

UNIVERSITÀ DEGLI STUDI DI SALERNO
DIPARTIMENTO DI CHIMICA E BIOLOGIA
“ADOLFO ZAMBELLI”
DOTTORATO DI RICERCA IN CHIMICA

XIV CICLO (Nuova serie)

***BIODEGRADABLE AND FUNCTIONAL
ALIPHATIC CO-POLYESTERS***

Tiziana Fuoco

TUTOR
Prof.^{ssa} Daniela Pappalardo

CO-TUTORS
*Prof.^{ssa} Marina
Lamberti
Prof.^{ssa} Anna Finne-
Wistrand*

COORDINATORE
Prof. Gaetano Guerra

INDEX

ABSTRACT	VI
LIST OF ABBREVIATIONS	IX
1. INTRODUCTION	1
1.1. Aliphatic polyesters: generalities	1
1.2. Synthesis of aliphatic poly(ester)s: polycondensation <i>versus</i> ring-opening polymerization	3
1.2.1. Metal-based catalysts for the ROP of lactones and lactides	6
1.3. Properties and applications of the aliphatic polyesters object of this thesis.....	10
1.4. Copolyesters	13
1.5. Functional aliphatic polyesters by ROP	15
1.6. Polyesters <i>polyethylene-like</i>	17
AIMS OF THE THESIS	19
References	21
2. RING-OPENING COPOLYMERIZATION OF GLYCOLIDE, <i>rac</i>-LACTIDE AND ϵ-CAPROLACTONE ..	25
2.1. Introduction.	25
2.2. Results and Discussion	29
2.2.1. Catalysts synthesis	29
2.2.2. Homo- and copolymerization of <i>rac</i> -lactide and glycolide in bulk	30
2.2.2.1. End groups analysis by NMR of poly(<i>rac</i> -lactide-co-glycolide)s prepared in bulk.....	36
2.2.2.2. Determination of molecular weight of poly(<i>rac</i> -lactide-co-glycolide)s prepared in bulk.....	39

2.2.2.3. <i>Thermal characterization of poly(glycolide-co-rac-lactide)s prepared in bulk.</i>	41
2.2.3. Copolymerization of <i>rac</i> -lactide and glycolide in solution ...	43
2.2.4. Block copolymerization of <i>rac</i> -lactide and glycolide.	46
2.2.5. Copolymerization of glycolide and ϵ -caprolactone.	49
2.2.5.1. <i>Thermal characterization of poly(ϵ-caprolactone-co-glycolide)</i>	57
2.2.6. Terpolymerization of glycolide, <i>rac</i> -lactide and ϵ -caprolactone.	59
2.2.6.1. <i>Thermal characterization of terpolymers</i>	66
CONCLUSIONS	68
References.	70

3. SYNTHESIS OF ALIPHATIC POLY(ESTER)S WITH PENDANT THIOL GROUPS: FROM MONOMER DESIGN TO EDITABLE POROUS SCAFFOLDS 74

3.1. Introduction	74
3.2. Results and discussion.....	78
3.2.1. Design and synthesis of the sulfur-functionalized monomer	78
3.2.2. Copolymerization	82
3.2.3. Polymer modifications	88
3.2.4. Scaffold preparation and characterization	91
3.2.5. Peptide binding on 3D porous scaffolds and cytotoxicity evaluation	94
CONCLUSIONS.....	99
References	101

4. RING-OPENING POLYMERIZATION OF ω -6-HEXADECENLACTONE: A ROUTE TO

SEMICRYSTALLINE AND FUNCTIONAL POLY(ESTER)S

.....	106
4.1. Introduction	106
4.2. Results and discussion.....	109
4.2.1. Ring-opening polymerization of ω -6-hexadecenlactone.....	109
4.2.2. Functionalization of poly(ω -6-hexadecenlactone)	117
4.2.2.1. <i>Thermal and structural analysis of poly(ω-6-hexadecenlactone) and its functionalized derivatives</i>	120
4.2.3. Copolymerization of ω -6-hexadecenlactone with small and medium size lactones	124
CONCLUSIONS	133
References	135
CONCLUDING REMARKS	140

5. EXPERIMENTAL SECTION

5.1. General experimental methods	144
5.1.1. Materials and methods	144
5.1.2. Instruments and measurements	145
5.2. Catalysts synthesis and characterization	147
5.2.1. Synthesis of {[2-O-C ₆ H ₄]CH=NC ₆ F ₅ }Al(CH ₃) ₂ (1).....	147
5.2.2. Synthesis of {[3- ^t Bu-2-O-C ₆ H ₃]CH=NC ₆ F ₅ }Al(CH ₃) ₂ (2)...	148
5.2.3. Synthesis of {[3,5-C(CH ₃) ₂ C ₆ H ₃ -2-O-C ₆ H ₂]CH=NC ₆ F ₅ }Al(CH ₃) ₂ (3).....	148
5.3. Copolymerization of <i>rac</i> -lactide and glycolide	149
5.3.1. Hopolymerization in bulk	149
5.3.2. Copolymerization in bulk	150
5.3.3. Copolymerization in solution	151
5.3.4. Synthesis of poly(glycolide)- <i>block</i> -poly(<i>rac</i> -lactide)	152

5.4. Copolymerization of glycolide and ϵ -caprolactone	153
5.5. Terpolymerization of glycolide, ϵ -caprolactone and <i>rac</i> -lactide	154
5.6. Synthesis and ROP of TrtS-LA, post-polymerization modification and scaffolding	155
5.6.1. Synthesis of 3-methyl-6-(tritylthiomethyl)-1,4-dioxane-2,5- dione (TrtS-LA)	155
5.6.2. Copolymerization of 3-methyl-6-(tritylthiomethyl)-1,4- dioxane-2,5-dione (TrtS-LA) with L-lactide (LA).....	158
5.6.3. Copolymerization of 3-methyl-6-(tritylthiomethyl)-1,4- dioxane-2,5-dione (TrtS-LA) with ϵ -caprolactone (CL).....	158
5.6.4. Copolymerization of 3-methyl-6-(tritylthiomethyl)-1,4- dioxane-2,5-dione (TrtS-LA) with ϵ -caprolactone (CL) and L-lactide (LA).....	159
5.6.5. Cleavage of trityl groups of poly[(TrtS-LA)- <i>co</i> -CL].....	160
5.6.6. Reaction of poly[(HS-LA)- <i>co</i> -CL] with 2,2'-dipyridyl disulfide.....	161
5.6.7. Synthesis of poly(L-lactide- <i>co</i> - ϵ -caprolactone) (PCLA)	162
5.6.8. Scaffold preparation	162
5.6.9. Binding of the H-Arg-Gly-Asp-Cys-OH (RGDC) peptide to the scaffolds	163
5.6.10. Cytotoxicity of the scaffolds' extracted liquid	163
5.7. Ring-opening of 6HDL and post-polymerization modifications	164
5.7.1. Synthesis of poly(6- ω -hexadecenlactone).....	164
5.7.2. Kinetic experiments	165
5.7.3. Epoxidation of poly(6,7-epoxy- ω -hexadecenlactone)	165
5.7.4. Reaction of poly(6,7-epoxy- ω -hexadecenlactone) with NaCNBH ₃	166
5.7.5. Reaction of poly(6- ω -hexadecenlactone) with 6-mercapto-1- hexanol.....	166

5.7.6. Synthesis of poly[(6- ω -hexadecenlactone)- <i>ran</i> -(ϵ -caprolactone)].....	167
5.7.7. Synthesis of poly(6- ω -hexadecenlactone)- <i>block</i> -poly(ϵ -caprolactone).....	168
5.7.8. Synthesis of poly(6- ω -hexadecenlactone)- <i>block</i> -poly(<i>rac</i> -lactide).....	169
5.7.9. Synthesis of poly[(6- ω -hexadecenlactone)- <i>ran</i> -(ϵ -caprolactone)]- <i>block</i> -poly(<i>rac</i> -lactide)	170
References	172
ACKNOWLEDGMENTS.....	174

ABSTRACT

Over the past decades, aliphatic polyesters have found rapidly increasing interest. Linear aliphatic polyesters, such as poly(glycolide) (PGA), poly(lactide) (PLA), poly(ϵ -caprolactone) (PCL) and their copolymers have found a wide range of practical applications, from packaging to more sophisticated biomedical devices. This class of materials is biocompatible and biodegradable; the degradation products are excreted via the citric acid cycle.

The uniqueness of this class of polymers lies in its immense diversity and synthetic versatility. They can be prepared by a variety of monomers via different approaches. The ring-opening polymerization of cyclic esters and lactone is the best strategy.

There is still need for improvements to provide materials with enhanced features to address the new requirements of use. A precise control over properties, like hydrophilicity, glass transition, the presence of functional group is important to regulate the biodegradation rate, the thermomechanical properties and it relies on a controlled synthetic pathway.

This doctoral thesis was focused on the development of synthetic pathways to obtain aliphatic polyesters with different and controlled microstructures and functional groups by extending the expertise in the ring-opening polymerization of cyclic esters by dimethyl(salicylaldiminato)aluminum compounds.

Dimethyl(salicylaldiminato)aluminum compounds with a different steric hindrance at the ortho position of the phenolato ring were tested as catalysts in the ring-opening homo- and co-polymerization of GA, rac-LA and CL. These complexes resulted active for the production of PLGA copolymers with variable microstructure.

This copolymer is one of the most used in biomedical field as temporary scaffolds and as drug delivery device. The degradation profile of PLGA is strongly influenced by the microstructure.

The copolymerization of GA and LA were performed in bulk and in solution, by varying comonomers ratio, monomer/catalyst feed ratio, temperature, reaction time and solvent. By changing the reaction conditions, copolymers from random, to blocky, to di-block were obtained, demonstrating the versatility of such system in modulating the copolymers microstructure and the related thermal properties.

The same catalytic approach was extended to the copolymerization of GA with CL and to the terpolymerization of GA, CL and rac-LA. The formation of random copolymers was favored by the steric hindrance of the catalyst and transesterification reactions contributed to randomize the structure. All the terpolymer samples resulted random and amorphous, the incorporation of the monomers is in this case determined by the bulkiness of the catalyst and by the higher coordination ability of the cyclic esters.

While the physical properties can be tailored by copolymerization, the introduction of functional group extends the possible applications to new areas, especially in biomedical field where the binding of biological motifs could enable interactions with cells.

Due to the ubiquity of thiol groups in the biological environment and to the pliability of thiol chemistry, an ad hoc lactide-type monomer possessing a pendant thiol-protected group, the 3-methyl-6-(tritylthiomethyl)-1,4-dioxane-2,5-dione was designed and synthesized. Then, this molecule was used as a “building block” for the preparation of functionalized aliphatic co-polyesters by copolymerization with LA and CL promoted by dimethyl(salicylaluminum)aluminum compounds. After polymerization, the pendant groups incorporated along the chains were converted into pyridyl disulfide functionalities. This derivative was used to prepare porous scaffolds by salt-leaching method after blend with PCLA.

The pyridyldisulphide groups, which are very reactive in the disulphide exchange reaction, embedded in the 3D porous scaffolds were exploited to graft a cysteine terminated RGD peptide demonstrating the potential of such prepared materials.

Finally, dimethyl(salicylaldiminato)aluminum compounds were employed as catalyst in the ring-opening polymerization of an unsaturated large lactone, the ω -6-hexadecenlactone (6HDL). Semicrystalline polyethylene-like unsaturated polyesters were obtained with a good control over the chain growth.

The double bonds along the polymeric backbones were used to carry out further modification, which occurred without any change in the degree of polymerization, however, modifying the thermal and structural polymer features.

Copolymerization of the 6HDL with the smaller ring size CL produced a true random semicrystalline copolymer. The pseudo-living behaviour of the catalytic system and the absence of transesterification reactions allowed also the preparation of linear block copolymers of 6HDL with CL and/or rac-LA by sequential addition of the monomers. These block copolymers were also semicrystalline.

LIST OF ABBREVIATIONS

6HDL	(ω -6-hexadecenlactone)
AIBN	2,2'-azobis(2-methylpropionitrile)
Ar	Aryl
bs	Broad singlet
BP	Benzoyl peroxide
Cap	Caproyl unit
Cat	Catalyst
CGM	Cell growth medium
CL	ϵ -caprolactone
d	Doppietto
dd	Doppio doppietto
D,L-LA	D,L-Lactide
DMSO	Dimethyl sulfoxide
DSC	Differentials scanning calorimetry
DTT	Dithiothreitol
<i>E</i>	Elactic modulus
FTIR	Fourier transform spectroscopy
G	Glycolyl unit
GA	Glycolide
GG	Glycolidyl unit
GPC	Gel permeation chromatography
h	Hour(s)
hDF	Human dermal fibroblast
L	Lactyl unit
LA	L-Lactide
L _{6HDL}	Average length of hexadecenlactoyl sequences
L _{Cap}	Average length of caproyl sequences

L _{CL}	Average length of caproyl sequences
L _{GG}	Average length of glycolidyl sequences
LL	Lactydyl unit
L _{LL}	Average length of lactidyl sequences
m	Multipletto
MALDI-Tof-MS	Matrix assisted laser desorption/ionization-time of flight mass
mCPBA	<i>meta</i> -Chloroperbenzoic acid
<i>meso</i> -LA	<i>meso</i> -Lactide
min	Minute(s)
M _n	Number average molecular weight
M _w	Weight average molecular weight
NMR	Nuclear magnetic resonance
P6HDL	Poly(ω -6-hexadecenlactone)
PBS	Phosphate buffer saline
PCL	Poly(ϵ -caprolactone)
PCLA	Poly(ϵ -caprolactone- <i>co</i> -lactide)
PDL	Pentadecalactone
PDS	Pyridyl disulfide
PE	Poly(ethylene)
PGCA	Poly(glycolide- <i>co</i> - ϵ -caprolactone)
PGLC	Poly(glycolide- <i>co</i> -lactide- <i>co</i> - ϵ -caprolactone)
Ph	Phenyl
PLGA	Poly(lactide- <i>co</i> -glycolide)
PPDL	Poly(pentadecalactone)
q	Quartet
<i>rac</i> -LA	<i>rac</i> -Lactide
R _g	Radius of gyration
RGD	Arginine-glycine-aspartic acid sequence

RGDC	Arginine-glycine-aspartic acid-cysteine sequence
RGDS	Arginine-glycine-aspartic acid-serine sequence
ROP	Ring-opening polymerization
rt	Room temperature
s	Singlet
SEC	Size-exclusion chromatography
SEM	Scanning electron microscopy
T	Temperature
t	Time
t	Triplet
TFA	Trifluoroacetic acid
T_g	Glass transition temperature
THF	Tetrahydrofuran
T_m	Melting temperature
Trt	Trityl
TrtS-LA	3-methyl-6-(tritylthiomethyl)-1,4-dioxane-2,5-dione
UV	Ultraviolet

1. INTRODUCTION

1.1. Aliphatic polyesters: generalities

Aliphatic polyesters are a class of natural and synthetic polymers with good mechanical and thermal properties.¹ Among them, linear aliphatic polyesters represent one of the most promising family and, up to now, are the most extensively investigated (Figure 1.1.).

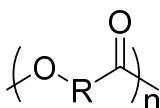


Figure 1.1. General formula for linear aliphatic polyesters.

Linear aliphatic polyesters are thermoplastic polymers with hydrolytically esters linkages in their backbone. Their degradation process can occur through an enzymatic route or by hydrolytically cleavage of the ester bonds, which is easier to control by chemists.²

Although all polyesters are theoretically degradable, as esterification is a chemically reversible process, only aliphatic polyesters with reasonably short aliphatic chains between the ester bonds, R, can degrade over the period required for most of the applications. Therefore, materials with different degradation rate can be obtained by varying the lengths of the aliphatic chains as well as by copolymerization processes.

To date, aliphatic polyesters with short aliphatic chains, such as poly(glycolide) (PGA), poly(lactide) (PLA) and poly(ϵ -caprolactone) (PCL), have a leading position among the various class of biodegradable polymers. Biodegradable polymers, generally speaking, have been defined as those materials which are degraded in biological environments not through oxidation, photolysis, or radiolysis but through enzymatic or non-enzymatic hydrolysis.

Moreover, PLA, PGA, PCL and related copolymers have been extensively investigated since their hydrolysis generates metabolites, which are excreted *via* the citric acid cycle (Figure 1.2), therefore, they are biocompatible and bioresorbable materials.³

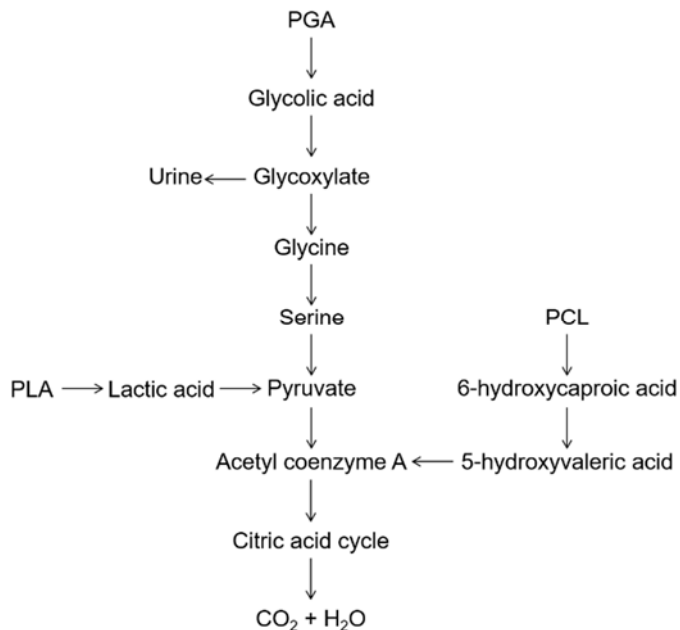


Figure 1.2. Breakdown of biodegradable/bioresorbable polymers.

Indeed, such polymers currently find application as biodegradable materials that contribute to the medical care of patients, as well as ecological materials that preserve the environment. In details, they have been used in medical products such as sutures, bone screws, tissue engineering scaffolds and drug delivery systems. Moreover, aliphatic polyesters have found a broad range of practical applications from packaging for industrial products to films in agriculture.

On the contrary, aliphatic polyesters with long aliphatic chains have been recently envisaged as *poly(ethylene)-like* materials, therefore suitable for long term applications. *Poly(ethylene)-like* polyesters are those with a

relatively large number of methylene groups (i.e. $-\text{CH}_2- \geq 5$) whose chains can adopt a planar zigzag structure.²

1.2. Synthesis of aliphatic polyesters: polycondensation versus ring-opening polymerization

The uniqueness of the aliphatic polyesters lies in their immense diversity and synthetic versatility. Indeed, they can be prepared by a variety of monomers via enzymatic route or synthetic approaches, i.e. ring-opening polymerization or polycondensation routes.

The synthetic approaches for the synthesis of aliphatic polyesters allow a better control over macromolecular features than the enzymatic route, which usually leads to low molecular weights with molecular weight dispersity (M_w/M_n) higher than 2.⁴ Moreover, the enzymatic approach is more expensive than the synthetic ones, because of the large quantity of enzymes required for polymerization. On the other hand, the enzymatic route can be regarded as an environment-friendly synthetic process, which can occur in mild conditions.⁵

The traditional synthetic route for the preparation of aliphatic polyesters is the step-growth polymerization or polycondensation of diols with diacids (or diesters), or of hydroxyacids. The advantages of the polycondensation route are the access to a large range of monomer feedstocks and the low cost. However, direct polycondensation suffers from several drawbacks such as the need for high temperature, the continuous removal of by-products (most often water), and long reaction time, often favoring side reaction. Moreover, the molecular weights of the resulting polymers are typically low, with large dispersities, thus resulting in products having poor mechanical properties. The method, finally, do not allow the preparation of block copolymers.⁶

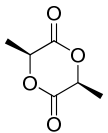
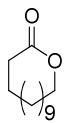
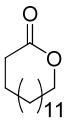
In contrast to the limitations of the step-growth polycondensation techniques, ring-opening polymerization (ROP) of cyclic esters,⁷ despite the restriction on monomers, may provide high-molecular weight aliphatic polyesters under mild conditions. The ROP can be performed in bulk (absence of solvent), in solution or in emulsion. Under given conditions (temperature, solvent, initiator, catalyst), the ROP proceeds in controlled manner. In the presence of proper catalyst and conditions, the ROP may also display the features of a “*living*” polymerization, enabling the prediction of molecular weights for polyesters by controlling the initial monomer-to-initiator molar ratio, thus the synthesis of well-defined polyesters with a low degree of polydispersity is achieved.⁸ Moreover, block copolymers can be obtained by *living* ROP by sequential addition of the different monomers.

Cyclic diesters and lactones, such as glycolide (GA), lactide (LA), β -butyrolactone (β -BL), ϵ -caprolactone (CL) have been the most investigated monomers in the ROP. Recently the ROP of large ring-size lactones, such as pentadecalactone (PDL), have been also studied (Table 1.1).

The ability of a cyclic ester to polymerize by ROP, i. e. the conversion of the monomer molecules into macromolecules, must be allowed both thermodynamically and kinetically. Practically, this means that (1) the monomer-macromolecule equilibrium has to be shifted to the right-hand side, and (2) the corresponding polymerization mechanism should enable the conversion of monomer molecules into polymer, within an operable polymerization time.^{9,10}

The thermodynamic parameters, (the standard enthalpy, ΔH_p^0 , and entropy, ΔS_p^0) characterizing the ability to polymerize for some representative cyclic esters, are showed in Table 1.1.¹¹

Table 1.1. Standard thermodynamic parameters of polymerization of selected cyclic esters.^{10,11}

Monomer	Ring size	ΔH_p^0 (298 K) [kJmol ⁻¹ K ⁻¹]	ΔS_p^0 (298 K) [Jmol ⁻¹ K ⁻¹]	
β -propiolactone (PL)		4	-82.3	-74
γ -Butyrolactone (γ -BL)		5	5.1	-29.9
δ -Valerolactone (VL)		6	-27.4	-65.0
L-Lactide (L-LA)		6	-22.9	-41.1
ϵ -Caprolactone (CL)		7	-28.8	-53.9
Tridecanolactone (TDL)		14	-8	26
Pentadecanolactone (PDL)		16	3	23

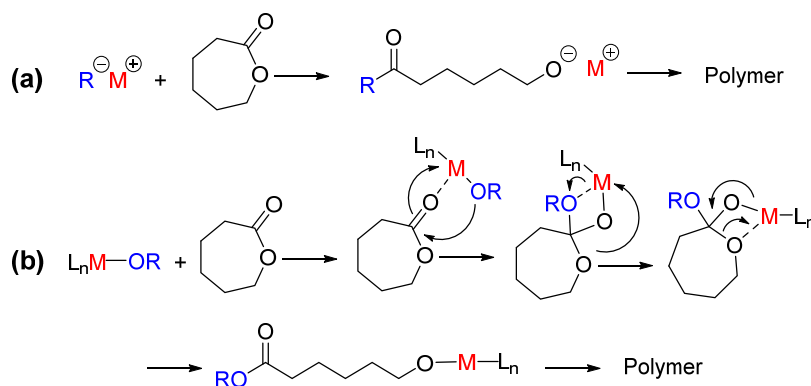
The driving force for the polymerization of the majority of cyclic esters is their ring strain. In fact, enthalpy of polymerization is often a measure of the ring strain. Due to the loss of the translational degrees of freedom, polymerization is often accompanied by an entropy decrease. In particular, the six-member L-lactide assumes irregular skew-boat conformation, in which two ester groups can adopt planar conformation, and it has, therefore, a relatively high enthalpy of polymerization equal to $-22.9 \text{ kJ mol}^{-1}$.¹² This value is very close to the ring strain of δ -valerolactone (VL)¹³ and ϵ -caprolactone (CL).¹⁴ The thermodynamic

data in Table 1.1 for large lactones (tridecanolactone and pentadecanolactone) suggest that an increase in the ring size leads to a rather small ring strain and to an increase in the polymerization entropy.¹⁵ The latter is due to a relatively high flexibility of the long polymethylene sequences in the resulting polymer chains.

1.2.1. Metal-based catalysts for the ROP of lactones and lactides

The ROP processes can be promoted by different kind of catalysts, including metal coordination complexes, enzymes and simple organic molecules. Depending on monomers, catalytic system, nature of active species, ROP can proceed as a radical, coordinative, anionic or cationic polymerization. Anionic and coordinative ROP by metal-based catalysts allow to obtain the highest polymerization yields and molecular weights in short reaction times.⁵

Simple metal-based initiators, such as butyl lithium, lithium/potassium *tert*-butoxide and potassium methoxide, can mediate anionic ROP. The polymerization generally occurs *via* attack of the initiating or propagating alkoxide at the carbonyl group of cyclic ester with ring-opening occurring quantitatively at the acyl-oxygen bond (Scheme 1.1a).¹⁶



Scheme 1.1. Metal-catalysed ring-opening polymerization of ϵ -caprolactone. (a) Anionic polymerization and (b) coordination-insertion polymerization.

Different metal salts and well-defined single site catalysts are able to mediate ROP by coordination-insertion mechanism.^{4,5} In this mechanism, the first step is the coordination of the monomer to the metal centre through the carbonyl oxygen, followed by the insertion of the monomer in the metal-initiator group bond, typically an alkoxide. Subsequently the polymerization proceeds by propagation by a metal alkoxide species (Scheme 1.1b).

One of the most commonly used catalysts for the ROP of cyclic esters is tin (II) octanoate, SnOct_2 ,¹⁷ which is also the most frequently used catalyst for the ROP of cyclic esters in industry (Figure 1.3).¹⁸

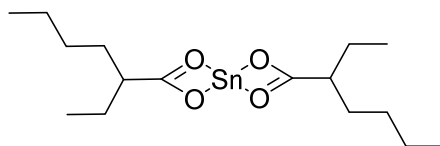


Figure 1.3. Molecular structure of tin (II) octanoate.

A coordination-insertion mechanism is active in this case. SnOct_2 is an efficient catalyst for the ROP of a wide range of cyclic esters, although it is generally only active at elevated temperatures. Moreover, SnOct_2 promotes transesterification side reactions throughout the polymerization, that leads to a decreased control, manifested by broad molecular weight dispersities in the obtained polyesters.

Besides SnOct_2 , tin triflate and aluminium compounds have also been shown to be highly efficient catalysts for the ROP of cyclic monomers. In particular, aluminium tris(isopropoxide) has received extensive attention.¹⁹ A great interest has been recently devoted to the development of single-site homogeneous metal-based catalysts, which might remove the mechanistic complexity resulting from the aggregation-disaggregation exchange reactions, in which multiple-site alkoxides are usually engaged, thus allowing a better control over chain growth.²⁰

Single-site catalysts for ROP have been recently developed, and can be described by the general formula L_nM-OR . The enchainment of monomer occurs at a metal centre, M , the active site, which is bound to carefully designed ancillary ligands, L_n . The ancillary ligand remains bound to the metal throughout the entire catalytic reaction, and it may tune the reactivity and selectivity of the metal centre, decreasing the occurrence of side reactions.²¹

A wide variety of single-site aluminium complexes has received a great deal of attention as catalyst for ROP. The first example was the use of aluminium complexes bearing a tetraphenylporphyrin ligand, which were able to catalyse the immortal ROP of various cyclic esters with good control.²² More recently, the use of tetradentate salicylaldehyde ligands (*salen*) for the preparation of aluminium complexes has been investigated (Figure 1.4a). These catalyst are highly active in the ROP of cyclic esters as well as in the ability to control the stereochemistry of the ROP of *rac*-lactide.²³

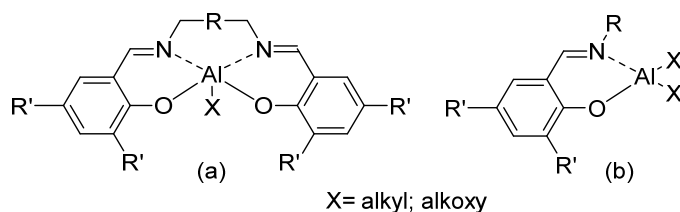


Figure 1.4. Aluminium complex bearing (a) *salen* and (b) *half-salen* ligands for ROP.

Interestingly, the related half-salen aluminium complexes (Figure 1.4b) have been shown as efficient catalysts for ROP of cyclic esters.²⁴

Recently, our research group has described a set of dimethyl(salicylaldehyde)aluminium compounds, with variable Ar-imino substituents and with a bulky tert-butyl at the *ortho*-position of the phenolato ring (Figure 1.5) as efficient and versatile initiators in the ROP of CL and LA, when activated by addition of 1 equiv. of MeOH.²⁵

Indeed, this class of catalysts is usually synthesized as alkyl aluminium compounds and the active aluminium-alkoxide species is formed *in situ* by addition of the appropriate alcohol followed by alkane elimination. The alkoxy moiety is then incorporated as the α -chain end of the polymer quantitatively.²²⁻²⁵

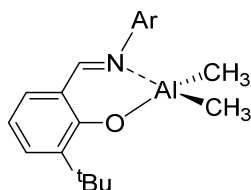


Figure 1.5. Dimethyl(salicylaldiminato)aluminum complexes reported for the ROP of CL and LA.²⁵

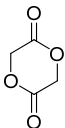
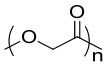
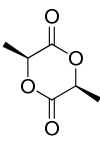
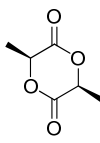
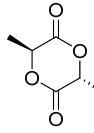
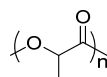
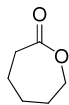
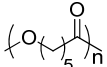
This class of initiators displayed a good control over chain growth and molecular weight, not only in the homopolymerization but also in the copolymerization under mild reaction conditions, by proper choice of the Ar group. In particular, when Ar = C₆F₅ the related compound exhibited a *living* behaviour allowing the synthesis of block copolymers. Random copolymers of CL and La were also obtained with a controlled chain growth in the absence of transesterification reactions.²⁵

The ability of such complexes to readily tune polymer features, producing polymers with narrow molecular weight dispersities, end groups fidelity and almost complete absence of transesterification side reactions, provides attractive options in the synthesis of advanced polymer architecture. Moreover, the simple formulation, the straightforward synthesis and the easy activation are advantageous features with respect to other aluminum catalysts bearing more complex polydentate ligand systems.

1.3. Properties and applications of the aliphatic polyesters object of this thesis.

Poly(lactide) (PLA), poly(glycolide) (PGA), poly(ϵ -caprolactone) (PCL), which are usually obtained by ROP of the related cyclic monomers (i.e. LA, GA and CL), and their copolymers are among the most extensively investigated aliphatic polyesters, and they have already found important applications. The features of these polyesters are summarized in Table 1.2.³

Table 1.2. Selected cyclic esters and related polymers.

Cyclic Monomer	Polymer	T_g (°C)	T_m (°C)	E (GPa)	Degradation rate (months)
 Glycolide (GA)	 Poly(glycolide) PGA	35-40	225	12.5	6-12
 L-Lactide (L-LA)	 D-Lactide (D-LA)				
 <i>meso</i> -Lactide (<i>meso</i> -LA)	 Poly(lactide) PLA	<i>Isotactic</i> 55-60	170	2.7	24-60
		<i>Atactic</i> 45-55	-	1.9	12-16
 ϵ -Caprolactone (CL)	 Poly(ϵ -caprolactone) PCL	-60	65	0.4	24-36

Polyglycolide (PGA) was the first commercially successful synthetic biodegradable polymer used as biomedical material. PGA is a highly crystalline polymer (45-55%) and therefore it shows excellent mechanical properties, it exhibits a high tensile modulus, E , approximately 12.5 GPa.

However, it shows a very low solubility in organic solvent. The glass transition temperature of the polymer ranges from 35 to 40 °C and the melting point is greater than 200 °C (Table 1.2.). Due to its excellent fiber forming ability, PGA was initially investigated for developing resorbable sutures, and it has been used as bone internal fixation devices.²⁶

PGA is a bulk degrading polymer by hydrolysis of the ester linkages. The polymer is known to lose its strength in 1-2 months when hydrolyzed and loses mass within 6-12 months. In the body, PGA is broken down into glycine, which can be excreted or converted in CO₂ and water via the citric acid cycle (Figure 1.2). The high rate of degradation, acid degradation and low solubility, however, represent a drawback and limit the biomedical applications.

On the other hand, lactide, which can be obtained from renewable resources, exists in three forms, two optically active forms, L-lactide and D-lactide, and in the meso form. The polymerization of L or D-lactide leads to the formation of isotactic PLA, which is semi-crystalline hard and brittle polymer, with a modulus E of 2.7 GPa. The melting point is around 170 °C and the glass transition temperature in the range 55-60 °C. In the absence of a stereocontrolled polymerization, the ROP of racemic (D,L)-lactide or *meso*-lactide results of course in the formation of atactic amorphous polymers, with a glass transition temperature of 45-55 °C and a modulus of 1.9 GPa. PLAs degrade by hydrolytic chain scission into lactic acid, a natural intermediate in carbohydrate metabolism, Figure 1.2.

The degradation rate of isotactic PLLA is very low; it takes between 2 and 5-6 years to be completely resorbed, which is due to its hydrophobic nature and high degree of crystallinity.²⁷ Even though the polymer loses the strength in approximately 6 months when hydrolyzed, no significant changes in mass occur after a very long time. This has dramatic consequences in the case of its use as biomedical implants, with undesirable

inflammatory response, highlighted in a certain number of clinical studies, with the necessity to remove the implants afterward.

The long degradation time and the high crystallinity make PLLA an ideal material for load-bearing application. Since the first use as multifilament sutures in the 1980s, it has been used to develop bone screw, plates and different prosthetic devices.

On the other hand, the atactic PDLLA loses its strength within 1–2 months when hydrolyzed and undergoes a loss in mass within 12–16 months.²⁸ Therefore, it is the preferred candidate for developing drug delivery vehicles and as low strength scaffolding material for tissue regeneration.

The ring opening polymerization of the cheap monomer ϵ -caprolactone (Table 1.2), firstly performed by Carothers in the early 1930s,²⁹ yields the poly(ϵ -caprolactone) (PCL), a semicrystalline, tough, flexible and highly processable polymer, soluble in a wide range of organic solvents. It shows a melting point of about 65 °C and a glass-transition temperature of -60 °C, much below room temperature. Thus, the PCL is in the rubber state at room temperature, with an *E* modulus of 0.4 GPa. However, the PCL is highly hydrophobic with a long degradation time of the order of two years. It degrades by hydrolytic degradation as well as by enzymatic attack. Hydrolysis yields 6-hydroxy caproic acid, which enters the citric acid cycle and it is completely metabolized (Figure 1.2). PCL has been exploited to develop long-term drug/vaccine delivery system and scaffolds for bone tissue engineering.

Several disadvantages of these aliphatic polyesters, such as the difficulty to dissolve the PGA in most organic solvents, the brittleness of the PLA and the low degradation rate of PCL, can be overcome by copolymerization process. Indeed, copolymerization is an important tool to change the base properties of homopolyesters and tune them to the need of a given application.

While the physical properties, such as glass transition temperature, mechanical features, rate of degradation, can be modulated by copolymerization process, a further drawback of aliphatic polyesters is the lack of functional groups, which limits the applications especially in biomedical field. Indeed, the presence of reactive groups along the polymeric chains can enlarge the range of properties and applications and allow the functionalization with biologically relevant molecules in order to enhance a positive response when these materials are used for medical purposes.

Therefore, it is important to develop strategies toward the synthesis of aliphatic polyesters with controlled properties and functional groups to give materials for demanding applications.

1.4. Copolyesters

As discussed above, ring-opening polymerization enables the synthesis of polymers with predictable features, offering the possibility to obtain a wide range of poly(ester)s that display different thermal and degradative properties with potentials in very different fields.

To obtain a product with particular combination of desirable features, copolymerization techniques have been extensively used. Physical properties, such as T_g , melting temperature and crystallinity can be significantly affected by copolymerization. Moreover, a well-controlled ROP process may allow also the synthesis of copolymers with different architectures, from random, to alternating, block, multiblock, or graft, which display different properties (Figure 1.6).

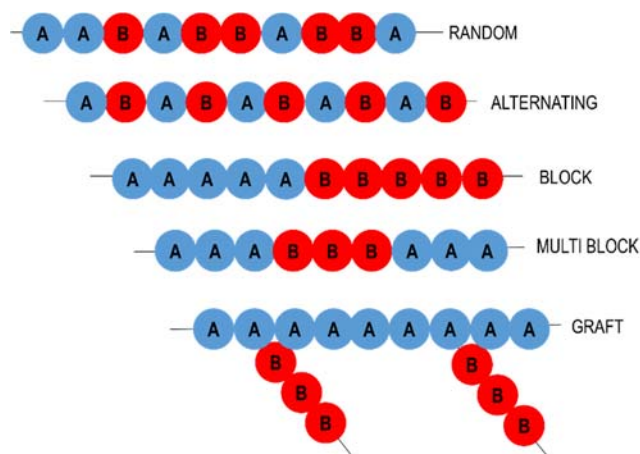


Figure 1.6. Schematic overview of selected copolymer architectures.

Random copolymers can be synthesized by polymerization of more than one lactone using suitable initiators. The copolymer composition can be tuned by adjusting the composition of the feed and it is regulated by the reactivity ratio of the monomers. The copolymer composition and microstructure are important factors that influence the degradation rate.³⁰ Thus, a proper control of the polymerization parameters is of outmost importance to prepare a material with the desired physical properties and with the required degradation rate.

In this regard, copolymerization of GA and LA has been widely used to engineer the properties of PGA and PLA. The poly(glycolide-*co*-lactide), PGLA, is one of the most used aliphatic polyesters in biomedical field, especially for tissue engineering applications since it demonstrates good cell adhesion and proliferation. PLGA is less stiff compared to the parent homopolymers, and in the composition range of 25-75% forms amorphous polymers. Copolymers with different ratios of two monomers have been commercially developed and are being investigated for a wide range of biomedical applications. The 50/50 PLGA degrades in approximately 1-2

months, the 75/25 (LA/GA) in 4-5 months and the 85/15 (LA/GA) in 5-6 months.³¹

On the other hand, due to the slow degradation rate of PCL, several copolymeric system containing PCL have been investigated to improve the properties of the native polymer. Copolymers of CL with DL-lactide have yielded materials with more rapid degradation rate. Similarly, copolymers of CL and GA resulted in fibers, currently on the market, that were less stiff than those made of PGA.

1.5. Functional aliphatic polyesters by ROP

While the physical properties of the aliphatic polyesters can be tailored *via* copolymerization, a major limitation towards application in new areas results from the lack of readily accessible side-chain functionalities.³²

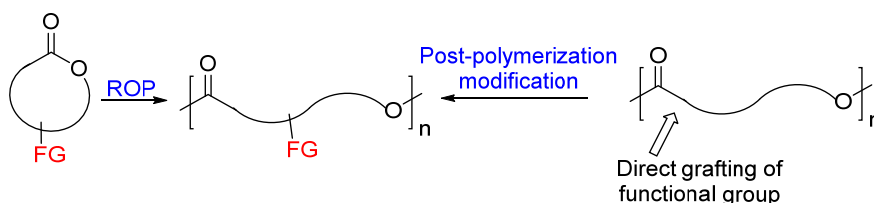
According to their structure merely the chain ends of linear aliphatic polyesters may be utilized to introduce functionalities. This functionalization strategy can be accomplished by using functional initiators for ROP³³ and/or through end-capping reactions.³⁴ Aliphatic polyesters with reactive end groups can be used as macromonomers for post polymerization, copolymerization or cross-linking reactions.³⁵

However, more functionalities are often required to meet the demand of a greater manipulation throughout the macromolecular structure. The synthesis of degradable polymers susceptible to further modifications is highly desired, since the presence of a functional group could allow to tune the physical and mechanical properties as well as to improve hydrophilicity and biocompatibility. For application in biomedical field, such as tissue engineering, a functional group could provide an anchoring site for biologically active ligands, thus, improving cell adhesion and function.³⁶

Thus, methods to integrate functionality into aliphatic polyesters for fine-tuning their physical and biological properties have been sought. However,

derivatization of aliphatic polyesters is particularly delicate as compared to non degradable polymers, because any reaction condition that allows the cleavage of the ester bond could be responsible for premature polymer degradation. A lot of efforts are thus currently devoted to the preparation of tailored-made functionalized aliphatic polyesters, that represent promising materials for different applications.³⁷

Two main strategies have been proposed to synthesize aliphatic polyesters with functionalities incorporated as side groups (Scheme 1.2). ROP of suitable monomers bearing a functional group, FG, or post-polymerization modification on preformed polyester chains.



Scheme 1.2. Main strategies for the synthesis of aliphatic polyesters with pendant functional group.

Post-polymerization modifications on preformed aliphatic polyesters chains is an appealing strategy because from a single easily available precursor a wide range of functional groups can be attached in one further step. However, the main drawback of this strategy is that side reactions often occur, such as chain scission, with a consequent drop of the polymeric properties.^{38,39} Hence, the method is generally used only to modify the surface without affecting the polymer bulk.⁴⁰ Therefore, post-polymerization functionalization is not the preferred route to obtain functional polyesters.

On the other hand, synthesis and ring-opening polymerization of functionalized lactones or cyclic diesters bearing side reactive groups, may allow the introduction of functional groups throughout the polymer chains (Scheme 1.2). If the process occurs in a controlled fashion the

copolymerization of the functionalized monomers may offer the way to tailor the functional group density over a wide range. Therefore, this strategy represents the most versatile synthetic method toward functional aliphatic polyesters. Indeed, a great deal of cyclic monomers, bearing different functionalities, has been reported and their ring-opening (co)polymerization investigated.⁴¹

However, functional monomers need to be synthesized and then polymerized and protection is necessary for functionalities, that can react with the catalyst or other species involved in the polymerization. The choice of the protecting group is also an important issue because the cleavage after polymerization should proceed cleanly under mild condition, leaving the polymeric backbone intact.⁴¹

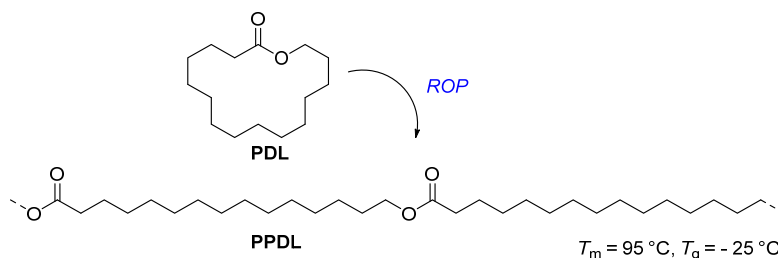
1.6. Polyesters *polyethylene-like*

Among the aliphatic polyesters, the poly(ω -hydroxy fatty acid) family is recently receiving an increasing attention. Indeed, this class of polyesters could be derived from biobased feedstock and thanks to the long methylene chain they are semicrystalline polymers with good mechanical properties.

In the 2010, Mecking *et al.* reported an elegant route to the synthesis of PE-like polyesters *via* methoxy carbonylation of unsaturated fatty acids followed by polycondensation.⁴² However, the obtaining of high molecular weight polymers by polycondensations remains a big challenge.

Alternatively, the ROP of large fatty acid based lactones represents a straightforward route for the synthesis of this class of polyesters. For example, the poly(ω -pentadecalactone) (PPDL), which can be obtained by ROP of the ω -pentadecalactone (PDL), is a semicrystalline polymer resembling the mechanical properties of low density polyethylene (LDPE) (Scheme 1.3). It owes its PE-like properties to the high crystallinity of the 14 methylene units,⁴³ giving it a melting point (T_m) around 95 °C and a glass

transition temperature (T_g) of $-25\text{ }^\circ\text{C}$ analogous to LDPE ($T_m = 97 - 117\text{ }^\circ\text{C}$; $T_g = -25\text{ }^\circ\text{C}$). Furthermore, PPDL presents good mechanical properties,⁴⁴ which has led to recent investigation in coating and fiber applications.⁴⁵



Scheme 1.3. ROP of PDL.

However, the ROP of large lactones is scarcely explored. The reason is that the ROP of these macrolactones differs from the behaviour of small or medium size lactones because the polymerization reactions are driven mainly by entropy (see Table 1).⁴⁶ Indeed, as the ring strain decreases with increasing lactone size so does the reactivity in ROP. Not surprisingly, a limited number of catalytic approaches have been reported for the synthesis of polyesters from macrolactones, mainly enzymatic⁴⁷ and anionic polymerization.⁴⁸ Only recently the ring-opening polymerization of large-ring size lactones by single-site metal initiators has been investigated.⁴⁹ Notably, the ROP of suitable macrolactones could also be an appealing strategy for the preparation of functional aliphatic polyesters. Indeed, available macrocycles can contain reactive groups in the main chain, such as double bond, that may not interfere with the ROP activity. Hence chemical moiety can be subsequently added in the polymer main chain for optimizing their physical properties, degradation rate and for introducing functionalities.⁵⁰

AIMS OF THE THESIS

It is evident that a precise control over properties, like hydrophilicity, glass transition temperature, T_g , crystallinity and the presence of functional groups are of utmost importance for thermomechanical properties, biodegradation rate, and bioadherence of aliphatic polyesters, and relies on the availability of an adequate synthetic pathway.

Although aliphatic polyesters have been used for many years for different applications, there is still need for improvements to provide materials with enhanced features and to address the new requirements of use.

Therefore, the purpose of this doctoral thesis was the development of synthetic approaches for the preparation of aliphatic polyesters with controlled microstructure and functional groups, extending the achieved expertise in the ROP of cyclic esters by salicylaldiminato aluminum complexes to suitable monomers.

In details, the main aims were:

1. The synthesis of aliphatic copolyesters by ring-opening polymerization of glycolide, rac-lactide and ϵ -caprolactone with controlled properties, such as microstructure and molecular weight, since these features determine the thermal and mechanical properties as well as the rate and mechanism of degradation of the final materials.
2. The synthesis of aliphatic polyesters by ROP of a suitable monomer bearing a functional group to allow the synthesis of editable polymers with tunable features and able to bind biological motifs. A *lactide-type* monomer bearing a pendant thiol-protected group was designed in order to combine the features of biodegradability

and biocompatibility of aliphatic polyesters with the great versatility of the thiol functionality.

3. The synthesis of polyesters “*poly(ethylene)-like*” by ROP of an unsaturated 17-members ring lactone. Such a monomer appeared a useful starting point for the synthesis of semicrystalline and functional materials thanks to the presence of a long methylene chain and a *trans* double bond. The double bond represented a convenient functionality for post-polymerization modifications. Moreover, by copolymerization with smaller lactones or cyclic diesters, the synthesis of different polymeric architectures was explored.

References

- ¹ *Biodegradable Polyesters* **2015**, Stoyko Fkirow Ed.; Wiley.
- ² Y. Ikada, H. Tsuji, *Macromol. Rapid. Commun.* **2000**, *21*, 117-132.
- ³ J.-M. Raquez, R. Mincheva, O. Coulembier, P. Dubois, *Polymer Science: A Comprehensive Reference*. Amsterdam, Elsevier, **2012**, *4*, 761-777.
- ⁴ S. Kobayashi, H. Uyama, S. Kimura, *Chem. Rev.* **2001**, *101*, 3793-3818.
- ⁵ (a) A.-C. Albertsson, R. K. Srivastava, *Adv. Drug Delivery Rev.* **2008**, *60*, 1077-1093. (b) S. Kobayashi, *Polym. Adv. Technol.* **2015**, *26*, 677-686.
- ⁶ M. Okada, *Prog. Polym. Sci.* **2002**, *27*, 87-133.
- ⁷ C. Jérôme, P. Lecomte, *Adv. Drug. Deliv. Rev.* **2008**, *60*, 1056-1076.
- ⁸ A.-C. Albertsson, I. K. Varma, *Biomacromolecules* **2003**, *4*, 1466-1486.
- ⁹ A. Duda, A. Kowalski, J. Libiszowski, S. Penczek, *Macromol. Symp.* **2005**, *224*, 71-83.
- ¹⁰ A. Duda, A. Kowalski, in *Handbook of ring Opening Polymerization* **2009**; Wiley Ed.; 1-51.
- ¹¹ A. Duda in *Polymer Science: A Comprehensive Reference*. Amsterdam, Elsevier, **2012**, *4*, 213-245.
- ¹² A. Duda, S. Penczek, *Macromolecules* **1990**, *23*, 1636-1639.
- ¹³ A. A. Evstropov, B. V. Lebedev, T. G. Kulagina, N. K. Lebedev, *Vysokomol. Soedin. Ser. A* **1982**, *24*, 568-574.
- ¹⁴ B. V. Lebedev, A. A. Evstropov, N. K. Lebedev, *Vysokomol. Soedin. Ser. A* **1978**, *20*, 1974-1980.
- ¹⁵ A. Duda, A. Kowalski, S. Penczek, H. Uyama, S. Kobayashi, *Macromolecules* **2002**, *35*, 4266-4270.
- ¹⁶ K. M. Stridsberg, M. Ryner, A.-C. Albertsson, in *Advance in Polymer Science*. Berlin, Springer, **2002**, *157*, 41-65.
- ¹⁷ M. Ryner, K. Stridsberg, A.-C. Albertsson, H. von Schenck, M. Svesson, *Macromolecules* **2001**, *34*, 3877-3881.

-
- ¹⁸ A. Stjern Dahl, A.F. Wistrand, A.C. Albertsson, *Biomacromolecules* **2007**, *8*, 937–940.
- ¹⁹ (a) P. Dubois, C. Jacobs, R. Jérôme, P. Teyssie, *Macromolecules* **1991**, *24*, 2266–2270. (b) P. Vanhoorne, P. Dubois, R. Jérôme, P. Teyssie, *Macromolecules* **1992**, *25*, 37–44. (c) D. Mecerreyes, R. Jérôme, *Macromol. Chem. Phys.* **1999**, *200*, 2581–2590.
- ²⁰ B.J. O’Keefe, L. E. Breyfogle, M. A. Hillmyer, W. B. Tolman, *J. Am. Chem. Soc.* **2002**, *124*, 4384–4393.
- ²¹ B. M. Chamberlain, M. Cheng, D. R. Moore, T. M. Ovitt, E. B. Lobkovsky, G. W. Coates, *J. Am. Chem. Soc.* **2001**, *123*, 3229–3238.
- ²² S. Inoue, *J. Polym. Sci., Part A: Polym. Chem.* **2000**, *38*, 2861–2871.
- ²³ (a) A. Leborgne, V. Vincens, M. Jouglard, N. Spassky, *Makromol. Chem., Macromol. Symp.* **1993**, *73*, 37–46. (b) T. M. Ovitt, G. W. Coates, *J. Am. Chem. Soc.* **2002**, *124*, 1316–1326. (c) N. Nomura, R. Ishii, M. Akakura, K. Aoi, *J. Am. Chem. Soc.* **2002**, *124*, 5938–5939. (d) Z. Y. Zhong, P. J. Dijkstra, J. Feijen, *J. Am. Chem. Soc.* **2003**, *125*, 11291–11298. (e) K. Majerska, A. Duda, *J. Am. Chem. Soc.* **2004**, *126*, 1026–1027. (f) N. Nomura, R. Ishii, Y. Yamamoto, T. Kondo, *Chem. Eur. J.* **2007**, *13*, 4433–4451.
- ²⁴ (a) N. Nomura, T. Aoyama, R. Ishii, T. Kondo, *Macromolecules* **2005**, *38*, 5363–5366. (b) J. Liu, N. Iwasa, K. Nomura, *Dalton Trans.* **2008**, 3978–3988. (c) N. Iwasa, J. F. Liu, K. Nomura, *Catal. Commun.* **2008**, *9*, 1148–1152. (d) N. Iwasa, M. Fujiki, K. Nomura, *J. Mol. Catal. A: Chem.* **2008**, *292*, 67–75. (e) N. Iwasa, S. Katao, J. Y. Liu, M. Fujiki, Y. Furukawa, K. Nomura, *Organometallics* **2009**, *28*, 2179–2187. (f) M. Normand, B. Dorcet, E. Kirillov, J.-F. Carpentier, *Organometallics* **2013**, *32*, 1694–1709.
- ²⁵ D. Pappalardo, L. Annunziata, C. Pellecchia, *Macromolecules* **2009**, *42*, 6056–6062.

-
- ²⁶ (a) H. Montes de Oca, I.M. Ward, *Polymer* **2006**, *47*, 7070-7077. (b) M. Niaounaski, in *Biopolymers: Processing and Products*, Elsevier **2015**, 76-116.
- ²⁷ J. C. Middleton, A. J. Tipton, *Biomaterials* **2000**, *21*, 2335-2346.
- ²⁸ P. B. Maurus, C. C. Kaeding, *Oper. Tech. Sport Med.* **2004**, *12*, 158-160.
- ²⁹ F. J. Van Natta, J. W. Hill, W. H. Carothers, *J. Am. Chem. Soc.* **1934**, *56*, 455-457.
- ³⁰ K. K. L. Phua, E. R. H. Roberts, K. W. Leong in *Comprehensive Biomaterials* **2011**, *1*, 381-415.
- ³¹ J. C. Middelton, A. J. Tipton, *Biomaterials* **2000**, *21*, 2335-2346.
- ³² M. Heiny, J. J. Wurth, V. P. Shastri, in *Natural and synthetic Biomedical Polymers*. Elsevier, **2014**, 167-180.
- ³³ (a) B. Bogdanov, A. Vidts, A. Van Den Bulcke, R. Verbeeck, E. Schacht, *Polymer* **1998**, *39*, 1631-1636. (b) R. Savić, L. Luo, A. Eisenberg, D. Maysinger, *Science* **2003**, *300*, 615-618.
- ³⁴ (a) M. Mizutani, S. C. Arnold, T. Matsuda, *Biomacromolecules* **2002**, *3*, 668-675. (b) F. Nederberg, T. Bowden, J. Hilborn, *Macromolecules* **2004**, *37*, 954-965.
- ³⁵ M. Schappacher, A. Soum, S. M. Guillaume, *Biomacromolecules* **2006**, *7*, 1373-1379.
- ³⁶ (a) M. Vert, *Biomacromolecules* **2005**, *6*, 538-546. (b) C. K. Williams, *Chem. Soc. Rev.* **2007**, *36*, 1573-1580. (c) M. S. Soichet, *Macromolecules* **2010**, *43*, 581-591. (d) H. Seyednejad, A. H. Ghassemi, C. F. van Nostrum, T. Vermonden, W. E. Hennik, *J. Control. Release* **2011**, 168-176.
- ³⁷ H. Tian, Z. Tang, X. Zhuang, X. Chen, X. Jing, *Prog. Polym. Sci.* **2012**, *37*, 237-280.
- ³⁸ S. Ponsart, J. Caudane, M. Vert, *Biomacromolecules* **2000**, *1*, 275-281.
- ³⁹ B. Saulier, S. Ponsart, J. Caudane, H. Garreau, M. Vert, *Macromol. Biosci.* **2004**, *4*, 232-237.

-
- ⁴⁰ (a) H. Sun, A. Wirsén, A.-C. Albertsson, *Biomacromolecules* **2004**, *5*, 2275–2280. (b) B. Guo, A. Finne-Wistrand, A.-C. Albertsson, *Macromolecules* **2012**, *45*, 652–659.
- ⁴¹ (a) X. Lou, C. Detrembleur, R. Jérôme, *Macromol. Rapid Commun.* **2003**, *24*, 162-172. (b) R. J. Pounder, A. Dove, *Polym. Chem.* **2010**, *1*, 260-271. (c) Y. Yu, J. Zou, C. Cheng, *Polym. Chem.* **2014**, *5*, 5854-5872.
- ⁴² D. Quinzler, S. Mecking, *Angew. Chem., Int. Ed.* **2010**, *49*, 4306-4308.
- ⁴³ M. Gazzano, V. Malta, M. L. Focarete, M. Scandola, R. A. Gross, *J. Polym. Sci.; Part B: Polym. Phys.* **2003**, *41*, 1009-1013.
- ⁴⁴ P. Skoglund, A. Fransson, *Polymer* **1998**, *39*, 1899-1906.
- ⁴⁵ M. de Geus, I. van der Meulen, B. Goderis, K. Vanhecke, M. Dorschu, H. van der Werff, C. E. Koning, A. Heise, *Polymer Chemistry* **2010**, *1*, 525-533.
- ⁴⁶ S. Strandman, J. E. Gautrot, X. X. Zhu, *Polym. Chem.* **2011**, *2*, 791-799.
- ⁴⁷ K. S. Bisht, L. A. Henderson, R. A. Gross, *Macromolecules* **1997**, *30*, 2705-2711.
- ⁴⁸ R. Nomura, A. Ueno, T. Endo, *Macromolecules* **1994**, *27*, 620-621.
- ⁴⁹ I. Van der Meulen, E. Gubbels, S. HUIjser, R. Sablong, C. E. Koning, A. Heise, R. Duchateau, *Macromolecules* **2011**, *44*, 4301-4305.
- ⁵⁰ Z. Ates, P. D. Thornton, A. Heise, *Polym. Chem.* **2011**, *2*, 309-312.

2. RING-OPENING COPOLYMERIZATION OF GLYCOLIDE, *rac*-LACTIDE AND ϵ -CAPROLACTONE

2.1. Introduction

Poly(lactide-*co*-glycolide) copolymers (PLGA) are among the most widely used biodegradable materials.¹ Indeed, poly(glycolide) (PGA) is a biodegradable and biocompatible polymer, however it is hydrolytically unstable, hardly processable, and too brittle for many applications. Modifications of its physical and chemical properties, such as degradation rate, have been therefore obtained by incorporation of lactide, LA, into the PGA chains.

All the practical uses of PLGAs involve their biodegradable character; consequently, the decomposition profile has to be precisely matched to the needs of application. The rate and mechanism of degradation are affected not only by environmental factors, such as temperature and pH, but also by several intrinsic parameters, such as copolymer composition and sequence of monomeric units, molecular weight and molecular-weight dispersity, polymer chain-ends, structure of copolymer.²

In detail, the copolymer ratio (LA to GA) determines the hydrophilicity of the polymer matrix since the LA is more hydrophobic and GA is more hydrophilic. Indeed, glycolide-glycolide bonds and glycolide-lactide bonds are preferentially hydrolyzed than lactide-lactide bonds.³

Moreover, the degree of crystallinity and the glass transition temperature of polymeric matrix, which depend on the above-mentioned parameters, such as copolymer composition, microstructure and molecular weight, have additional effects on degradation rate.²

On the contrary, copolymer of GA with ϵ -caprolactone (CL) have been less explored than PLGAs. However, CL could impart different hydrophilicity, elasticity, solubility, crystallization and degradation rates; copolymers of GA and CL could allow a broad variation of properties for the final obtained poly[glycolide-*co*-(ϵ -caprolactone)] (PGCA) materials.⁴ In turn, the incorporation of CL into PLGA chains, resulting into poly[(glycolide-*co*-lactide-*co*-(ϵ -caprolactone))] (PGLC) terpolymer, has been also found to be beneficial for the application of these materials in drug delivery and tissue engineering.⁵

ROP of GA, LA and CL represents the most efficient method to produce these polymers, however, it requires an appropriate catalyst to proceed in reasonable conditions and to afford polymers with controlled properties.⁶ Indeed, when a specific degradation kinetic is required, an absolute control on the polymer microstructure and monomers sequences is necessary. Therefore, there is an increasing interest in development of reproducible and controlled synthetic pathways, which allow the preparation of PLGAs with controlled microstructure, i. e. well predictable thermal and mechanical properties as well as degradation rate.

Currently, the most used initiator for the homo- and copolymerization of GA is tin octanoate, SnOct₂.⁶ However, the first systematic studies on the preparation of PLGAs copolymers by this initiator revealed that the synthesized copolymers did not show a truly random monomer distribution.^{7,8} Because of the higher reactivity of GA in comparison to LA, the copolymers initially formed were richer in GA than the monomer feed mixture. Therefore, random copolymers with a blocky microstructure were prepared. PLGAs with shorter block lengths were obtained carrying out the copolymerization at 150 °C, due to transesterification side reactions.⁹ Moreover, one drawback of the use of the SnOct₂ is the poor control of the polymerization and the scarce reproducibility of the polymerization results. As a consequence, the properties of the copolymers widely vary from batch

to batch. Furthermore, because of the blocky microstructure, the hydrolysis pattern of such copolymers involved very fast initial degradation due to hydrolysis of glycolic units, followed by a very slow degradation of the residual material, mainly lactic units.¹⁰

To overcome these limitations, two different approaches have been reported in literature, which allow the synthesis of PLGAs with a controlled microstructure. In one strategy, reported by Feng *et al.*, truly alternated poly(glycolide-*alt*-lactide) copolymers were obtained by polymerization of the monomer 3-methyl-1,4-dioxan 2,5- dione, synthesized ad hoc.¹¹ The other approach, reported by Meyer *et al.*,¹² involved the preparation of poly(lactic-*co*-glycolic acid) copolymers by condensation polymerization of preformed segments comprising high degree of sequence and stereocontrol. The work of Meyer allowed a really extensive, systematic and thorough investigation of PLGA microstructure. Remarkably, they demonstrated how the primary structure of PLGA strongly influences the degradation properties. Indeed, while PLGAs obtained by ROP of GA and LA employing SnOct₂ exhibited non-homogeneous hydrolysis pattern, due to the “blocky” microstructure, alternating PLGAs degraded with a uniform profile, the molecular weight loss was nearly linear throughout the process.¹³ Meyer and co-workers extended the same approach to the preparation of sequence-defined PGAs and PGLCs.¹⁴

Although both the above-mentioned approaches allowed the preparation of sequence-controlled copolymers,¹⁵ they are less efficient and more expensive than ROP, since they require synthetic efforts for the preparation of monomer or preformed segments. Therefore, the search for novel catalysts active in the controlled ROP of GA with LA and CL is a field of increasing academic and industrial interest.

In fact, in addition to SnOct₂, in literature several initiators have been reported for GA/LA copolymerization. Early studies include the testing of commercially available chlorides, alkoxides, oxides or sulfides of main

groups and transition metals (Sn, Al, Zr, Ti, Pd, Cd, and Zn).¹⁶ In this study only tin-based initiators were claimed to produce “random” copolymers, however the average blocks sequences were not reported. Cationic copolymerization in the presence of organic acids and salts was also investigated and non-random macromolecules with average blocks sequences higher than 2 were obtained.¹⁷ Afterward, homoleptic metal-complexes of Li and Mg,¹⁸ Al and Zn,^{9,19} Ca,²⁰ Zr,²¹ Fe,²² and Bi²³ have been also tested and produced multiblock non random copolymers.

Initiators based on Fe, Al and Zn,^{4a} Zr,^{4e-f,24} Ca,^{4d} Mg^{4h} and Bi²⁵ were also tested in the ROP of GA and CL to synthesize PGCAs. However, in the case of PGLCs, besides SnOct₂, only two other initiators were tested based on Zr^{5c,26} and Bi.^{5d}

Recently, the research group where the present project thesis has been developed reported that dimethyl(salicylaldiminato) aluminum compounds were able to efficiently catalyze the living ROP of L- and *rac*-lactide and ϵ -caprolactone, allowing the controlled synthesis of block and random copolymers in the absence of transesterification reactions.²⁷ This class of catalysts was studied for the ROP of a variety of cyclic esters,²⁸ however, it had not been used for the homo- and copolymerization of glycolide.

It was envisioned that this class of compounds could have represented also a class of suitable catalysts for the ROP of GA and for copolymerization of GA with LA and CL. Therefore, dimethyl(salicylaldiminato) aluminum compounds, with a different steric hindrance at the *ortho* position of the phenolato ring, were tested as precatalysts in the homo- and copolymerization of GA with *rac*-LA. The feasibility of random and block copolymerization was studied in different experimental conditions.

As an extension of the investigation, this class of catalysts was also tested in the ROP of GA and CL, and in the terpolymerization of GA with both CL and LA.

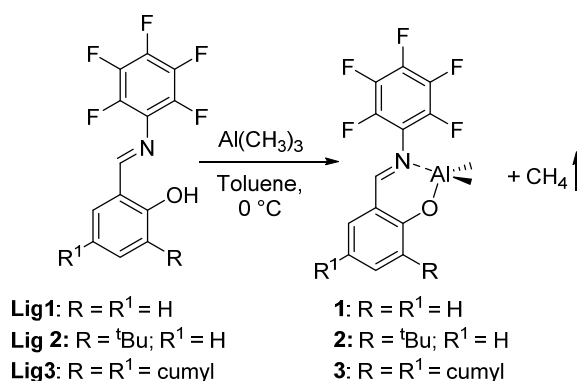
A detailed microstructural analysis of the obtained co- and terpolymers was carried out by means of NMR spectroscopy, and the effect of microstructure on thermal behavior was investigated.

2.2. Results and discussion

2.2.1. Catalysts synthesis

Dimethyl(salicylaldiminato) aluminum complexes **1-3**, bearing a different steric hindrance at the *ortho* position of the phenolato ring, were synthesized in toluene by the alkane elimination reaction between the corresponding proligand and $\text{Al}(\text{CH}_3)_3$ (Scheme 2.1). Notably, complexes **1**, **3** were never reported before. The aluminum complexes²⁹ and the corresponding proligands³⁰ were prepared according to literature procedures.

The phenoxy-imine compounds coordinate to the aluminum atom as monoanionic ligands, yielding the dimethyl compounds **1-3** (Scheme 2.1) and one equivalent of methane.



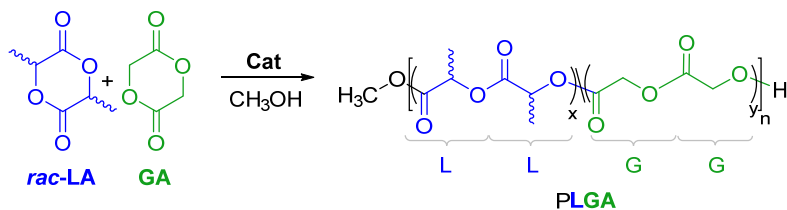
Scheme 2.1. Synthetic route for complexes **1-3**.

The synthesized complexes, **1** and **3**, were fully characterized by multinuclear NMR spectroscopy. The ¹H and ¹³C NMR spectra indicated

the formation of the desired complexes bearing one salicylaldiminato ligand and two methyl groups. In the ^1H NMR spectra sharp singlets at -0.28 ppm and -0.57 ppm, respectively for complexes **1** and **3**, were observed for the methyl protons of the $\text{Al}(\text{CH}_3)_2$. The pattern of the protons of the salicylaldiminato ligands showed significant shifts with respect to the signals of the protons of free proligands. Accordingly, the ^{19}F NMR spectra showed three signals for the ortho, meta, and para-fluorine atoms on the aromatic ring bound to the nitrogen. ^{13}C NMR characterization was coherent with these data showing; for the methyl carbons on the aluminum signals at -9.2 and -10.3 ppm, respectively for complexes **1** and **3**.

2.2.2. Homo- and copolymerization of *rac*-lactide and glycolide in bulk

The complexes **1** and **3** were tested in the ring-opening copolymerization of *rac*-LA and GA (Scheme 2.2), using methanol as cocatalyst, under several experimental conditions.



Scheme 2.2. Ring-opening copolymerization of *rac*-lactide (*rac*-LA) and glycolide (GA).

The homo- and copolymerizations of GA and *rac*-LA were first performed in bulk at 140 °C in the presence of catalysts **1** or **3** and one equivalent of methanol. The obtained polymer samples were characterized by ^1H and ^{13}C NMR spectroscopy, GPC and DSC analysis. The main results are summarized in Tables 2.1, 2.2 and 2.3.

Table 2.1. Homo- and copolymerization of glycolide and *rac*-lactide in bulk.^a

Run	Cat	f_{GA}^b	Yield (%)	F_{GA}^c	L_{GG}^d	L_{LL}^d	T_{LGL}^e	T_{GLG}^e
1	1	100	>99	100	-	-	-	-
2	1	0	76	-	-	-	-	-
3	3	100	>99	100	-	-	-	-
4	3	0	92	-	-	-	-	-
5	1	70	78	70	3.55	1.52	1.59	0.01
6	1	50	62	51	1.67	1.61	1.19	0.07
7	1	30	73	30	1.17	2.72	0.71	0.11
8	3	80	89	81	6.13	1.44	4.39	0.10
9	3	70	83	72	3.44	1.34	1.85	0.08
10	3	60	92	59	2.29	1.59	1.34	0.10
11	3	50	77	53	2.05	1.82	1.07	0.15
12	3	40	81	41	1.40	2.01	0.90	0.12
13	3	30	89	34	1.14	2.21	0.94	0.15
14	3	20	74	22	1.18	3.05	0.74	0.32

^a**Polymerization conditions:** precatalyst = 25 μ mol; MeOH = 25 μ mol (0.25 mL of a 0.1 M toluene solution); T = 140 $^{\circ}$ C; t = 75'; mol ratio of monomer(s) to precatalyst in the feed = 100.

^bMolar percentage of glycolide in the feed.

^c F_{GA} , molar percentage of glycolide in the copolymer, as determined by 1 H NMR (DMSO- d_6 , 100 $^{\circ}$ C).

^dAverage length of glycolidyl (GG) and lactydyl (LL) blocks in the copolymer; calculated from 13 C NMR (DMSO- d_6 , 100 $^{\circ}$ C).

^eYield of the second mode of transesterification (%) of glycolidyl (LGL) and lactydyl (GLG) sequences; calculated from 1 H NMR (DMSO- d_6 , 100 $^{\circ}$ C).

For both the catalysts, after 75 minutes of reaction, full conversion in the homopolymerization of glycolide was assessed; almost complete conversion of *rac*-lactide was reached in the same time (Table 2.1, runs 1-4).

The copolymerizations were performed systematically varying the comonomers ratio and the monomer/catalyst feed ratio, and almost

complete monomer conversion was reached in 75 minutes with both the catalysts. As shown in Table 2.1, the composition of the copolymers, evaluated by the ^1H NMR spectrum, parallels the feed ratio, as it would be expected for a copolymer at full conversion.

A detailed microstructural analysis was performed through inspection of the carbonyl region of the ^{13}C spectra, and by analysis of the methine region in ^1H NMR spectra.

The carbonyl regions of the ^{13}C NMR spectra (DMSO- d_6 , 100 °C) of the copolymer samples prepared with catalyst **1** with different monomers feed (Table 2.1, runs 5-7) are shown in Figure 2.1. For comparison, the ^{13}C NMR spectrum (DMSO- d_6 , 100 °C) of a poly(*rac*-lactide) prepared in the same conditions (Table 2.1, run 2) is also shown (Figure 2.1i).

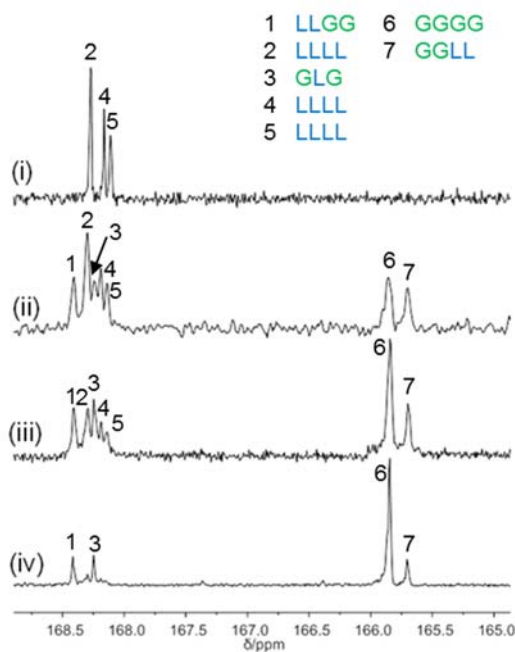


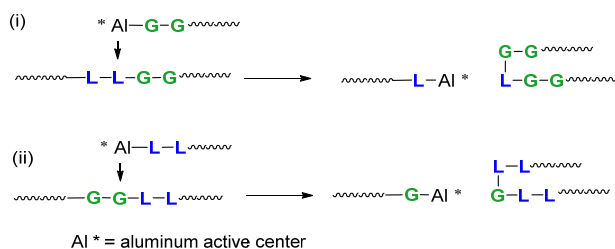
Figure 2.1. ^{13}C NMR (75 MHz, DMSO- d_6 , 100 °C) spectra in the carbonyl region of polymers obtained with complex **1**: (i) poly(*rac*-lactide) (Table 2.1, run 2); (ii) poly(glycolide-*co-rac*-lactide) $F_{\text{GA}} = 30$ (Table 2.1, run 7); (iii) poly(glycolide-*co-rac*-lactide) $F_{\text{GA}} = 51$ (Table 2.1, run 6); (iv) poly(glycolide-*co-rac*-lactide) $F_{\text{GA}} = 70$ (Table 2.1, run 5).

The chemical shifts of the carbonyl carbons are highly sensitive to their surroundings.^{4a} Providing that L and G represent respectively a lactyl –CH(CH₃)C(O)O– and a glycolyl –CH₂-C(O)O– moiety, two resonances attributable to the hetero- and homosequences centered on the carbonyl of the glycolyl (GGLL at δ 165.7 ppm and GGGG at δ 165.8 ppm) were observed, accordingly with the literature.^{9,21}

At lower field, in the region centered on the carbonyl of the lactyl group, five resonances were observed. According to a detailed microstructural analysis by NMR spectroscopy of poly(glycolide-*co*-L-lactide) reported in literature, the resonance at δ 168.4 ppm was attributed to the heterosequence LLGG, while the resonance at δ 168.2 ppm was attributed to the GLG sequence.²¹ The latter sequence cannot be formed by ring opening of LA and GA during the chain growth, but it derives from the transesterification of the second mode, during which the lactidyl and glycolidyl units undergo bond cleavage.²¹

The transesterification processes involve side reactions between the growing chain and preformed polymeric segments and, specifically, transesterifications of the second mode lead to sequences cannot be formed by ROP of GA or LA.^{6a}

Notably, the GLG sequence could be generated by a transesterification reaction involving the attack of an active glycolidyl chain end –GGAl* on a preformed LLGG sequence (Scheme 2.3i).



Scheme 2.3. Transesterification processes of the second mode occurring during the copolymerization.

The remaining three resonances (at δ 168.3, 168.15, 168.1 ppm) are attributable to the different stereochemical combination of the atactic LLLL homosequence (Figure 2.1).³¹ Indeed, the same resonances appeared in the ^{13}C NMR spectrum (DMSO- d_6) of the poly(*rac*-lactide) homopolymer prepared with the same catalyst (Figure 2.1i).

The average lengths of glycolidyl and lactidyl blocks (L_{GG} and L_{LL}) were calculated by using previously reported equations.^{8,17} The so-calculated lengths were also confirmed by using as control the monomers composition ratio ($F_{\text{GA}}/F_{\text{LA}}$) evaluated by ^1H NMR.¹⁷

The average block lengths linearly depend on the copolymer composition ratio as shown in Figure 2.2. Interestingly, with catalyst **3** the L_{GG} and L_{LL} values were close to the value of 2 (Table 2.1, run 11), as it is expected for a random copolymer in the case of a 50 to 50 monomer feed composition.³² The copolymers microstructure could be easily tuned by adjusting the feed.

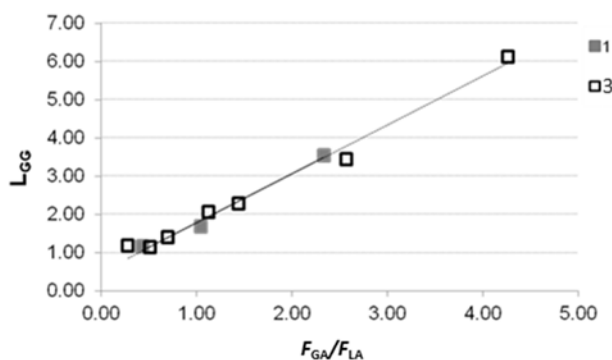


Figure 2.2. Plot of average length of glycolidyl (GG) blocks vs copolymer composition ratio (G/L) for the copolymers obtained with complexes **1** and **3** (Table 2.1, runs 5-7 and 8-14).

More information on the copolymers microstructures can be derived from the ^1H NMR spectra in the methylene region. Signals at 4.83 ppm were attributed, according to the literature, to the presence of LGL sequences.⁹ In details, the LGL sequence is generated when an active lactidyl chain end attacks a preformed glycolidyl segment (Scheme 2.3ii).

The amount of transesterification sequences LGL and GLG (see above) were evaluated by using the coefficients of the second mode of transesterification, T_{LGL} and T_{GLG} , as previously reported.^{9,21} According to the definitions, the T_{LGL} and T_{GLG} values are close to 1 when the contribution of glycolyl and lactyl units in the chain are close to Bernoulian statistics, while they are higher than 1 when longer alternate sequences are present in the chains.²¹

The T_{LGL} values increase by increasing the amount of glycolide in the feed, and values higher than 1 are calculated for the copolymers obtained when the molar percentage of glycolide in the feed is higher than 50%. For both catalysts, T_{LGL} values are higher than T_{GLG} ones of one order of magnitude, thus indicating that the transesterification reaction involving the attack of active lactidyl chain end on preformed glycolidyl segments is preferred (Scheme 2.3ii). This behavior is definitely in contrast with previous results obtained with the classical $\text{Sn}(\text{Oct})_2$ catalyst, and with $\text{Zr}(\text{acac})_2$ ²¹ or Fe based catalysts,²² where T_{GLG} values were higher than T_{LGL} ones.

This feature can be tentatively explained taking into account that in the homopolymerization of *rac*-LA by this class of aluminium catalysts, transesterification reactions are completely absent.²⁷ It is therefore confirmed that the tendency of these complexes to break the lactidyl unit into two lactyl fragments is low.

Overall, the two initiators showed roughly analogous behavior in the polymerization performed in bulk. An accurate analysis of the copolymerization results, however, showed that transesterifications of the second mode were slightly higher for catalyst **3**, bearing a bulky cumyl groups as *ortho*-phenoxy substituents. Probably the steric hindrance of this group could have an influence on the relative rate of chain propagation and transesterification reaction.

The final microstructure of copolymer chain should reasonably result from the reactivity of comonomers as well as transesterification processes taking

place together with the main copolymerization reaction. In particular, the main transesterification process operating in this system is involving the attack of active lactidyl chain end on preformed glycolidyl segments.

2.2.2.1. End groups analysis by NMR of poly(*rac*-lactide-co-glycolide)s prepared in bulk

In order to get more information on the mechanism involved in these copolymerization reactions an accurate end group analysis was carried out by ^1H NMR spectroscopy (DMSO- d_6 , 100 °C). For this purpose, low molecular weight copolymer samples were prepared by conversion of 20 equivalents of each monomer. The assignment of the different end groups was made by comparison with the spectra of the homopolymer samples (Figures 2.3i and 2.3ii) and some literature data.¹¹

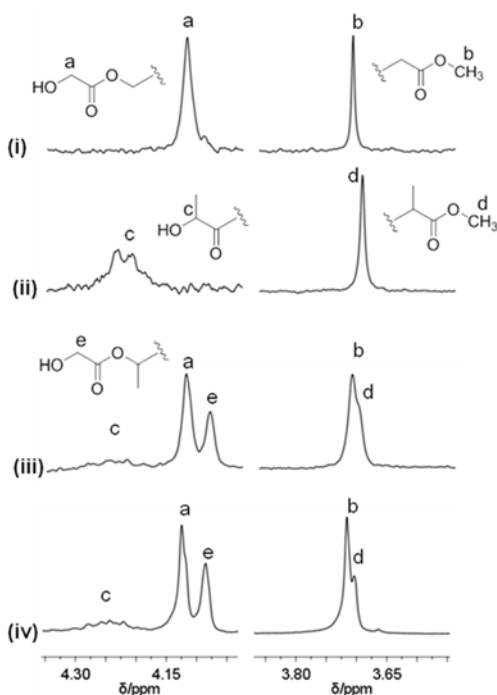
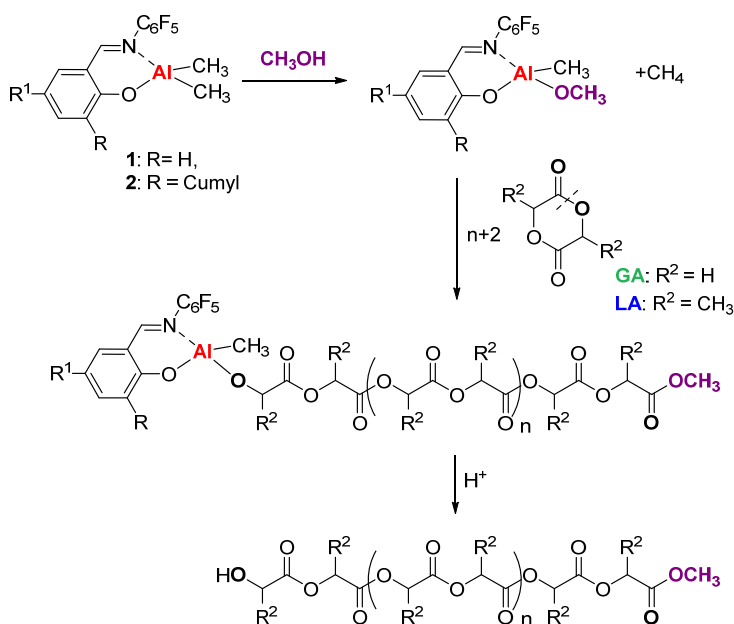


Figure 2.3. ^1H NMR (300 MHz, DMSO- d_6 , 100 °C) spectra of: (i) poly(glycolide) obtained with complex **1** (Table 2.1, run 1); (ii) poly(*rac*-lactide) obtained with complex **1** (Table 2.1, run 2); (iii) poly(glycolide-co-*rac*-lactide) obtained with

complex **1** (Table 2.2, run 15); (iv) poly(glycolide-*co-rac*-lactide) obtained with complex **3** (Table 2.2, run 16).

Easily recognizable were the singlets due to the terminal alkoxide OCH_3 group: the signals at 3.72 and 3.70 ppm were assigned respectively to the $-\text{CH}_2\text{C}(=\text{O})-\text{OCH}_3$ (G- OCH_3 ; **b**) and to the $-\text{CH}(\text{CH}_3)\text{C}(=\text{O})-\text{OCH}_3$ (L- OCH_3 ; **d**) end groups in the copolymers (Figures 2.3iii and 2.3iv) by comparison with the homopolymers spectra (Figures 2.3i and 2.3ii). The presence of both signals indicated that the first step of these copolymerization reactions can be the insertion of either glycolide unit or lactide unit into the $\text{Al}-\text{OCH}_3$ bond. Although the partial overlapping of these signals did not permit an exact estimation of their relative abundance, it is possible to claim that, for both complexes, the preferred first step is the insertion of the glycolide monomer into the $\text{Al}-\text{OCH}_3$ bond (Scheme 2.4). This is in agreement with the higher reactivity of this monomer with respect to that of lactide. Moreover, the observed preference is more significant with catalyst **3** (Figure 2.3iv) suggesting a stronger discrimination in favour of the less hindered monomer by the most encumbered complex.



Scheme 2.4. Mechanism of polymerization.

The hydroxyl end groups, such as HOCH₂C(O)OCH₂- (HOGG-; **a**) and the HOCH₂C(O)OCH(CH₃)- (HOGL-; **e**) respectively at 4.13 ppm and 4.09 ppm (Figures 2.3iii and 2.3iv), are reasonably generated by hydrolysis of the growing chain. Interestingly, the latter may only derive from transesterification reactions generating the LGL sequence (Scheme 2.3ii). As a matter of fact, this kind of transesterifications was the most abundant for the explored aluminum catalysts (see above).

Accordingly, signals due to the hydroxyl end groups bound to a lactyl unit (HOL-; **c**) in the range 4.23-4.18 ppm, showed low intensity (Figure 2.3). This result may be rationalized taking into account that the Al-lactidyl active centers, from which these end groups can be generated, are the most involved in the transesterification reactions.

The whole picture suggests that a coordination-insertion mechanism, proceeding through acyl-oxygen cleavage of both the monomers, should be operative in these systems (Scheme 2.4). Moreover, the occurrence of the

different transesterification reactions with the relative frequencies detailed above well explain the relative ratio of the observed end groups.

2.2.2.2. Determination of molecular weight of poly(*rac*-lactide-co-glycolide)s prepared in bulk

The molecular weights of PLGAs prepared in bulk were evaluated by Gel Permeation Chromatography (GPC) and by NMR, being known the end group signals (see above). Representative results are reported in Table 2.2.

Table 2.2. Homo- and copolymerization of glycolide and *rac*-lactide in bulk: molecular weights and molecular-weight dispersities.^a

Run	Cat	F_{GA}^b	$M_{n,th}$ (kDa) ^c	$M_{n,NMR}$ (kDa) ^d	$M_{n,GPC}$ (kDa) ^e	M_w/M_n^e
2	1	0 ^f	11.0	8.9	11.4 ^{g,h}	1.6g
4	3	0 ^f	13.9	13.9	12.2 ^{g,h}	1.5g
5	1	70	12.2	9.2	24.8	2.4
6	1	51	12.7	9.4	41.3	2.2
7	1	30	8.9	15.4	49.6	1.9
8	3	81	11.7	10.7	14.1	1.3
10	3	59	12.0	8.3	17.0	1.4
13	3	34	12.2	7.3	8.0	1.3
14	3	22	12.2	8.1	46.0	1.8
15 ⁱ	1	50	5.2	4.3	3.7 ^g	2.0 ^g
16 ⁱ	3	55	5.2	5.5	7.1 ^g	1.4 ^g
17 ^j	1	53	34.1	27.2	27.8	1.6
18 ^j	3	53	32.7	19.0	38.8	2.0

^a**Polymerization conditions:** precatalyst = 25 μ mol; MeOH = 25 μ mol (0.25 mL of a 0.1 M toluene solution); T = 140 °C; t = 75'; mol ratio of monomer(s) to precatalyst in the feed =100.

^b F_{GA} , content of glycolide in the copolymer (mol %), as determined by ¹H NMR (DMSO-*d*₆, 100 °C).

^cTheoretical molecular weight.

^dMolecular weight determined by ¹H NMR.

^eMolecular weights and polydispersivities determined by gel permeation chromatography (GPC) vs. polystyrene standards, elution solvent mixture: chloroform/ HFIP 99/1.

^fPoly(*rac*-LA).

^gElution solvent: tetrahydrofuran (THF).

^hMolecular weights of poly(*rac*-lactide) have been corrected by a 0.58 factor.

ⁱThe mol ratio of monomer(s) to precatalyst in the feed =40.

^jThe mol ratio of monomer(s) to precatalyst in the feed =300.

The molecular weight of the poly(*rac*-lactide)s obtained in bulk were evaluated by GPC vs. polystyrene standards, using THF as elution solvent, corrected by a factor of 0.58,³³ resulted $M_{n, \text{GPC}} = 11.4$ for run 2 and 12.2 kDa for run 4. Monomodal molecular weight distributions were observed. A good agreement with both the molecular weight evaluated by NMR, $M_{n, \text{NMR}}$, and the theoretical molecular weight, $M_{n, \text{th}}$, calculated by the monomer/catalyst feed ratio was observed.

On the contrary the assessment of the molecular weights for PGA homopolymers (Table 2.1, runs 1 and 3) was not possible by either GPC or NMR analysis, since the polymer is insoluble in most of the organic solvents.^{4a}

The determination of the molecular weights of the PLGAs samples was performed by GPC in a chloroform/HFIP 99/1 solvents mixture. Low molecular weight samples, prepared by a lower monomer/initiator feed ratio, dissolved even in THF, therefore in these cases the GPC analysis was performed by using THF as eluent.

As previously underlined in the literature, the radius of gyration R_g of the PLGA samples is extremely sequence and solvent dependent,¹² thus the values obtained by GPC should be regarded with special care. However, the GPC analysis performed on all the samples disclosed monomodal molecular weight distributions with variable molecular-weight dispersities (1.3-2.4). Interestingly, the molecular weights evaluated by NMR are in reasonable agreement with the theoretical molecular weight, $M_{n, \text{th}}$, obviously indicating that the molecular weight could be tuned by adjusting the monomer/catalyst feed ratio.

2.2.2.3 Thermal characterization of poly(glycolide-co-*rac*-lactide)s prepared in bulk

Thermal analysis of the copolymers was carried out by means of differential scanning calorimetry (DSC), from - 20 to + 260 °C. The glass transition temperature, T_g , and the melting temperature, T_m , are given in Table 2.3. Values are reported for the second heating cycle and the heating rate is 10 °C min⁻¹.

Table 2.3. Homo- and copolymerization of glycolide and *rac*-lactide in bulk: thermal properties.^a

Run	Cat	f_{GA}^b	F_{GA}^c	T_g (°C) ^d	T_m (°C) ^d	ΔH_m (J g ⁻¹) ^d
3	3	100	100	n.o.	222.6	83.8
4 ^e	3	0	0	48.3	n.o.	n.o.
5	1	70	70	43.5	n.o.	n.o.
6	1	50	51	47.2	n.o.	n.o.
7	1	30	30	49.2	n.o.	n.o.
8	3	80	81	41.2	201.3	50.3
10	3	60	59	40.7	n.o.	n.o.
12	3	40	41	45.8	n.o.	n.o.
14	3	20	22	51.4	n.o.	n.o.

^a**Polymerization conditions:** precatalyst = 25 μmol; MeOH = 25 μmol (0.25 mL of a 0.1 M toluene solution); T = 140 °C; t = 75'; mol ratio of monomer(s) to precatalyst in the feed = 100.

^b f_{GA} , molar percentage of glycolide in the feed.

^c F_{GA} , content of glycolide in the copolymer (mol %), as determined by ¹H NMR (DMSO-*d*₆, 100 °C).

^dValues reported for the second heating cycle.

^e F_{LA} = 100.

n.o. = not observed.

In Figure 2.4 are shown the thermograms of the PGA and of PLGA samples obtained with catalyst **3**. The thermogram of the PGA displays a melting peak at 226 °C, with endotherm of fusion of 83.8 Jg⁻¹ (Figure 2.4i). The T_g

of PGA was not observed with our analytical settings in agreement with the thermal behavior of PGA with analogous molecular weight.³⁴

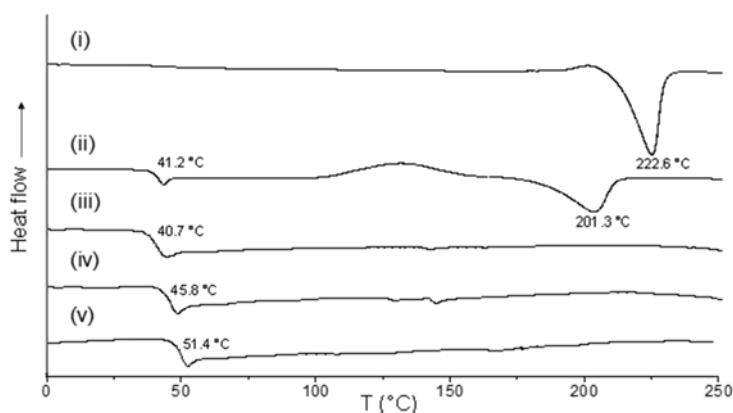


Figure 2.4. DSC thermograms (run II) of poly(glycolide-*co-rac*-lactide) obtained with complex 3: (i) $F_{GA} = 100$ (Table 3, run 3); (ii) $F_{GA} = 81$ (Table 2.3, run 8); (iii) $F_{GA} = 59$ (Table 2.3, run 10); (iv) $F_{GA} = 41$ (Table 2.3, run 12); (v) $F_{GA} = 22$ (Table 2.3, run 14).

All the copolymers were amorphous, apart from the sample prepared with 80 mol % of GA (Table 2.3, run 8; Figure 2.4); in this case a melting peak, with a T_m of 201.3 °C can be seen in the thermogram. This observation is in agreement with previously reported cases of PLGAs with a content of glycolide of 80 mol % or higher.^{7,21,22}

The DSC thermograms recorded during the second scan for all the samples displayed a unique glass transition temperature with values intermediate between those of the pure homopolymers and changing as a function of the composition. The experimental T_g values linearly increase by decreasing the GA content in the copolymer (Figures 2.4), which in turn reflects the feed composition.

2.2.3. Copolymerization of *rac*-lactide and glycolide in solution

Copolymerization of GA and *rac*-LA were also performed in solution. In order to elucidate the influence of the reaction conditions on yield, molecular weights and composition and microstructure of copolyesters, the following experimental parameters were systematically varied: i) nature of the catalyst, ii) nature of the solvent, iii) temperature, and iv) reaction time. In all the cases equimolar amounts of the two monomers were used.

The obtained polymeric samples were characterized by ^1H and ^{13}C NMR, GPC and DSC analysis. The main results are summarized in Tables 2.4 and 2.5.

Table 2.4. Copolymerization of *rac*-lactide and glycolide promoted by complexes 1-3 in solution.^a

Run	Cat	Solvent	T (°C)	Yield (%)	F_{GA}^b	L_{GG}^c	L_{LL}^c	T_{LGL}^d	T_{GLG}^d
1	1	Toluene	90	45	99	n.d.	n.d.	n.o.	n.o.
2	1	chlorobenzene	90	68	72	5.91	2.32	0.28	0.05
3	1	chlorobenzene	120	66	54	2.94	2.50	0.63	n.o.
4	1	Xylenes	90	43	90	7.23	0.80	n.o.	0.94
5	1	Xylenes	130	66	59	2.96	2.06	0.73	0.13
6	3	Toluene	90	41	89	n.d.	n.d.	n.o.	n.o.
7	3	chlorobenzene	120	67	66	2.75	1.32	1.39	0.08
8	3	Xylenes	130	79	49	1.94	2.02	0.95	0.09

^a**Polymerization conditions:** precatalyst = 25 μmol ; MeOH = 25 μmol (0.25 mL of a 0.1 M toluene solution); solvent = 5 mL; glycolide = 2.50 mmol, *rac*-lactide = 2.50 mmol, $t = 180'$.

^b F_{GA} , content of glycolide in copolymer (mol %), as determined by ^1H NMR ($\text{DMSO-}d_6$, 100 °C).

^cAverage sequences length of glicolidyl (GG) and lactidyl (LL) blocks in the copolymer; as calculated by ¹³C NMR (DMSO-*d*₆, 100 °C).

^dYield of the second mode of transesterification (%) of glycolidyl (LGL) and lactydydyl (GLG) sequences; calculated from ¹H NMR (DMSO-*d*₆, 100 °C).

n.d. = not determined; n.o. = not observed.

Carrying out the polymerization experiments in toluene at 90 °C, only polyglycolide was obtained with catalyst **1** (Table 2.4, run 1), while a copolymer with a GA content of 89 % was obtained with catalyst **3** (Table 2.4, run 6) in agreement with its higher reactivity. Then, two solvents of different polarity, chlorobenzene and xylenes, were chosen as reaction medium. The reactions performed at 90 °C, using catalyst **1**, afforded copolymers with higher incorporation of glycolide and very long glycolide sequences (Table 2.4, runs 2 and 4). When the polymerizations were conducted at higher temperatures (120 or 130°C) with both catalysts (Table 2.4, runs 3, 5, 7 and 8) polymeric samples with a glycolide content ranging between 49 and 66% were obtained showing that, in these experimental conditions, comparable incorporation of both monomers was obtained.

The randomness of these copolymers was assessed by the calculation of the block lengths of *rac*-LA and GA within the copolymer chain, while the occurrence of the second mode of transesterification was quantified by analysis of the signals due to the GLG and LGL groups in the NMR spectra of the copolymers.^{9,21}

For copolymers produced by complex **1** in the two different solvents, the average block lengths were higher than 2 (Table 2.4, runs 3 and 5), indicating a non-random copolymer chain. DSC analysis of these samples obtained by complex **1** showed two *T_g* values (Table 2.5, runs 3, 5). Melting endotherm of glycolide blocks crystalline phase was observed for the copolymer obtained in run 21, whereas the sample obtained in run 23 should have shorter glycolide blocks in agreement with the presence of the GLG sequences. The whole picture is compatible with the formation of copolymer samples with a blocky structure showing a first sequence

comprising glycolidyl blocks separated by short lactyl and lactidyl groups and a second part of the chain with a complementary distribution of the two monomers.

Copolymers obtained by complex **3** showed lower L_{GG} and L_{LL} values, and higher second mode of transesterification values (Table 2.4, runs 7, 8). In particular, average lactide and glycolide block lengths for the copolymer obtained in run 8 was close to 2, the value expected for a completely random copolymer. Accordingly, these samples displayed unique glass transition temperature (Table 2.5, runs 7, 8), as observed in the copolymerizations performed in bulk (see above).

To get more insights on the copolymerization behavior of catalyst **3**, the effect of the polymerization time was studied. A polymerization run was performed in the same condition ($f_{GA} = 50$) than run 6 in Table 2.4, but for shorter reaction time (0.5 h). Comparison of the two products showed that in the beginning of the polymerization the L_{GG} (2.95) were higher than L_{LL} (0.89), thus indicating that glycolide was polymerized first ($F_{GA} = 70$). At higher conversion the L_{GG} and L_{LL} values were close to 2, as expected for a random copolymer. Thus, the transesterification reactions, taking place during the polymerizations, are mainly responsible of the random structure. End group analysis performed by ^1H NMR spectroscopy on the obtained copolymers showed polymer chains end-capped with a methyl ester and a hydroxyl group.

Table 2.5. Molecular weights characterization and thermal analysis of PLGA prepared with complexes **1**, **3** in solution.^a

run	$M_{n,th}$ (kDa) ^b	$M_{n,NMR}$ (kDa) ^c	$M_{n,GPC}$ (kDa) ^d	M_w/M_n GPC ^d	T_g (°C) ^e	T_m (°C) ^e	ΔH_m (J g ⁻¹) ^e
3	21.4	22.3	79.7	1.3	41.3; 51.1	199.0	36.7
5	23.6	22.8	84.9	1.3	42.0; 52.7	n.o.	n.o.
7	21.0	14.9	19.9	1.3	42.7	187.7	6.9
8	26.0	21.4	n.d.	n.d.	45.9	n.o.	n.o.

^aGeneral conditions: precatalyst = 25 μmol ; MeOH = 25 μmol (0.25 mL of a 0.1 M toluene solution); solvent = 5 mL; glycolide, 2.50 mmol, *rac*-lactide = 2.50 mmol; $t = 180^\circ$.

^bTheoretical molecular weight.

^cMolecular weight determined by ^1H NMR (DMSO-*d*₆, 100 $^\circ\text{C}$).

^dDetermined by gel permeation chromatography (GPC) vs. polystyrene standards, elution solvent mixture: chloroform/HFIP 99/1.

^eValues reported for the second heating cycle.

n.d. = not determined; n.o. = not observed.

The molecular weights of the polymers were evaluated by GPC in chloroform/HFIP 99/1 solvents mixture. As discussed above, GPC analysis is not reliable for the assessment of the real molecular weight of the glycolide/lactide copolymers. Nevertheless, the GPC results indicated narrow molecular-weight dispersities ($M_w/M_n = 1.3$), with values inferior than those of the copolymers prepared in bulk ($M_w/M_n = 1.3$ - 2.4; see Table 2.2). Molecular weights calculated from ^1H NMR spectra are in good agreement with the theoretical values for the samples obtained with catalyst **1**, while they are lower for the samples obtained with catalyst **3**. This could be the result of the transesterification reactions, that are predominant with catalyst **3**.

2.2.4. Block copolymerization of *rac*-lactide and glycolide

The synthesis of block copolymers was attempted by using catalyst **1** in xylenes at 130 $^\circ\text{C}$. The block copolymer was obtained by sequential addition of the two monomers, polymerizing first the *rac*-LA. After 4.5 h an aliquot was withdrawn from the reaction mixture to assess the molecular weight of the poly(lactide) block by NMR (2.5 kDa). The addition of the GA to the mixture yielded the product in 10 minutes, and the precipitated polymer was analyzed by NMR (Figure 2.5).

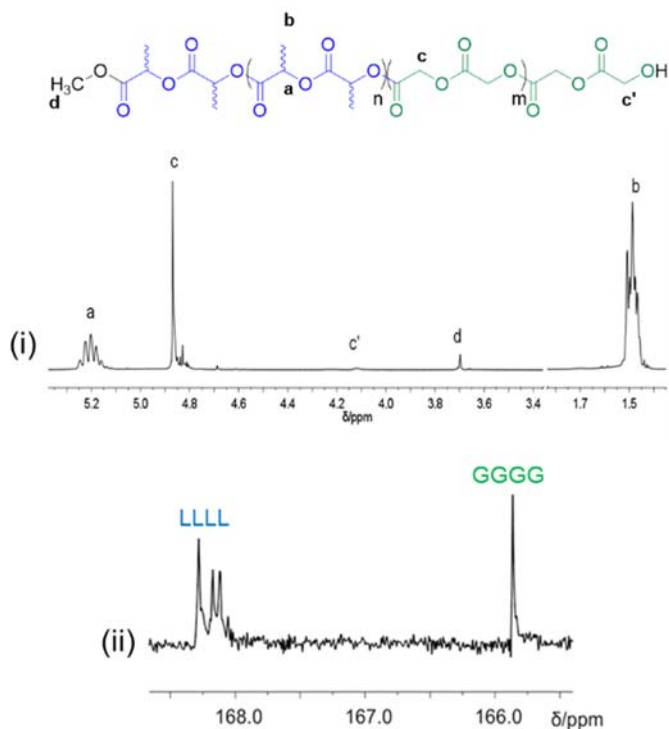


Figure 2.5. ^1H NMR (300 MHz, $\text{dmsO}-d_6$, 100 °C) (i) and carbonyl region of ^{13}C NMR (300 MHz, $\text{dmsO}-d_6$, 100 °C) (ii) of poly(*rac*-lactide)-block-poly(glycolide).

The ^1H NMR analysis of the copolymer confirmed the reflection of the feed in the monomer composition in the copolymer (Figure 2.5i). End group analysis showed the exclusive presence of end groups LLOCH_3 at 4.23 ppm (**d**), derived from the insertion step of the *rac*-lactide monomer into the $\text{Al}-\text{OCH}_3$ bond, and the HOGG - end group at 3.70 ppm (**c'**), generated by hydrolysis of the growing poly(glycolide) block.

The ^{13}C NMR analysis showed the exclusive presence of the carbonyl signals attributed to the homosequences LLLL and GGGG (Figure 2.5ii). Signals due to transesterification processes were negligible. The lengths of the glycolidyl and lactidyl blocks were determined by evaluation of the integrals of the main signals, and were found to be as follows: $L_{\text{GG}} = 15$; $L_{\text{LL}} = 31$.

Formation of the poly(*rac*-lactide)-*block*-poly(glycolide) copolymer was definitely proved by DOSY NMR experiment (Figure 2.6). This experiment, indeed, providing diffusion coefficients of molecules related to hydrodynamic radius and molecular weight, is becoming a very powerful tool in investigating polymer properties.³⁵

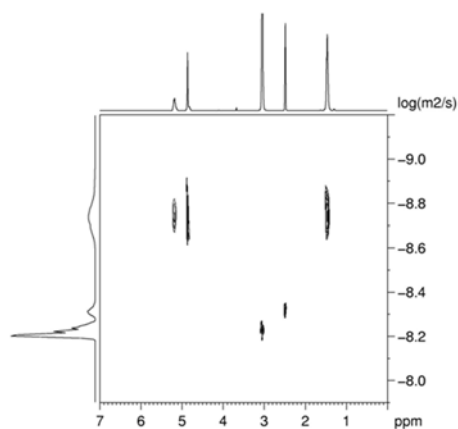


Figure 2.6. 2D DOSY NMR (400 MHz, DMSO-*d*₆, 80 °C) of the block copolymer obtained with compound **1**. Signals at 2.50 and 3.06 ppm are relative to the deuterated solvent (DMSO-*d*₆) and adventitious water, respectively.

In our case, the DOSY spectrum of the sample obtained by the block copolymerization reaction showed that the multiplets of the poly(*rac*-lactide) block (centered at 5.20 and 1.49 ppm) and the singlet of the poly(glycolide) block (at 4.87 ppm) lied at the same diffusion coefficient, and therefore belonged to the same polymeric chains.

The molecular weight estimated by NMR was found to be close to the theoretical one ($M_{n,NMR} = 3.7$ kDa vs $M_{n,th} = 3.1$ kDa). DSC analysis evidenced the presence of only one T_g at 45.4 °C, attributable to the *rac*-lactide block, while no T_g was observed for the homo-glycolide block, as observed above for the poly(glycolide) (Figure 2.4a; Table 2.3, run 3).

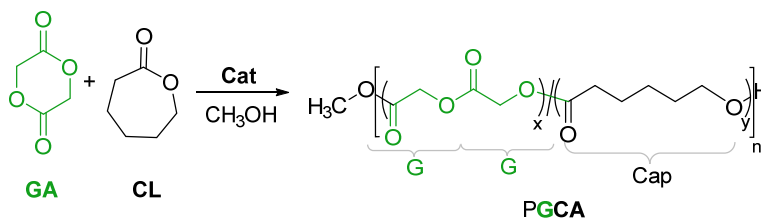
Thus, the sequential addition of the two monomers leads to the achievement of a poly(*rac*-lactide)-*block*-poly(glycolide) copolymer, which represents

an experimental evidence of the tendentially *living* behavior of the polymerization promoted by this class of initiators.

It was found, moreover, that, in order to obtain the block copolymer, glycolide had to be added to living PLA chains. The opposite sequence of monomers addition led mainly to poly(glycolide) and a low amount of the block copolymer. The importance of the order of the monomer addition in the block copolymerization was previously underlined in the literature.³⁶

2.2.5. Copolymerization of glycolide and ϵ -caprolactone

The aluminum complexes **1-3** were tested as precatalysts in the ring-opening copolymerization of glycolide and ϵ -caprolactone in the presence of one equivalent of methanol, in bulk at 140 °C (Scheme 2.5).



Scheme 2.5. Copolymerization of glycolide and ϵ -caprolactone.

The polymeric samples were fully characterized by ¹H and ¹³C NMR, GPC and DSC analysis. The main results are reported in Tables 2.6-2.8.

Table 2.6. Copolymerization of glycolide and ϵ -caprolactone in bulk at 140 °C.^a

Run	Cat	f_{GA}^b	Yield (%)	F_{GA}^c	L_{GG}^d	L_{Cap}^d	T_{II}^e
1	1	70	85	57 (77 ^f)	2.01	1.52	0.66
2	1	50	83	40	1.15	1.73	0.86
3	1	30	87	32	0.76	1.62	0.97
4	2	70	94	62 (73 ^f)	2.66	1.63	0.20
5	2	50	76	50	1.90	1.90	0.31

5bis ^g	2	50	96	50	1.55	1.56	0.75
6	2	30	90	28	0.81	2.07	2.11
7	3	70	82	70 (80 ^f)	3.36	1.44	0.14
8	3	50	93	52	1.65	1.52	0.36
9	3	30	82	24	0.63	2.01	0.90
10 ^h	2	33	96	33	1.02	2.08	1.43

^aPolymerization conditions: precatalyst = 12 μ mol; MeOH = 12 μ mol (0.12 mL of a 0.1 M toluene solution); T = 140 °C; t = 75 min; mol ratio of monomers to precatalyst in the feed = 200.

^b f_{GA} , molar percentage of glycolide in the feed. ^c F_{GA} , content of glycolide (% mol) in the copolymer, as determined by ¹H NMR (DMSO-*d*₆, 100 °C).

^dAverage length of glycolidyl (GG) and caproyl (Cap) blocks in the copolymer; calculated from ¹H NMR (DMSO-*d*₆, 100 °C).

^eYield of the second mode of transesterification (% CapGCap) of the glycolidyl sequences; calculated from ¹H NMR (DMSO-*d*₆, 100 °C).

^fCalculated from ¹H NMR (CDCl₃/TFA 1/1, RT) data of monomers conversion. TFA = 2,2,2-trifluoroacetic acid.

^gSame conditions as run 5, but t = 150 min.

^hPolymerization conditions: precatalyst = 25 μ mol; MeOH = 25 μ mol; T = 140 °C; t = 7 hours; mol ratio of monomers to precatalyst in the feed = 900.

Characterization of the polymers microstructure was attained by ¹H NMR analysis, according to the literature.^{4c} In Figure 2.7 the methylene regions of the ¹H NMR spectra of the PGCA's obtained with initiator **3** at different composition are reported. The signals (1-7) in the glycolide methylene region were attributed to one homosequence and eight different heterosequences (*vide infra*); the two triplets in the caprolactone ϵ -methylene region were attributed to two diads (one homo- and one heterosequence).

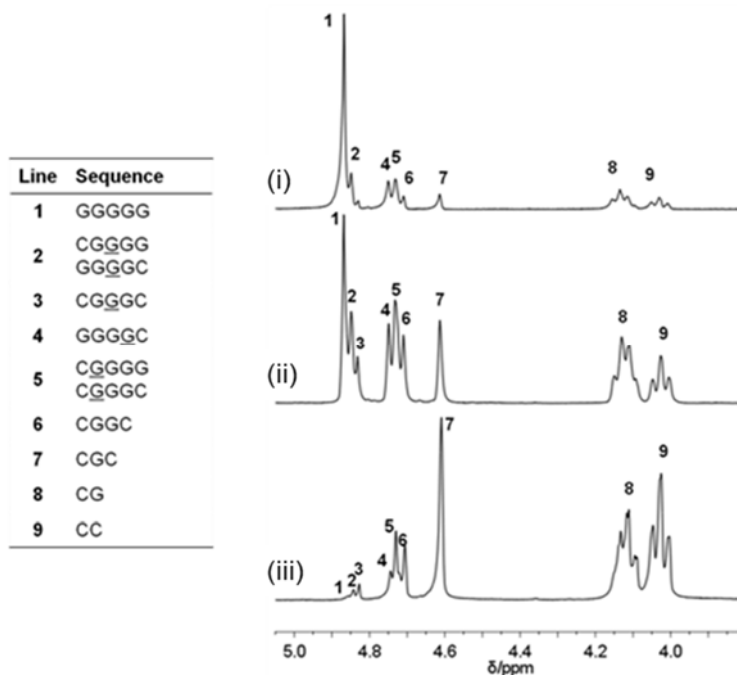


Figure 2.7. ^1H NMR (300 MHz, $\text{DMSO-}d_6$, $100\text{ }^\circ\text{C}$) spectra in the methylene region of PGCA copolymers obtained with complex **3**: (i) $F_{\text{GA}} = 70$ (Table 2.6, run 7), (ii) $F_{\text{GA}} = 52$ (Table 2.6, run 8), (iii) $F_{\text{GA}} = 24$ (Table 2.6, run 9).

The copolymers compositions were evaluated by these data. However, since the solubility of PGCA having high amount of glycolide is very poor, when the monomer feed is 70% in glycolide, the NMR analysis in $\text{DMSO-}d_6$ highlights a glycolide content lower than expected. However, the glycolide content calculated from conversion data is more in line with the feed, thus evidencing the presence of insoluble fraction.

The average lengths of glycolidyl (GG) and caproyl (Cap) blocks (namely L_{GG} and L_{Cap} , respectively) of the copolymers obtained with catalysts **1-3** were calculated from ^1H NMR data, according to literature formulas.³⁷ Confirmation of the glycolide lengths was achieved by using as control the monomers composition ratio ($F_{\text{GA}}/F_{\text{Cap}}$).^{4c} Nicely, glycolidyl block lengths linearly increase by increasing the incorporation of GA into the copolymer (Figure 2.8).

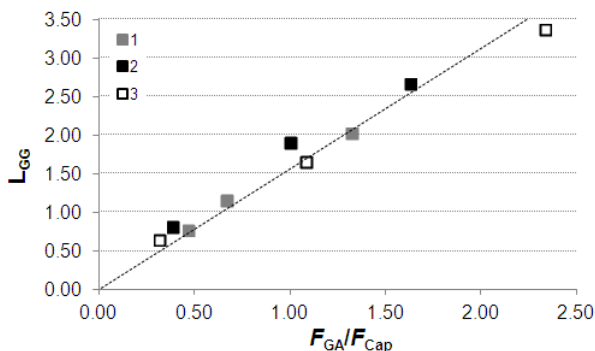


Figure 2.8. Plot of average length of glycolidyl (L_{GG}) blocks vs copolymer composition (F_{GA}/F_{Cap}) for the copolymers obtained with catalysts **1-3** at 140 °C (Table 2.6, runs 1-9).

While for any given feed composition, the L_{Cap} values do not differ significantly, being in the range of 1.44 to 2.07, the L_{GG} glycolidyl blocks lengths vary depending both on the feed and on the catalyst. When the feed is enriched in CL ($f_{GA} = 30$) the GA content in the copolymer slightly decreases by increasing the steric bulk on the catalyst. The L_{GG} values are lower than 1 for all the catalysts, indicating the cleavage of the glycolidyl blocks into glycolyl units, as also observed with other catalysts.^{3c,4c} This behaviour is clearly shown in the 1H NMR spectra of Figure 2.7. While for the $f_{GA} = 70$ copolymers (Figure 2.7i) there is the predominance of the GGGGG pentad (line 1), for the $f_{GA} = 30$ copolymers (Figure 2.7ii) this pentad is almost completely absent in favour of the CapGCap line (line 7). The latter cannot be formed by the ROP of GA, but can derive from a transesterification reaction of the second mode, involving the attack of an active ϵ -caproyl chain end on the preformed -CapGG- sequence.^{4a} The yield of this transesterification process, T_{II} , was calculated by using literature formula.^{4f}

At $f_{GA} = 50$, catalyst **1** incorporates only 40 % of the GA into the polymeric chains, while catalysts **2** and **3** have similar values of F_{GA} (50 and 52) and T_{II} (0.31 and 0.36). The L_{GG} values are below 2 (1.15-1.90), indicating

random materials, and the presence of CapGCap sequences. A polymerization test was performed in identical conditions of run 5, but increasing the polymerization time, to allow the system to reach almost full conversion (Table 2.6, run 5bis). An increase of the transesterification yield was noticed, while the L_{GG} and L_{Cap} decrease and become close to 1.5.

When the feed is enriched in glycolide ($f_{GA} = 70$), the polymeric samples are not completely soluble in DMSO. Thus, the NMR analysis take into account only the soluble fraction (see above).

A copolymerization test was performed by increasing the monomers/Al molar ratio to 900/1 (run 10). Higher M_n was obtained (*vide ultra*), while no significant effect on the polymer microstructure was noticed, thus proving the ability of the catalytic systems to produce high molecular weight polymers.

To get more insight on the origin of the copolymer microstructure, the analysis of end groups of the obtained materials was carried out by ^1H NMR in $\text{DMSO-}d_6$ at 100 °C (Figure 2.9). The resonances were assigned by comparison with the spectra of homopolymer samples, synthesized in the same experimental conditions. The three singlets at 3.71, 3.70 and 3.60 ppm were attributed to the GGGG-OCH₃ (**a**), CapGG-OCH₃ (**d**) and Cap-OCH₃ (**b**) end groups, respectively, generated by the insertion of the monomer into the Al-OCH₃ bond, formed by reaction of the aluminum dimethyl complex with methanol. The relative abundance of the signals suggests a predominance of the GA insertion with respect to the CL insertion. The triplet at 3.42 ppm is attributed to the hydroxyl end group bound to a caproyl unit HOCap- (**c**), and it is generated by hydrolysis of the polymeric chain. The hydroxyl end group of the glycolide-capped polymeric chains (HOGG-), which is expected at 4.13 ppm, could not be identified, since it may be overlapped with the signal of ϵ -caprolactone heterosequences.

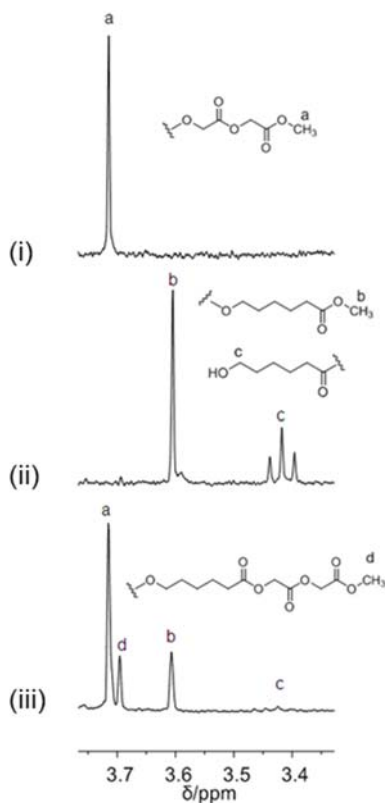


Figure 2.9. End groups analysis: ^1H NMR (300 MHz, $\text{DMSO-}d_6$, 100 $^\circ\text{C}$) spectra of: (i) poly(glycolide); (ii) poly(ϵ -caprolactone); (iii) poly(glycolide-*co*- ϵ -caprolactone) (Table 2.6, run 5).

The above data, together with the analysis of the copolymer microstructure, provides a clear picture of the polymerization reaction: the first reaction steps privilege the insertion of the glycolide into the Al-OCH_3 bond, ensued by the formation of a predominantly glycolide block which allow ϵ -caprolactone insertion by transesterification processes, i.e. insertion of a caproyl chain end on preformed glycolidyl sequences. This picture is corroborated by: the end-group analysis, that confirms the more readily pathway of the GA insertion into the Al-OCH_3 ; the ϵ -caproyl block lengths, that remain overall unaltered at any given feed ratio; the CapGCap

transesterification yield, that increases by increasing the CL content and/or the reaction time.

Interestingly, the behaviour of the catalysts **1-3** shows some differences. Information on this issue can be retrieved from end group analysis of the copolymers (Figure 2.10).

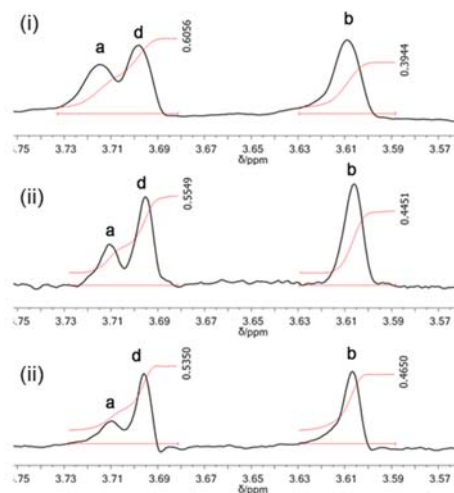


Figure 2.10. ^1H NMR (300 MHz, DMSO-d_6 , $100\text{ }^\circ\text{C}$) spectra of PGCA with $f_{\text{GA}30}$ feed, obtained with: (i) complex **1** ($F_{\text{GA}} = 32$; Table 1, run 3); (ii) complex **2** ($F_{\text{GA}} = 28$; Table 1, run 6); (iii) complex **3** ($F_{\text{GA}} = 24$; Table 1, run 9). End groups region.

Notably, the comparison of the intensity of peaks **a** (relative to the GGGG-OCH₃ end group) and **d** (relative to the CapGG-OCH₃ end group), for the polymerization runs carried out with the different catalysts at the same feed ratio ($f_{\text{GA}} = 30$), is indicative of the second insertion after the glycolide first insertion, and could be a representation of the relative rate of the two monomers during the polymer propagation steps.

In particular, the ratio **d/a** increases from catalyst **1** to catalyst **3** indicating that increasing the steric hindrance of the catalyst, the insertion rate of the glycolide monomer decreases. As a result, for the most encumbered catalyst **3** the insertion rates of the two monomers are closer than for the other

catalysts. Remarkably, this observation indicates that with catalyst 3 the two monomers have very similar propagation rates, which is a required condition to get random copolymers.

The molecular weights for the polymers were evaluated by GPC and by NMR in solution, being known the polymer end groups determined by NMR. Representative results are reported in Table 2.7.

Table 2.7. Copolymerization of glycolide and ϵ -caprolactone: molecular weight and molecular-weight dispersities.^a

Run	Cat	F_{GA}^b	$M_{n,th}$ (kDa) ^c	$M_{n,NMR}$ (kDa) ^d	M_w/M_n^e
1	1	57	19.6	23.2	-
2	1	40	19.1	20.3	-
3	1	32	20.8	22.1	1.6
4	2	62	21.7	n.d.	-
5	2	50	17.4	19.6	-
6	2	28	20.8	25.5	1.6
7	3	70	19.0	22.3	-
8	3	52	21.4	20.4	-
9	3	24	19.6	18.5	1.3
10 ^f	2	33	98.5	n.d.	1.4
11 ^g	1	49	9.3	10.2	-
12 ^g	3	45	10.5	12.6	-

^aPolymerization conditions: precatalyst = 12 μ mol; MeOH = 12 μ mol (0.12 mL of a 0.1 M toluene solution); $T = 140$ °C; $t = 75$ min; mol ratio of monomers to precatalyst in the feed = 200.

^b F_{GA} , content of glycolide in the copolymer (mol %), as determined by ¹H NMR (DMSO-*d*₆, 100 °C).

^cTheoretical molecular weight.

^dMolecular weight determined by ¹H NMR (DMSO-*d*₆, 100 °C).

^eMolecular-weight masses dispersities determined by GPC (THF, 35 °C) vs polystyrene standards.

^fPolymerization conditions: precatalyst = 25 μ mol; MeOH = 25 μ mol; $T = 140$ °C; $t = 7$ hours; mol ratio of monomers to precatalyst in the feed = 900; $M_{n,GPC} = 89.3$ kDa.

^gPrecatalyst = 25 μ mol; MeOH = 25 μ mol (0.25 mL of a 0.1 M toluene solution); mol ratio of monomers to precatalyst in the feed = 100.

As a consequence of the low solubility of PGCA having high amount of GA,¹² GPC analysis was allowed only for the copolymers with a high content of CL (Table 2.7, runs 3, 6, 9, 10), soluble in THF. In these cases, the GPC evidenced monomodal distribution with dispersities in the range 1.3 - 1.6. The catalytic system is also able to produce high molecular weight polymers (Table 2.7, run 10).

The GPC analysis is not reliable for the determination of their M_n , since the radius of gyration R_g is extremely sequence and solvent dependent, while the NMR analysis is more reliable. Indeed, a good agreement between the molecular weights evaluated by NMR, $M_{n,NMR}$, and the theoretical molecular weights, $M_{n,th}$, calculated by the monomer/catalyst feed ratio was observed.

2.2.2.5.1. Thermal characterization of poly(ϵ -caprolactone-co-glycolide)

Thermal analysis of the copolymers was carried out by means of differential scanning calorimetry (DSC), from - 60 to + 260 °C. The glass transition temperature, T_g , and the melting temperature, T_m , are given in Table 2.8. Representative thermograms of polymeric samples obtained with complex **3** are reported in Figure 2.11.

Table 2.8. Copolymerization of glycolide and ϵ -caprolactone: thermal properties.^a

Run	Cat	F_{GA}^b	$T_{g,th} (^{\circ}C)^c$	$T_g (^{\circ}C)^d$	$T_m (^{\circ}C)^d$	$\Delta H (J g^{-1})^d$
1	1	77 ^e	-1.7	-	209.1	42.0
2	1	40	-33.1	-41.1	202.4	23.8
3	1	32	-38.9	-40.8	-	-
4	2	73 ^e	-5.5	-	201.4	35.2
5	2	50	-25.3	-34.8	173.7	15.7
6	2	28	-41.8	-44.4	-	-
7	3	80 ^e	1.2	-	204.2	48.0

8	3	52	-23.7	-24.4	185.9	8.2
9	3	24	-44.6	-46.2	-	-

^aPolymerization conditions: precatalyst = 12 μmol ; MeOH = 12 μmol (0.12 mL of a 0.1 M toluene solution); $T = 140\text{ }^{\circ}\text{C}$; $t = 75\text{ min}$; mol ratio of monomers to precatalyst in the feed = 200.

^b F_{GA} : content of glycolide in the copolymer (mol %), as determined by $^1\text{H NMR}$ ($\text{DMSO-}d_6$, $100\text{ }^{\circ}\text{C}$).

^cTheoretical values, as calculated with the Fox equation, using the following T_g values for the homopolymers: PCL = $-60\text{ }^{\circ}\text{C}$;³⁸ PGA = $22.0\text{ }^{\circ}\text{C}$.³⁹

^dValues reported for the second heating cycle.

^eCalculated from $^1\text{H NMR}$ (CDCl_3/TFA 1/1, RT) data of monomers conversion.

For the PCGAs with a glycolide content $F_{\text{GA}} > 50$, a neat melting peak due to the glycolide homo-sequences is observable, evidencing semi-crystalline copolymers.

When the ϵ -caprolactone content is increased ($F_{\text{GA}} \sim 50$), a glass transition peak is present in each thermograms. In particular, for the copolymer obtained with catalyst **3** the observed T_g is in perfect agreement with that calculated by Fox's equation for random copolymers, while the T_g values observed for the other two copolymers are lower than those calculated. A melting peak is observed in each case, although it results affected by the more frequent GG-Cap junction points. Moreover, the heat of fusion decreases from catalyst **1** to catalyst **3** indicating the formation of a less crystalline copolymer in the last case.

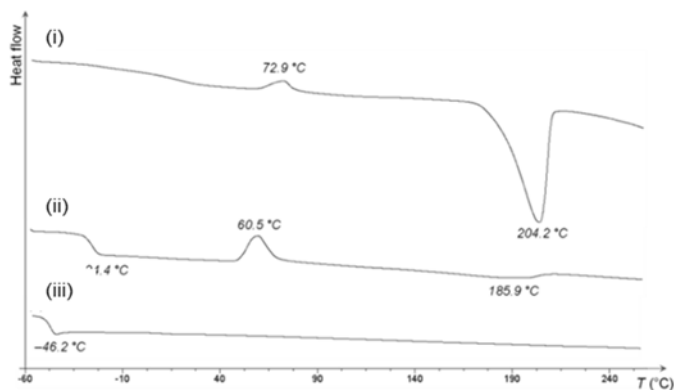


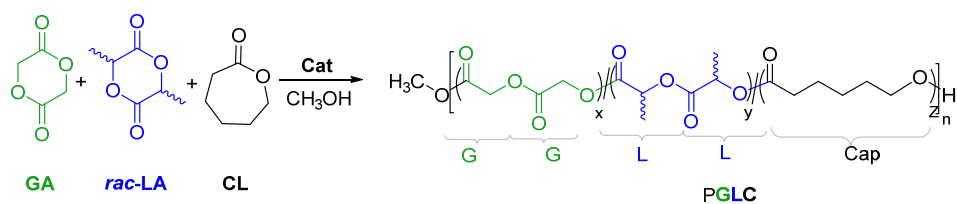
Figure 2.11. DSC thermograms (run II) of poly[glycolide-*co*-(ϵ -caprolactone)] obtained with complex **3**: (i) $F_{GA} = 70$ (Table 2.6, run 7), (ii) $F_{GA} = 52$ (Table 2.6, run 8), (iii) $F_{GA} = 24$ (Table 2.6, run 9).

Thus, the DSC results are in line with the previous speculations, confirming the higher propensity of complex **3**, with respect to catalyst **1** and **2**, to give random copolymers.

For copolymers with higher ϵ -caprolactone content, no melting endotherm is observed for the glycolide blocks, as expected from the values of the average block lengths ($L_{GG} < 1$) and from the high transesterification values (Table 2.6). These observations confirm the picture of polymeric material where most of the glycolide units undergo G-G cleavage and glycolyl units are randomly distributed along with caproyl units, sometimes comprising –CapGG– blocks, as evidenced by ^1H NMR (Figure 2.7ii). The experimental T_g of these copolymers reveal a nice match with the values predicted by the Fox equation: this is the first time that such a correlation is found for a poly(glycolide-*co*-caprolactone) synthesized by ROP.¹⁴

2.2.6. Terpolymerization of glycolide, *rac*-lactide and ϵ -caprolactone

The complexes (**1-3**) were also tested as initiators in the terpolymerization of GA, *rac*-LA and CL (Scheme 2.6).



Scheme 2.6. Terpolymerization of glycolide, *rac*-lactide and ϵ -caprolactone.

The obtained polymer samples were characterized by NMR spectroscopy, GPC and DSC analysis. The results about composition and chain microstructural analysis are summarized in Table 2.9.

Table 2.9. Terpolymerization of glycolide, *rac*-lactide and ϵ -caprolactone.^a

Run	cat	f_{GA}^b	f_{LA}^b	f_{CL}^b	Yield (%)	F_{GA}^c	F_{LA}^c	F_{Cap}^c	L_{GG}^d	L_{LL}^d	L_{Cap}^d	T_{LGL}^e	$T_{CapGCap}^e$	T_{XLX}^e
1	1	33	33	33	83	37	37	26	1.69	2.26	1.26	0.3	0.8	n.o.
2	1	20	40	40	74	24	46	30	1.36	1.92	1.33	0.3	0.7	n.o.
3 ^f	1	20	20	60	90	18	16	66	0.85	0.95	1.91	0.2	0.9	0.1
4	2	33	33	33	85	41	24	35	1.40	1.66	1.28	0.4	0.7	n.o.
5	3	33	33	33	69	41	29	30	2.11	1.81	1.36	0.2	0.8	n.o.

^aPolymerization reactions: precatalyst = 25 μ mol; MeOH = 25 μ mol (0.1 M in toluene); $T = 140$ °C; $t = 75$ min; mol ratio of monomers to precatalyst in the feed = 100.
^bMolar percentage of glycolide (f_{GA}), *rac*-lactide (f_{LA}), ϵ -caprolactone (f_{Cap}) in the feed.
^cMolar percentage of glycolide (F_{GA}), *rac*-lactide (F_{LA}), ϵ -caprolactone (F_{Cap}) in the terpolymer, determined by ¹H NMR (DMSO-*d*₆, 100 °C).
^dAverage block lengths of glycolidyl (GG), lactidyl (LL) and caproyl (Cap) blocks in the terpolymer, determined by ¹H NMR (DMSO-*d*₆, 100 °C).
^eSecond mode of transesterification (%) of glycolidyl (CapGCap, LGL) and lactidyl (XLX) sequences, determined by ¹H NMR (DMSO-*d*₆, 100 °C).
^f $t = 150$ min.

Polymerizations were carried out in bulk at 140 °C in the presence of the selected catalyst and one equivalent of MeOH. The molar ratio of the comonomers to initiator was fixed at 100:1, and after 75 min of reaction, the polymeric samples were recovered in good yield (up to 85%) with all the used catalysts.

The chain microstructure of the terpolymers was studied by ^1H NMR analysis, in the methylene and methine regions. The resonances were assigned according to literature.²⁶ Selected regions of ^1H NMR spectra of the terpolymers samples for different compositions are shown in Figure 2.12. The calculation of average glycolidyl, L_{GG} , lactidyl, L_{LL} , and caproyl blocks, L_{Cap} , as well as the determination of contribution of sequences formed by transesterification of the second mode, were also obtained from the ^1H NMR analysis, by using literature formulas.^{5c}

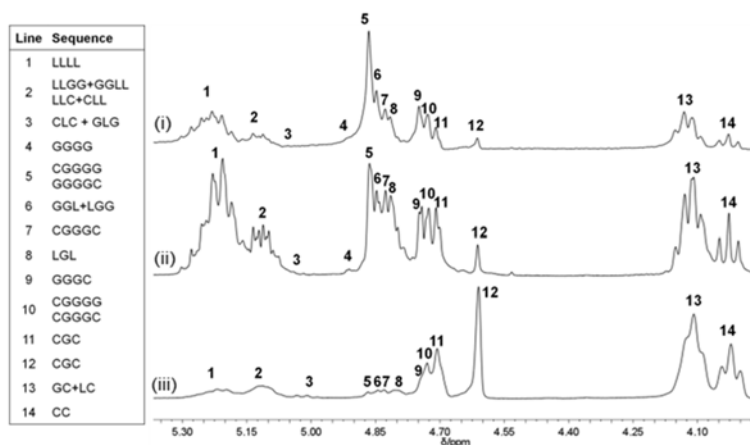


Figure 2.12. ^1H NMR (300 MHz, $\text{DMSO-}d_6$, 100 °C) of poly[glycolide-*co*-(*rac*-lactide)-*co*-(ϵ -caprolactone)] obtained with complex **1**: (i) $F_{\text{GA}} = 37$; $F_{\text{LA}} = 37$; $F_{\text{Cap}} = 26$ (Table 2.9, run 1); (ii) $F_{\text{GA}} = 24$; $F_{\text{LA}} = 46$; $F_{\text{Cap}} = 30$ (Table 2.9, run 2); (iii) $F_{\text{GA}} = 23$; $F_{\text{LA}} = 16$; $F_{\text{Cap}} = 61$ (Table 2.9, run 3).

The chemical composition of the terpolymers was determined through the ratio of the integrated values of the methylene signal of the caproyl segment $-\text{O}-\text{CH}_2-(\text{CH}_2)_4-\text{C}(\text{O})-$ (Cap, centered at 4.00 ppm ca.), the methylene signal

of the glycolyl segment $-O-CH_2-C(O)-$ (G, centered at 4.80 ppm ca.) and the methine signal of the lactyl segment $-O-CH(CH_3)-C(O)-$ (L, centered at 5.20 ppm ca.).

The effect of the catalyst was studied for equimolar amount of the three monomers (Table 2.9, runs 1, 4, 5). The effect of the monomers feed ratio was studied in the presence of complex **1** (Table 2.9, runs 1-3). The composition of the obtained polymeric samples was quite close to the feed in all the runs. GA was generally more easily incorporated than the other monomers with all the catalysts. Notably, for equimolar amount of the three monomers, the cyclic diesters (both GA and *rac*-LA) were preferred incorporated with respect to CL with complex **1**. On the contrary, when complexes **2** and **3** were used, the composition of the terpolymers follows the order: $F_{GA} > F_{Cap} > F_{LA}$. Thus, with the bulkier catalysts **2** and **3**, while the GA is still the most incorporated monomer, the CL is preferentially incorporated than *rac*-LA (Table 2.9, runs 1, 4, 5). This behavior should be explained on the basis of the bulkiness of the catalysts and of the higher coordination ability of the cyclic diesters with respect to that of the CL. Thus, the less encumbered catalyst **1** preferentially incorporates the cyclic diesters with respect to ϵ -caprolactone. However, with the more hindered complexes **2** and **3**, the bulkier *rac*-LA is disfavored, to the benefit of the less bulky and more flexible CL. A similar effect was reported by Nomura for the ϵ -caprolactone/lactide copolymerization.⁴⁰ Indeed, the higher reactivity of LA than CL, over the steric effect of the two methyl groups, in the copolymerization could be attributed to the higher coordination ability of LA than CL. However, the reactivity of LA could be reduced by increasing the bulkiness of the ligand.

The yield of transesterifications of the second mode, due to the attack of active chain end on the preformed segments, have been also evaluated by using the coefficient T_{LGL} , $T_{CapGCap}$, T_{XLX} as previous reported (Table 2.9).^{5c}

During the terpolymerization, the transesterification side reactions generated by the attack of active glycolidyl or caproyl chain ends on preformed lactidyl segments were absent or negligible (T_{XLX} higher value was 0.1 for run 3, Table 2.9). It is confirmed, therefore, the low tendency of this class of catalysts in breaking the lactidyl unit in two lactyl fragment.²⁷ The $T_{CapGCap}$ values, instead, are significantly higher, thus suggesting that the glycolidyl segment, GG, are quite completely broken by the attack of caproyl active chain end, as a result the glycolide is incorporated in CapGCap sequences along the polymeric chains. Coherently with this picture, Figure 2.12 shows that by increasing the amount of the ϵ -caprolactone, the CapGCap sequences increase and the GGGGG sequences decreases.

The ^1H NMR spectra showed also resonances attributable to the alkoxide - OCH_3 end groups. By comparison with the literature data, the signals due to the following end groups were recognized: $-\text{CH}_2\text{C}(\text{O})\text{OCH}_3$ (G- OCH_3), $-\text{CH}(\text{CH}_3)\text{C}(\text{O})\text{OCH}_3$ (L- OCH_3) and $-(\text{CH}_2)_4\text{CH}_2\text{C}(\text{O})\text{OCH}_3$ (Cap- OCH_3 , Figure 2.13).

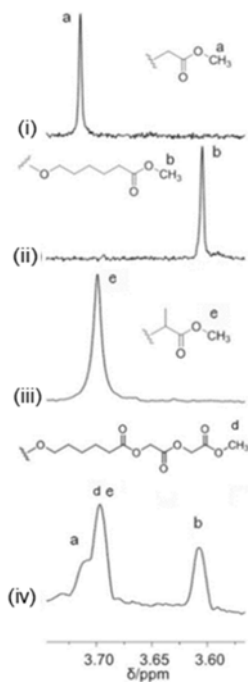


Figure 2.13. End groups analysis: ^1H NMR (300 MHz, $\text{DMSO-}d_6$, $100\text{ }^\circ\text{C}$) spectra of: (i) polyglycolide; (ii) poly(ϵ -caprolactone); (iii) poly(*rac*-lactide); (iv) poly[glycolide-*co*-(*rac*-lactide)-*co*-(ϵ -caprolactone)].

The presence of all the three signals indicates that the first step of these copolymerization reactions could be the insertion of all the three monomers into the Al-OCH_3 bond. However, the signals relative to the first insertion of lactide on the Al-OCH_3 bond is overlapped with the signals of the -CapGGOCH_3 end group, therefore the relative intensities of the end groups signals could not be evaluated.

The molecular weights of the obtained polymers were evaluated by gel permeation chromatography (GPC) and by ^1H NMR, being known the end group signals (Figure 2.13). The results are reported in Table 2.10.

Table 2.10. Terpolymerization of glycolide, *rac*-lactide and ϵ -caprolactone: analysis of molecular weights.^a

Run	Cat	F_{GA}^b	F_{LA}^b	F_{Cap}^b	$M_{n,th}$ (kDa) ^c	$M_{n,NMR}$ (kDa) ^d	$M_{n,GPC}$ (kDa) ^e	M_w/M_n^e
1	1	37	37	26	10.4	9.7	8.0	1.4
2	1	24	46	30	9.5	11.7	20.9	1.5
3 ^f	1	18	16	66	10.9	20.2	27.0	1.4
4	2	41	24	35	10.5	11.0	21.9	1.7
5	3	41	29	30	8.5	7.4	16.4	1.5

^aPolymerization conditions: precatalyst = 25 μ mol; MeOH = 25 μ mol (0.25 mL of a 0.1 M toluene solution); T = 140 $^{\circ}$ C; t = 75 min; mol ratio of monomers to precatalyst in the feed = 100.

^bContent of glycolide (F_{GA}), *rac*-lactide (F_{LA}) and ϵ -caprolactone (F_{Cap}) in the terpolymer (mol %), as determined by 1 H NMR (DMSO- d_6 , 100 $^{\circ}$ C).

^cTheoretical molecular weight.

^dMolecular weight determined by 1 H NMR (DMSO- d_6 , 100 $^{\circ}$ C).

^eMolecular weights and molecular-weight dispersivities determined by gel permeation chromatography (GPC) vs. polystyrene standards, elution solvent: tetrahydrofuran (THF).

^f $t = 150$ min.

Since the terpolymer samples were soluble in THF, their molecular weights were evaluated by GPC, vs polystyrene standards, using THF as elution solvent at 35 $^{\circ}$ C. However, as previously underlined the values obtained by GPC should be regarded with special care. However, the GPC analysis performed on all the samples disclosed monomodal molecular weight distributions with variable molecular-weight dispersities, in the range 1.4-1.7. In detail, catalyst **1** produced the terpolymer having narrower dispersity than those obtained with the others catalysts for equimolar amount of three monomers. The observed values of molecular-weight dispersities may be due to the transesterification side reactions.

Molecular weights were also calculated by 1 H NMR analysis, being known the end group signals, and a good agreement between the latter values ($M_{n,NMR}$), and the theoretical molecular weights, $M_{n,th}$, calculated by the monomer to precatalyst feed ratio was observed in most runs.

2.2.6.1. Thermal characterization of terpolymers

Thermal properties of the terpolymers were studied by Differential Scanning Calorimetry (DSC) in the range from -60 °C to 260 °C at heating rate of 10 °C min⁻¹. The DSC thermograms were recorded for the second heating scan. Terpolymers transition temperatures were measured and the values are reported in Table 2.11.

Table 2.11. Thermal properties of terpolymers.^a

Run	Cat	F_{GA}^b	F_{LA}^b	F_{Cap}^b	$T_{g,th} (^{\circ}C)^c$	$T_g (^{\circ}C)^d$
1	1	37	37	26	2.6	6.3
2	1	24	46	30	0.5	13.5
4	2	41	24	35	-8.6	-3.1
5	3	41	29	30	-2.9	6.6; 29.6

^aPolymerization conditions: precatalyst = 25 μmol; MeOH = 25 μmol (0.25 mL of a 0.1 M toluene solution); T = 140 °C; t = 75 min; mol ratio of monomers to precatalyst in the feed = 100.

^bContent of glycolide (F_{GA}), *rac*-lactide (F_{LA}) and ε-caprolactone (F_{Cap}) in the terpolymer (mol %), as determined by ¹H NMR (DMSO-d₆, 100 °C).

^cTheoretical values, as calculated with Fox equation, using the following T_g values for the homopolymers: poly(CL) = -60 °C;³⁸ poly(GA) = 22.0 °C,³⁹ poly(D,L-LA) = 48.3 °C (Table 2.3, run 4).

^dValues reported for the second heating cycle.

All the polymeric samples were amorphous, and the measured T_g 's were below 37 °C. All polymers exhibited unique glass transition, except in one case (Table 2.11, run 5), confirming that a single phase was retained for all samples, even if the composition changed. Indeed, experimental T_g 's were in good agreement with the theoretical ones, $T_{g,th}$ determined by Fox Equation (Table 2.11).

The DSC thermograms, recorded for the second heating scan, of terpolymer samples obtained with different catalysts **1-3** for equimolar monomers feed are shown in Figure 2.14.

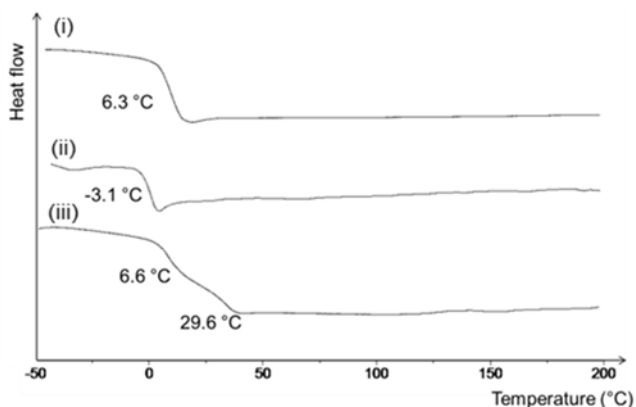


Figure 2.14. DSC thermograms (run II) of poly[glycolide-*co*-(*rac*-lactide)-*co*-(ϵ -caprolactone)] obtained with: (i) complex **1**, $F_{GA} = 37$; $F_{LA} = 37$; $F_{Cap} = 26$ (Table 2.9, run 1); (ii) complex **2**, $F_{GA} = 41$; $F_{LA} = 24$; $F_{Cap} = 35$ (Table 2.9, run 4); (iii) complex **3**, $F_{GA} = 41$; $F_{LA} = 29$; $F_{Cap} = 30$ (Table 2.9, run 5).

For terpolymers obtained with catalysts **1,2** the average glycolidyl block lengths were lower than 2, DSC analysis showed unique T_g . Whereas, for catalyst **3**, the thermogram showed two T_g values and glycolidyl block length was higher than 2, indicating a blocky structure of the terpolymer chain.

CONCLUSIONS

The most common degradable and biocompatible synthetic polymers are poly(glycolide), poly(lactide)s, poly(ϵ -caprolactone) and their respective comonomers. The poly(lactide-co-glycolide) is one of the most used biodegradable and biocompatible polymer in biomedical field.

There is a continuous search to precisely match the properties of these materials in terms of composition, rate of degradation, mechanical, and thermal properties to the needs of application. In this regard, the search for efficient ROP initiators for the synthesis of copolymers having controlled composition and microstructure is a very stimulating field.

Salicylaluminum compounds have been shown as efficient initiators in the homo- and copolymerization of glycolide, *rac*-lactide and ϵ -caprolactone. A highly versatile behavior has been recognized: by copolymerization of glycolide and *rac*-lactide, PLGAs having different microstructures, from random to blocky to multiblock, have been obtained as the polymerization conditions have been changed.

Copolymerization in bulk produced random copolymers, whose average block lengths linearly increase with the monomer feed ratio. The copolymers were amorphous, and their T_g could be nicely modulated by the feed. The copolymer microstructure reasonably should result from transesterification processes taking place together with the main copolymerization reaction. Interestingly, the values of the coefficients of the second mode of transesterification indicated that the transesterification reaction involving the attack of active lactidyl chain end on preformed glycolidyl segments was preferred in this case.

On the contrary, copolymerization performed in several solvents afforded mainly blocky copolymers, with sequence blocks lengths higher than 2. Finally, the sequential addition of the two monomers afforded di-block copolymers, thus indicating a certain *living* character of the polymerization.

In the copolymerization of glycolide with ϵ -caprolactone, performed in bulk, copolymers from semi-crystalline to amorphous were produced by decreasing the glycolide/ ϵ -caprolactone feed ratio. Interestingly, the net reactivities of the CL and GA comonomers could be controlled by changing the bulkiness of the substituents in the ortho positions of the phenoxide groups. In particular, the most encumbered complex **3** showed the highest propensity to furnish random copolymers.

In the case of the terpolymerization, all the polymeric samples were amorphous, and the composition could be modulated by the feed. The yield of transesterifications of the second mode, due to the attack of active chain end on the preformed segments contributed to the “randomized” structures. Notably, the transesterification side reactions generated by the attack of active glycolidyl or caproyl chain ends on preformed lactidyl segments were absent or negligible. It is thus confirmed that the tendency of these complexes to break the lactidyl unit into two lactyl fragments is low.

In all cases, GPC analysis disclosed monomodal molecular weight distribution with narrow molecular-weight dispersities. A reasonable agreement between the theoretical molecular weights and the experimental ones evaluated by NMR analysis was observed. The polymerization behavior of the catalysts is strongly related to the experimental conditions, and the copolymers molecular weight could be adjusted by regulating the monomers/initiator feed ratio.

These results should be of interest in applications where modulated thermal, physical and degradation properties of PGA/PLA/PCL based materials are required.

The results reported and discussed here were published in *Macromolecules*⁴¹ and in *Journal of Applied Polymer Science*.⁴²

References

- ¹ (a) I. Engelberg, J. Kohn, *Biomaterials* **1991**, *12*, 292–304. (b) R. Langer; J. P. Vacanti, *Science* **1993**, *260*, 920-926. (c) R. A. Jain, *Biomaterials* **2000**, *21*, 2475–2490. (d) H. Ueda, Y. Tabata, *Adv. Drug Deliv. Rev.* **2003**, *55*, 501–518. (e) S. S. D’Souza, P. P. De Luca, *Pharm. Res.* **2006**, *23*, 460-474. (f) Z. Pan, J. Ding, *Interface Focus* **2013**, *2*, 366-377.
- ² K. K. L. Phua, E. R. H. Roberts, K. W. Leong in *Comprehensive Biomaterials* **2011**, *1*, 381-415.
- ³ T. G. Park, *Biomaterials* **1995**, *16*, 1123–1130.
- ⁴ (a) H. R. Kricheldorf, T. Mang, J. M. Jonté, *Macromolecules* **1984**, *17*, 2173-2181. (b) H. R. Kricheldorf, J. M. Jonté, M. Berl, *Makromol. Chem.* **1985**, *Suppl. 12*, 25-38. (c) M. Bero, P. Dobrzyński, J. Kasperczyk, *Polym. Bull.* **1999**, *42*, 131-139. (d) P. Dobrzyński, J. Kasperczyk, M. Bero, *Macromolecules* **1999**, *32*, 4735-4737. (e) J. W. Pack, S. H. Kim, I. W. Cho, S. Y. Park, Y. H. Kim, *J. Polym. Sci., Part A: Polym. Chem.* **2002**, *40*, 544–554. (f) P. Dobrzynski, S. Li, J. Kasperczyk, M. Bero, F. Gasc, M. Vert, *Biomacromolecules* **2005**, *6*, 483-488. (g) S. Li, P. Dobrzynski, J. Kasperczyk, M. Bero, C. Braud, M. Vert, *Biomacromolecules* **2005**, *6*, 489-497. (h) P. Dobrzyński, J. Kasperczyk, K. Jelonek, M. Ryba, M. Walski, M. Bero, *J. Biomed. Mater. Res., Part A* **2006**, *79*, 865-873.
- ⁵ (a) Q. Cai, J. Bei, S. Wang, *J. Biomater. Sci., Polym. Ed.* **2000**, *11*, 273–288. (b) M. Srisa-ard, R. Molloy, N. Molloy, J. Siripitayananon, M. Sriyai, *Polym. Int.* **2001**, *50*, 891-896. (c) P. Dobrzynski, *J. Polym. Sci., Part A: Polym. Chem.* **2002**, *40*, 3129-3143. (d) H. R. Kricheldorf, S. Rost, *Polymer* **2005**, *46*, 3248-3256.
- ⁶ (a) A.-C. Albertsson, K. I. Varma, *Biomacromolecules* **2003**, *4*, 1466-1486. (b) O. Dechy-Cabaret, B. Martin-Vaca, D. Bourissou, *Chem. Rev.*

- 2004**, *104*, 6147-6176. (c) C. M. Thomas, *Chem. Soc. Rev.* **2010**, *39*, 165-173.
- ⁷ D. K. Gilding, A. M. Reed, *Polymer* **1979**, *20*, 1459-1464.
- ⁸ D. W. Grijpma, A. J. Nijenhuis, J. A. Pennings, *Polymer* **1990**, *31*, 2201-2206.
- ⁹ J. Kasperczyk, *Polymer* **1996**, *37*, 201-203.
- ¹⁰ (a) S. D. Allison, *J. Pharm. Sci.* **2008**, *97*, 2022-2035. (b) D. Hofmann, M. Entrialgo-Castano, K. Kratz, A. Lendlein, *Adv. Mater.* **2009**, *21*, 3237-3245.
- ¹¹ C.-M. Dong, K.-Y. Qiu, Z.-W. Gu, X.-D. Feng, *J. Polym. Sci., Part A: Polym. Chem.* **2000**, *38*, 4179-4184.
- ¹² R. M. Stayshich, T. Y. Meyer, *J. Am. Chem. Soc.* **2010**, *132*, 10920-10934.
- ¹³ (a) J. Li, R. M. Stayshich, T. Y. Meyer, *J. Am. Chem. Soc.* **2011**, *133*, 6910-6913. (b) J. Li, S. N. Rothstein, H. M. Edenborn, T. Y. Meyer, *J. Am. Chem. Soc.* **2012**, *134*, 16352-16359.
- ¹⁴ R. M. Weiss, E. M. Jones, D. E. Shafer, M. R. Stayshich, T. Y. Meyer, *J. Polym. Sci., Part A: Polym. Chem.* **2011**, *49*, 1847-1855.
- ¹⁵ C. M. Thomas, J.-F. Lutz, *Angew. Chem. Int. Ed.* **2011**, *50*, 9244-9246.
- ¹⁶ H. R. Kricheldorf, J. M. Jonté, M. Berl, *Makromol. Chem.* **1985**, *Suppl. 12*, 25-38.
- ¹⁷ H. R. Kricheldorf, I. Kreiser, *Mackromol. Chem.* **1987**, *188*, 1861-1873.
- ¹⁸ P. Dobrzyński, J. Kasperczyk, K. Jelonek, M. Ryba, M. Walski, M. Bero, *J. Biomed. Mater. Res., Part A* **2006**, *79*, 865-873.
- ¹⁹ I. Kreiser-Saunders, H. R. Kricheldorf, *Macromol. Chem. Phys.* **1998**, *199*, 1081-1087.
- ²⁰ P. Dobrzyński, J. Kasperczyk, M. Bero, *Macromolecules* **1999**, *32*, 4735-4737.
- ²¹ P. Dobrzyński, J. Kasperczyk, H. Janeczek, M. Bero, *Macromolecules* **2001**, *34*, 5090-5098.

- ²² P. Dobrzyński, J. Kasperczyk, H. Janeczek, M. Bero, *Polymer* **2002**, *43*, 2595-2601.
- ²³ H. R. Kricheldorf, G. Behnken, *J. Macromol. Sci., Part A: Pure Appl. Chem.* **2007**, *44*, 795-800.
- ²⁴ P. Dobrzynsky, *J. Polym. Sci., Part A: Polym. Chem.* **2002**, *40*, 1379-1394.
- ²⁵ (a) H. R. Kricheldorf, S. Rost, *Biomacromolecules* **2005**, *6*, 1345-1352. (b) H. R. Kricheldorf, H. Hachmann-Thiessen, *J. Polym. Sci., Part A: Polym. Chem.* **2005**, *43*, 3268-3277. (c) H. R. Kricheldorf, G. Behnken, *J. Macromol. Sci, Part A: Pure Appl. Chem.* **2008**, *45*, 693-697.
- ²⁶ J. Kasperczyk, Y. Hu, J. Jaworskam, P. Dobrzynski, J. Wei, S. Li, *J. Appl. Polym. Sci.* **2008**, *107*, 3258-3266.
- ²⁷ D. Pappalardo, L. Annunziata, C. Pellicchia, *Macromolecules* **2009**, *42*, 6056-6062.
- ²⁸ a) N. Nomura, T. Aoyama, R. Ishii, T. Kondo, *Macromolecules* **2005**, *38*, 5363-5366. (b) N. Iwasa, J. Liu, K. Nomura, *Catal. Commun.* **2008**, *9*, 1148-1152. (c) J. Liu, N. Iwasa, K. Nomura, *Dalton Trans.* **2008**, *30*, 3978-3988. (d) N. Iwasa, M. Fujiki, K. Nomura, *J. Mol. Catal. A: Chem.* **2008**, *292*, 67-75. (e) M. Normand, V. Dorcet, E. Kirillov, J.-F. Carpentier, *Organometallics* **2013**, *32*, 1694-1709.
- ²⁹ D. Pappalardo, C. Tedesco, C. Pellicchia, *Eur. J. Inorg. Chem.* **2002**, 621-628.
- ³⁰ (a) D.-P. Song, Y.-G. Li, R. Lu, N.-H. Hu, Y.-S. Li, *Appl. Organomet. Chem.* **2008**, *22*, 333-340. (b) K. V. Axenov, M. Klinga, O. Lehtonen, H. T. Laskela, T. Repo, *Organometallics* **2007**, *26*, 1444-1460.
- ³¹ K. A. M. Takur, R. T. Kean, E. S. Hall, J. J. Kolstad, T. A. Lindgren, M. A. Doscotch, J. I. Siepman, E. J. Munson, *Macromolecules* **1997**, *30*, 2422-2428.
- ³² G. Odian in *Principles of polymerization*, John Wiley & Sons. Eds.; **2004**; Chapter 6, 464-543.

-
- ³³ (a) I. Barak, P. Dubois, R. Jerome, P. Teyssie, *J. Polym. Sci., Part A: Polym. Chem.* **1993**, *31*, 505-514. (b) J. Baran, A. Duda, A. Kowalski, R. Szymanski, S. Penczek, *Macromol. Rapid Commun.* **1997**, *18*, 325-333.
- ³⁴ D. Cohn, H. Younes, G. Marom, *Polymer* **1987**, *28*, 2018-2022.
- ³⁵ (a) A. Chen, D. Wu, C. S. Johnson, *J. Am. Chem. Soc.* **1995**, *117*, 7965-7970. (b) C. F. Hansell, P. Espeel, M. M. Stamenović, I. A. Barker, A. P. Dove, F. E. Du Prez, R. K. O'Reilly, *J. Am. Chem. Soc.* **2011**, *133*, 13828-13831. (c) W. Li, H. Chung, C. Daeffler, J. A. Johnson, R. H. Grubbs, *Macromolecules* **2012**, *45*, 9595-9603.
- ³⁶ (a) C.-M. Feng, K.-Y. Qiu, Z.-W. Gu, X.-D. Feng, *J. Polym. Sci., Part A: Polym. Chem.* **2001**, *39*, 357-367.
- ³⁷ J. Kasperczyk, *Macromol. Chem. Phys.* **1999**, *200*, 903-910.
- ³⁸ P. Vanhoorne, P. Dubois, R. Jerome, P. Teyssie, *Macromolecules* **1992**, *25*, 37-44.
- ³⁹ I. Barakat, P. Dubois, C. Grandfils, R. Jerome, *J. Polym. Sci., Part A: Polym. Chem.* **2001**, *39*, 294-306.
- ⁴⁰ N. Nomura, A. Akita, R. Ishii, M. Mizuno, *J. Am. Chem. Soc.* **2010**, *132*, 1750-1751.
- ⁴¹ A. Meduri, T. Fuoco, M. Lamberti, C. Pellicchia, D. Pappalardo, *Macromolecules* **2014**, *47*, 534-543.
- ⁴² T. Fuoco, A. Meduri, M. Lamberti, C. Pellicchia, D. Pappalardo, *J. Appl. Polym. Sci.* **2015**, *132*, 42567 (1-11).

3. SYNTHESIS OF ALIPHATIC POLY(ESTER)S WITH PENDANT THIOL GROUPS: FROM MONOMER DESIGN TO EDITABLE POROUS SCAFFOLDS

3.1. Introduction

Given their versatile properties, synthetic polymeric materials have been employed in the biomedical field. Specifically, thanks to their biocompatibility and biodegradability, aliphatic poly(ester)s, such as poly(lactide) (PLA), poly(glycolide) (PGA), poly(ϵ -caprolactone) (PCL) and their copolymers, have become increasingly attractive in the design of temporary synthetic scaffolds in tissue engineering.¹

As previously underlined in this thesis, their properties and degradation profiles can be precisely tuned to match the needs of the final application. However, a major limitation to their application in highly specialized areas, such as the biomedical field, is the absence of readily accessible side-chain functionalities. For example, the bio-functionalization of polyester-based scaffolds with biologically relevant ligands could provide a host of opportunities to control cell adhesion and functions.² Specifically, conjugation with a peptide containing the sequence arginine-glycine-aspartic acid (Arg-Gly-Asp, or RGD) has been shown to improve the cytocompatibility and cellular attachment characteristics of temporary polymeric devices by promoting cellular adhesion through binding to integrin receptors.³

Therefore, the development of simple and controlled chemical synthetic approaches that allow the preparation of functionalized poly(ester)s is one of the main topics in this field.⁴

Two strategies can be followed to obtain polyesters with functionalities incorporated as side groups. First, post-polymerization modifications have been used to modify the surface of the polymers without impacting the bulk;⁵ however, these modifications are sometimes associated with side reactions, such as chain scission, with a consequent deterioration of the polymeric features.⁶

The second method, co-polymerization with functionalized monomers, allows the preparation of editable polymers through the polymeric chain, which can affect the material in the bulk.⁷

Following the Kimura's pioneering approach,⁸ functionalized lactide- and glycolide-type monomers featuring pendant-protected carboxyl, hydroxyl and amino groups have been prepared by diazotization of available amino acids, such as aspartic⁹ and glutamic acids,¹⁰ serine^{10a,11} or lysine,^{10a} into the corresponding α -hydroxy acids, followed by cyclization with α -haloacyl halides. Cyclic di-esters carrying aliphatic groups have also been obtained from their corresponding α -hydroxy acids.¹² Attempts to obtain the analogous hydroxy acid starting from the diazotization reaction of the cysteine were unsuccessful.^{13,14}

Due to the ubiquity of thiol groups in the biological environment and the versatility of thiol chemistry, it was envisaged a lactide-type monomer featuring a pendant cleavable thiol group as an attractive "building block" for the synthesis of functionalized aliphatic poly(ester)s. The polymerization of such a monomer could be a promising approach to combine the biodegradability of the aliphatic poly(ester) main chain with the great pliability of the pendant thiol groups.

Thiol synthesis, modification and functionalization are highly attractive and efficient in polymer and materials science and have immense application in

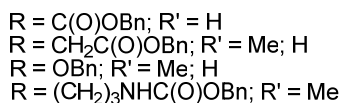
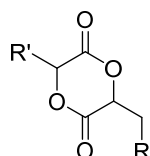
biological therapeutics and drug delivery.¹⁵ The abundance of the thiol-based amino acid cysteine may allow the use of thiol chemistry to easily conjugate polymers with peptides or proteins.¹⁶ Moreover, the thiol-ene click reaction represents an efficient tool for further polymer modifications.¹⁷ Following the example of nature, where disulfide bond formation plays an important role in the folding and stability of biopolymers, the oxidation of thiols into the corresponding disulphides should also be exploited as stimuli-responsive linkages to obtain improved and intelligent materials.¹⁸

Different approaches for the preparation of poly(ester)s with mercapto groups have already been reported. Exploiting their chemical structure, PCL samples functionalized with a thiol group on the chain-ends have been prepared.¹⁹ Additionally, amphiphilic PLA-based block copolymers functionalized with disulfides at the block junctions have been described.²⁰ Alternatively, poly(ester)s with thiol pendant groups grafted throughout the polymeric chains have been obtained by polycondensation reaction approaches, enzyme-catalyzed chemoselective reactions of mercaptosuccinate with different diols,²¹ or the polycondensation of dicarboxylic acid-containing thiol groups and diols in the presence of a metal initiator.²² In this regard, it was recently reported the polycondensation of suitably prepared sulfur-functionalized hydroxy acids in the presence of SnOct₂, which afforded low molecular weight samples.²³ With respect to the polycondensation reaction of hydroxy acids or dicarboxylic acid with diols, the ROP of cyclic esters can offer higher molecular weight, narrower dispersity, and better control in the microstructure of the final aliphatic poly(ester)s.²⁴

Thus, a further aim of this doctoral project was the development of an efficient chemical pathway toward aliphatic polyesters with pendant editable thiol group by ROP of a properly designed lactide-type monomer. Based on this, the 3-methyl-6-(tritylthiomethyl)-1,4-dioxane-2,5-dione

(TrtS-LA; Chart 3.1) was designed and synthesized. From a retrosynthetic point of view, this molecule can be considered as the cyclic diester related to the amino acid cysteine, analogue to other functionalized glycolide- and lactide-type monomers obtained from amino acids.⁸⁻¹¹

Previously described monomers



TrtS-LA

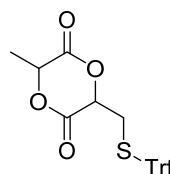


Chart 3.1. Previously described functionalized glycolide- and lactide-type monomers from amino acids;⁸⁻¹¹ 3-methyl-6-(tritylthiomethyl)-1,4-dioxane-2,5-dione (TrtS-LA).

The ROP of TrtS-LA with L-lactide (LA) and ϵ -caprolactone (CL) was then studied in the presence of the well-assessed dimethyl(salicylaldiminato)aluminum complex **2**.

The potentiality of the obtained functionalized poly(ester)s was ascertained through modifications of the pendant groups and by manufacturing porous scaffolds. The grafting of an RGD-containing oligopeptide on the scaffolds was also performed as a proof of concept.

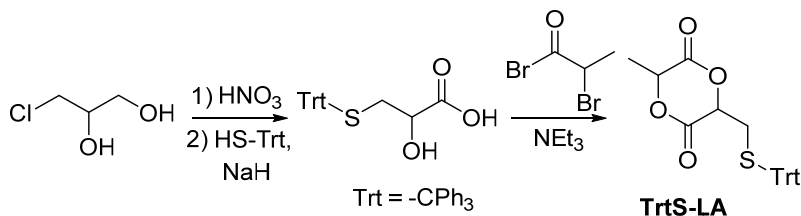
3.2. Results and discussion

3.2.1. Design and synthesis of the sulfur-functionalized monomer

In the design of the “optimum” sulfur-functionalized lactide-type monomer, it was considered that thiol groups are good nucleophiles; therefore, they could “poison” the electrophilic metal-based catalysts or give rise to initiation and side reactions during the polymerization. The “optimum” monomer should bear a sulfur-protecting group able to prevent disulfide formation and other side-reactions during the polymerization; moreover, the same sulfur-protecting group should be easily cleaved under mild conditions without affecting the poly(ester) main chain.

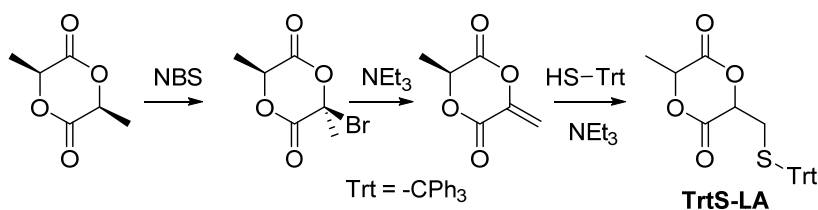
The trityl group (Trt) met these requirements²⁵ because it is stable in basic conditions, i.e., those affecting polymerization where the propagating species is a metal-alkoxide, and can also be cleaved quantitatively in mild conditions.

Following a well-established procedure for the preparation of analogous functionalized glycolide and lactide,⁸⁻¹² the synthesis of TrtS-LA (Chart 3.1) was first attempted by cyclization of the corresponding α -hydroxy acid, 2-hydroxy-3-(S-triphenylmethyl)-thiopropionic acid, with 2-bromopropionyl bromide (Scheme 3.1).



Scheme 3.1. Synthesis of 3-methyl-6-(tritylthiomethyl)-1,4-dioxane-2,5-dione (TrtS-LA) by cyclization of 2-hydroxy-3-(S-triphenylmethyl)-thiopropionic acid (route a).

2-Hydroxy-3-S-triphenylmethylthiopropionic acid cannot be prepared by diazotization of the S-trityl-L-cysteine,^{13,14} whereas this is possible for other amino acids.⁸⁻¹¹ Based on the literature, 2-hydroxy-3-S-triphenylmethylthiopropionic was therefore synthesized by an alternative two-step procedure, starting from 3-chloro-1,2-propanediol (Scheme 3.1).²⁶ The final cyclization with 2-bromopropionyl bromide using trimethylamine in CH₃CN afforded, after purification by chromatography, the desired product in low yield (30 %). Although the yield compared well with those obtained in the synthesis of previously described functionalized glycolide- and lactide-type monomers from amino acids,⁸⁻¹¹ another more convenient synthesis of the molecule was sought. Thus, a three-step route was developed in which the starting material was L-lactide (Scheme 3.2).



Scheme 3.2. Synthesis of 3-methyl-6-(tritylthiomethyl)-1,4-dioxane-2,5-dione (TrtS-LA) by modification of L-lactide (route b).

Following a previous procedure, L-lactide was converted to exo-methylene-lactide by radical bromination with N-bromosuccinimide, NBS, followed by dehydrobromination with NEt₃.²⁷ The exo-methylene-lactide was previously used as a dienophile in Diels-Alder reactions to construct tricyclic compounds by Hillmyer *et al.*²⁸ In this case, the Michael addition of the triphenylmethanethiol to the exo-methylene-lactide, catalyzed by NEt₃, afforded the desired product as a white solid with a yield of 68 %. The obtained 3-methyl-6-(tritylthiomethyl)-1,4-dioxane-2,5-dione (TrtS-LA) was characterized by NMR spectroscopy. The ¹H NMR spectrum (Figure 3.1) revealed the presence of two different patterns of signals.

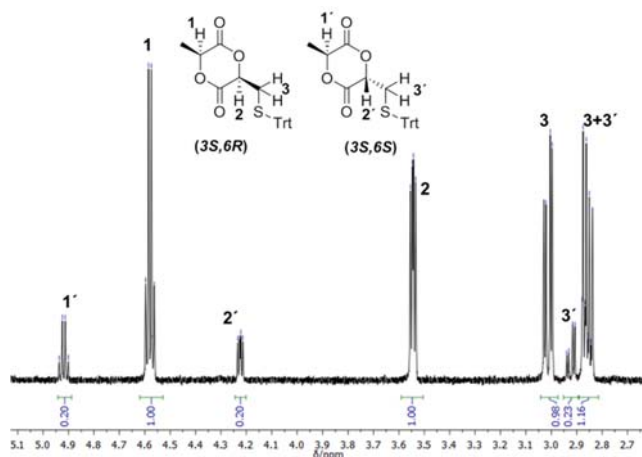


Figure 3.1. Selected region of ^1H NMR (600 MHz, CDCl_3 , RT) of the diastereoisomeric mixture of 3-methyl-6-(tritylthiomethyl)-1,4-dioxane-2,5-dione (TrtS–LA) obtained from route **b**.

In detail, two quartets at 4.92 and 4.58 ppm for the methine protons $-\text{CH}(\text{CH}_3)$ and two doublets of doublets at 4.22 and 3.54 ppm due to $-\text{CH}(\text{CH}_2\text{S}\text{Trt})$ coupled, in turn, with the two protons of the methylene $-\text{CH}_2\text{S}\text{Trt}$ group (partially overlapped, 3.00–2.85 ppm) were recognized (Figure 3.1). Moreover, two different methyl groups and signals in the aromatic region of the ^1H NMR related to the trityl group were observed. Two patterns of signals were also detected in the ^{13}C NMR spectrum. The two patterns of signals were diagnostic of two different diastereomers, formed by the attack of the thiol group on both of the prochiral faces of the *exo*-methylene-lactide. The diastereomeric ratio, calculated by ^1H NMR from the integral ratio of the methine protons (**1** vs **1'** or **2** vs **2'**), was 4:1, indicating that the reaction occurred preferentially at one of the two faces. ^1H NOESY NMR and 1D NOE experiments were performed to elucidate the configuration of the two diastereomers (Figure 3.2).

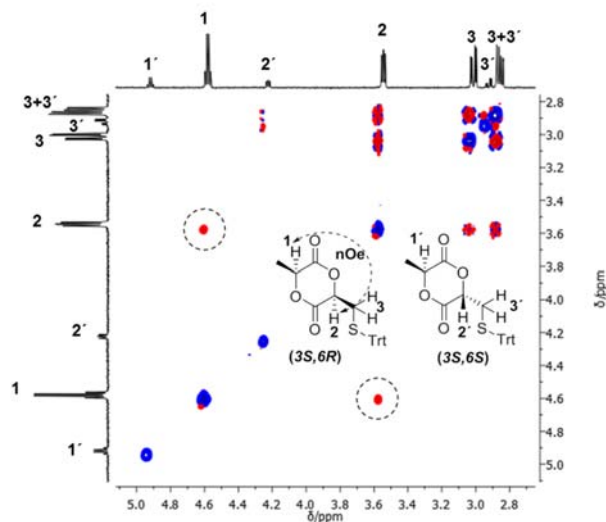


Figure 3.2. Selected section of ^1H NOESY NMR (600 MHz, CDCl_3 , RT) of the diastereomeric mixture of 3-methyl-6-(tritylthiomethyl)-1,4-dioxane-2,5-dione (TrtS-LA).

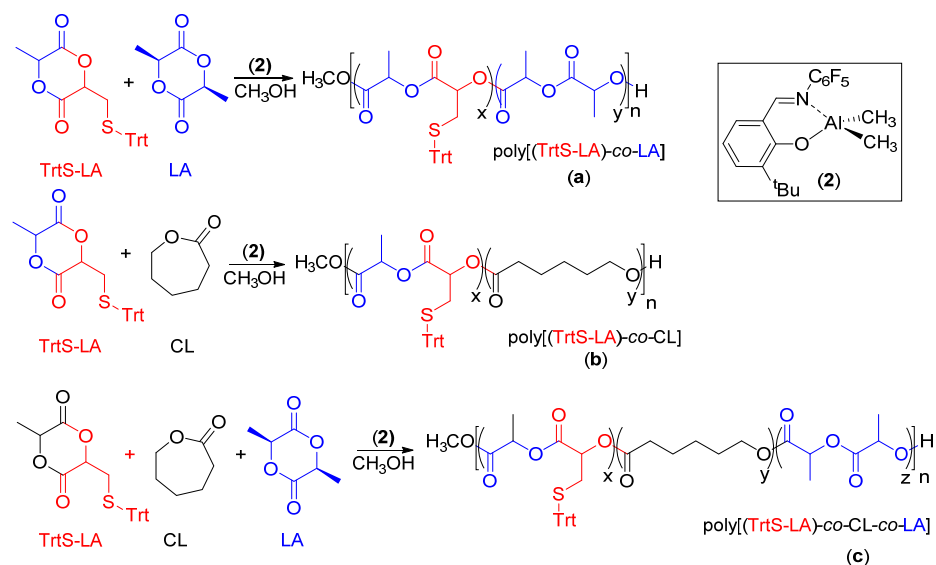
A NOE correlation was observed between the two methine protons (**1** and **2**), but no NOE correlations were observed between the pendant $-\text{CH}_2\text{S}\text{Trt}$ and $-\text{CH}_3$ groups for the major diastereomer (Figure 3.2). This result suggests that the two methine protons were on the same side of the ring, spatially close to each other, whereas the bulky $-\text{CH}_3$ and $-\text{CH}_2\text{S}\text{Trt}$ groups were apart from each other. Thus, the absolute configuration of the major diastereomer was deduced knowing that one of the stereogenic centers, which maintained the configuration (*S*) of the starting L-lactide. A configuration of *3S,6R* was assigned to the major isomer, while *3S,6S* the minor isomer. The (*3S,6R*)-favored product can probably adopt a twisted boat conformation in which the methine protons are located in axial positions and the pendant bulky groups are in equatorial positions pointing away from the six-member ring and from each other. The same conformation was observed in the solid-state by X-ray diffraction analysis of previously reported 1,4-dioxane-2,5-dione.^{10,11a}

During the course of this study, an analogous strategy was reported for the synthesis of a lactide functionalized with 4-hydroxythiobenzamide. Similar results were obtained regarding the configuration of the substituents on the ring for the major diastereoisomer.²⁹

3.2.2. Copolymerization

PLA, PCL and their copolymers are among the aliphatic polyesters most widely used in the biomedical field. However, the absence of functional groups available for further reaction strongly limits their applications. The copolymerization of 3-methyl-6-(tritylthiomethyl)-1,4-dioxane-2,5-dione (Trt-LA) with L-lactide (LA) and ϵ -caprolactone (CL) was investigated to include editable units in the main chain, which is useful for further reactions and/or the attachment of biological motifs. The polymerizations were carried out in toluene at 70 °C using the dimethyl(salicylaldiminato)aluminum complex (**2**), 1 equivalent of MeOH as an initiator, and a monomer-to-catalyst feed ratio of 100 to 1 (Scheme 3.3). The selected (salicylaldiminato)aluminum complex **2** was previously demonstrated as a well performing catalyst in the ROP of LA and CL, allowing controlled chain growth in the absence of transesterification reactions.³⁰

Three different aliphatic polyesters were synthesized: a PLLA with certain monomeric units bearing the S-trityl functionality (sample **a**), a PCLA copolymer enriched in CL with isolated and functionalized lactidyl units (sample **b**), and a PCLA copolymer enriched in LA obtained by copolymerization of the TrtS-LA with CL and LA (sample **c**).



The obtained copolymers were characterized by ^1H and ^{13}C NMR spectroscopy, SEC and DSC analysis. The related results are summarized in Tables 3.1 and 3.2.

Table 3.1. Copolymerization of TrtS–LA with CL and LA.^a

Sample	$f_{\text{TrtS-LA}}^b$	f_{LA}^b	f_{CL}^b	$F_{\text{TrtS-LA}}^c$	F_{LA}^c	F_{CL}^c	Yield (%)	$M_{n,\text{th}}^d$ (kDa)	$M_{n,\text{NMR}}^e$ (kDa)	$M_{n,\text{SEC}}^f$ (kDa)	M_w/M_n^f
a	15	85	-	14	86	-	90	18.3	21.5	21.2	1.1
b	30	-	70	35	-	65	92	18.9	19.2	22.6	1.2
c	10	70	20	10	63	27	84	16.5	16.3	25.9	1.4

^aPolymerization conditions: toluene = 2.0 mL; precatalyst = 25 μmol ; MeOH = 25 μmol (0.25 mL of a 0.1 M toluene solution); 96 hours.

^bMolar ratio of monomers to precatalyst in the feed.

^cMol % of monomeric units in the copolymers determined by ^1H NMR spectra.

^dDerermined from the monomer/catalyst feed ratio and conversion.

^eDetermined by ^1H NMR by comparison of the relative intensities of main chain signals and the $-\text{OCH}_3$ end group peak.

^JDetermined by SEC in CHCl₃ vs polystyrene standards.

The copolymers were produced in high yield (up to 92 %; Table 3.1). Copolymer compositions, calculated by the ratio of the signal intensities in the ¹H NMR spectra, were close to the feed in all cases.

The ¹H NMR spectrum of poly[(TrtS-LA)-*co*-LA] (Table 1, sample **a**) is shown in Figure 3.3. In addition to the signals due to the PLA main chain, signals relative to the functionalized units appeared. In detail, signals in the aromatic region (7.42-7.18 ppm) relative to the S-trityl group (**6**, **7** and **8**) and two signals at 5.01 and 4.53 ppm attributable to the two methine protons (**2** and **4**) of TrtS-LA unit were detected.

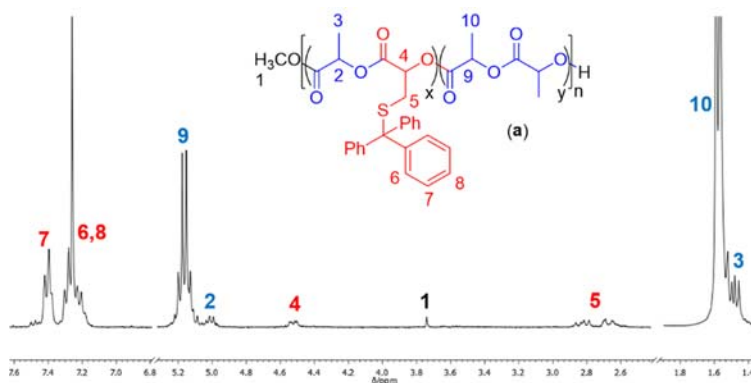


Figure 3.3. ¹H NMR (400 MHz, CDCl₃, RT) of poly[(TrtS-LA)-*co*-LA] (Table 3.1, sample **a**).

Moreover, a singlet relative to the methyl ester end group (**1**) at 3.74 ppm, probably generated by the insertion of the monomer units into Al-OCH₃, was also detected.^{30a} The copolymerization proceeded by the ROP of the 1,4-dioxane-2,5-dione core without affecting the pendant groups.

Interestingly, the ¹³C NMR of the poly[(TrtS-LA)-*co*-LA] showed four peaks in the carbonyl region. Having defined the lactyl moiety -C(O)CHCH₃- as **L** and the substituted lactyl moiety

$-C(O)CH(CH_2S\text{Trt})-$ as L^* , three of these peaks (169.8, 169.4 and 169.3 ppm) were attributed to those centered on the carbonyl group of a lactyl unit L according to their chemical shifts and relative intensities. In detail, the peak of higher intensity at 169.8 ppm was attributed to the homo-sequences (LL), and the other peaks were attributed to the hetero-sequences LL^* and L^*L . A signal at 167.5 ppm was attributed to the carbonyl group of the $-C(O)CH(CH_2S\text{Trt})-$, L^* , moiety. The simple pattern of signals suggests that the functional units $-C(O)CH(CH_2S\text{Trt})-$ were isolated in the polymeric chain.

The goal of the further copolymerizations was to prove the possibility of obtaining copolymers from TrtS-LA with CL and LA possessing different compositions. A copolymer whose main chain was made of $PCLA$, enriched in CL with isolated functionalized lactidyl units, was designed. The poly[(TrtS-LA)-*co*- CL] copolymer (Table 3.1, sample **b**) was prepared by copolymerization of TrtS-LA with CL (feed ratio of $\text{TrtS-LA}/CL = 30:70$). Another copolymer, enriched in LA , was obtained by copolymerization of TrtS-LA with CL and LA (poly[(TrtS-LA)-*co*- CL -*co*- LA] (Table 3.1, sample **c**) with a feed ratio of $\text{TrtS-LA}/LA/CL = 10:70:30$.

Selected regions of the 1H NMR spectra of poly[(TrtS-LA)-*co*- CL], sample **b**, and poly[(TrtS-LA)-*co*- CL -*co*- LA], sample **c**, (Table 3.1) are shown in Figure 3.4.

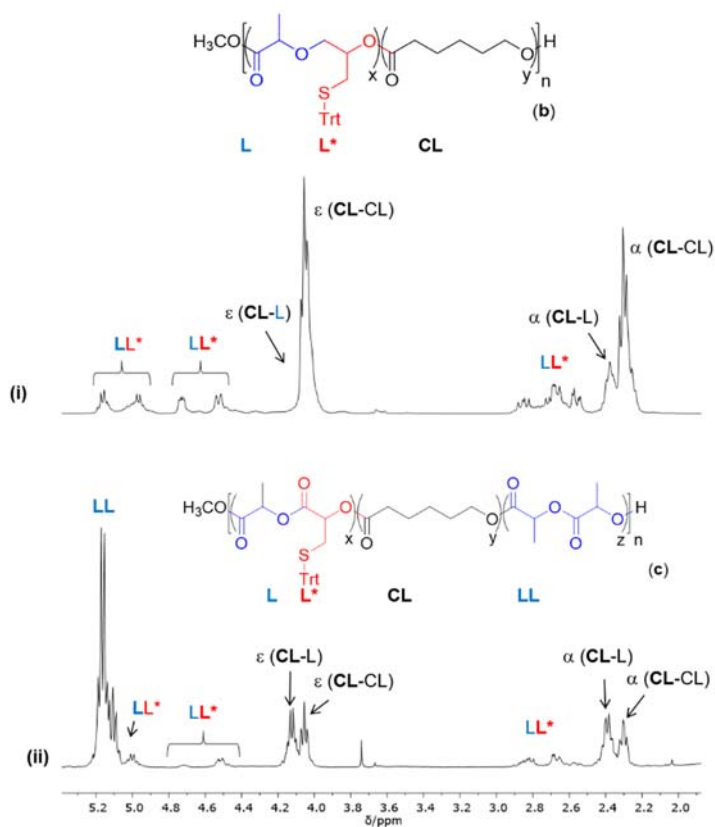


Figure 3.4. Selected regions of the ^1H NMR spectra (400 MHz, CDCl_3 , RT) of (i) poly[(TrtS-LA)-co-CL] (**b**) and (ii) poly[(TrtS-LA)-co-CL-co-LA] (**c**). Spectra not in scale.

In the NMR spectra, in addition to the signals relative to the opened TrtS-LA units, signals due to CL are observed. Moreover, signals due to the LL unit are recognized in the spectrum of sample **c** (Figure 3.4ii). Notably, the signals due to the α and ϵ methylene protons of the CL units revealed the presence of CL-L hetero-sequences (centered, respectively, at ca. 2.40 and 4.10 ppm), as previously observed for the PCLA copolymer.^{33a} Moreover, in the ^1H NMR spectrum of poly[(TrtS-LA)-co-CL] (sample **b**) four different signals were detected in the methine region. The two at higher chemical shifts 5.15 and 4.95 ppm were attributed to the methine proton of the L moiety, and the signals at 4.70 and 4.50 ppm were attributed to the

methine protons of the L^* moiety, which are coupled with the methylene protons at 2.75 ppm flanked by the functional group (Figure 3.4i).

Notably, an analogous pattern was observed in the carbonyl region of the ^{13}C NMR spectrum. The signal at 173.6 was attributed to the homo-sequence CL-CL, and the signals at 173.55, 172.7 and 172.6 were attributed to the hetero-sequences centered on the carbonyl groups of the CL unit. Moreover, two peaks at 170.0 and 169.9 ppm were attributed to the carbonyl groups of the L moiety, and two peaks at 168.1 and 160.8 ppm were attributed to those of the L^* moiety.

Because TrtS-LA has two different substituents in the α -positions with respect to the carbonyl groups, the number of signals observed in both the ^1H and ^{13}C NMR spectra is probably due to the cleavage of the two different acyl-oxygen bonds during ROP. Interestingly, consecutive L^*L^* sequences were not observed in any of the copolymers synthesized, even though all functional monomers had been incorporated. This could benefit the prefixed purposes because the monomer is totally incorporated and the functional groups are evenly distributed along the polymeric chain.

The molecular weights of the copolymers were evaluated by size exclusion chromatography (SEC) and by NMR in solution using the polymer end groups.^{30a,b} Good agreement between the molecular weight evaluated by NMR, $M_{n,\text{NMR}}$, and the theoretical molecular weights, $M_{n,\text{th}}$, calculated by the monomer/catalyst feed ratio was observed. SEC analysis performed on all samples revealed a monomodal molecular weight distribution with narrow dispersities of 1.1–1.4. The molecular weights measured by SEC, $M_{n,\text{SEC}}$, were 21.2–25.9 kDa, slightly higher than the $M_{n,\text{th}}$, which may be explained by considering that the analysis was performed using polystyrene standards.

Thus, the ring opening (co)polymerization of TrtS-LA with LA and CL, catalyzed by complex **2**, offers greater control over molecular weights and

molecular weight dispersities under relatively mild conditions compared to the polycondensation²³ or enzymatic approaches.²¹

Thermal properties of the synthesized copolymers were also evaluated by means of differential scanning calorimetry (DSC) from -80 to $+200$ °C. The glass transition, T_g , and melting temperatures, T_m , are given in Table 3.2.

Table 3.2. Copolymerization of TrtS–LA with CL and LA: thermal properties.^a

Sample	$F_{\text{TrtS-LA}}^b$	F_{LA}^b	F_{CL}^b	T_g^c (°C)	T_m^c (°C)	ΔH_m^c (Jg ⁻¹)
a	14	86	-	66.6	158.8	1.9
b	35	-	65	6.0	n.o.	n.o.
c	10	63	27	34.1	n.o.	n.o.

^aPolymerization conditions: toluene = 2.0 mL; precatalyst = 25 μmol ; MeOH = 25 μmol (0.25 mL of a 0.1 M toluene solution); 96 hours.

^bMol % of monomeric units in the copolymers determined by ¹H NMR spectra.

^cResult of the second scan of DSC analysis with a heating rate of 10 °C min⁻¹.

n.o. = not observed.

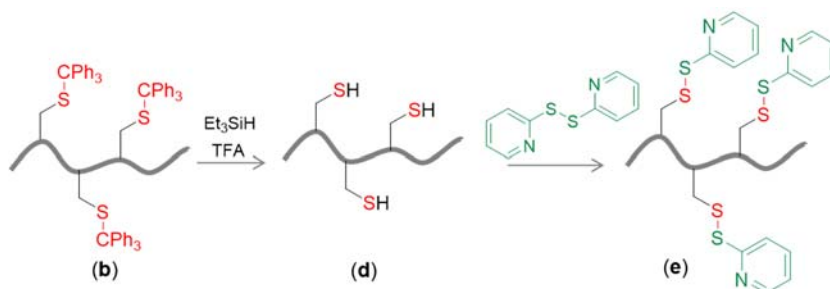
A content of 14 mol % of the TrtS–LA unit in a PLA chain does not affect the thermal properties of parent polymer, and poly[(TrtS–LA)-*co*-LA] (Table 3.2, sample **a**) has a T_g (66.6 °C) and T_m (158.8 °C) similar to those reported for isotactic PLA.³¹ The poly[(TrtS–LA)-*co*-CL] copolymer (Table 3.2, sample **b**), which appears waxy at room temperature, is amorphous, and the thermogram showed a T_g of 6.0 °C. Sample **c** (Table 3.2) is also amorphous with a T_g of 34.1 °C.

3.2.3. Polymer modifications

The thiol groups, protected as trityl thio-ether, are sites for further modifications, offering a wide range of possibilities for the fabrication of functional materials.

A polymeric sample bearing pyridyl disulfide groups (PDS) able to bind a cysteine-containing peptide was obtained by a two-step modification reaction. The pyridyl disulfide group is an attractive platform for post-polymerization modification *via* thiol-disulfide exchange reaction. This strategy has been previously exploited as a selective route to polymer-peptide conjugates in mild conditions and aqueous media.³² Bioconjugation with cysteine-containing peptides has been carried out at ambient temperature without the addition of any catalyst,³³ the formation of yellow 2-pyridinethiol allowed easy monitoring of the reaction by UV.

The copolymer sample poly[(TrtS-LA)-*co*-CL] (Table 3.1, sample **b**), richest in functional group, was chosen to perform the post-polymerization modification. After cleavage of the trityl groups, the modified copolymer bearing pyridyl disulfide pendant groups (PDS) was prepared (Scheme 3.4).



Scheme 3.4. Post-polymerization modification of poly[(TrtS-LA)-*co*-CL].

The selective removal of the trityl group is possible using a variety of conditions.²⁵ However, quantitative deprotection of the trityl thioethers has been achieved with trifluoroacetic acid (TFA) in the presence of triethylsilane (Et₃SiH).^{34,35} Treatment of the native sample **b** (Table 3.1) with an excess of TFA and Et₃SiH in CH₂Cl₂ selectively removed the protecting groups, and the copolymer bearing free thiol groups, poly[(HS-LA)-*co*-CL] (**d**), was obtained after 1 hour. The ¹H NMR analysis of this sample (Figure 3.5i) clearly showed the disappearance of

the signals related to the triphenylmethyl group in the aromatic region. Moreover, a shift of signals assigned to the methylene group near the sulfur $-CH_2S-$ (3) and methine $-CHCH_2S-$ (2) groups were observed (Figure 3.5i) by comparison with the 1H NMR of the native sample **b** (Figure 3.4i). The free thiol functionalities were then transformed into pyridyl disulfide groups (PDS) by reaction with an excess of 2,2'-pyridyl disulfide.³⁶ The modified sample poly[(PDS-LA)-*co*-CL] (**e**) was collected as a waxy solid, and the overall yield of the two steps was 90 %.

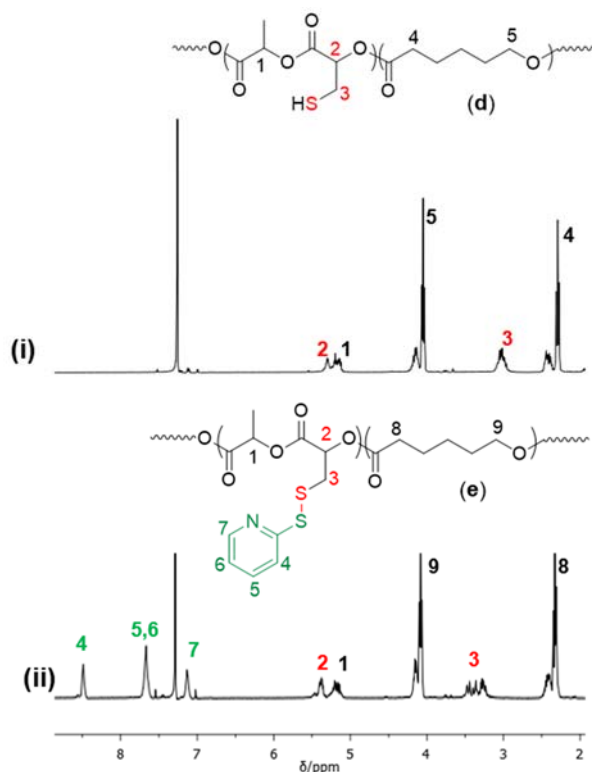


Figure 3.5. Selected region of the 1H NMR (400 MHz, $CDCl_3$, RT) of (i) poly[(HS-LA)-*co*-CL] (**d**) and (ii) poly[(PDS-LA)-*co*-CL] (**e**).

Three different signals due to the protons of the pyridyl ring could be recognized in the aromatic region of the 1H NMR spectrum of sample (**e**) (Figure 3.5ii), and a further shift of the methylene group $-CH_2S-$ was also detected. The other signals of the main chain remained unaffected by the

reactions, thus demonstrating that the initial copolymer composition did not vary at all. Further confirmation was derived from the SEC of poly[(PDS-LA)-*co*-CL] (**e**), which disclosed a monomodal molecular weight distribution with $M_n = 18.2$ kDa and $M_w/M_n = 1.6$. The decrease in molecular weight with respect to the native sample ($M_n = 22.6$ kDa; Table 1, sample **b**) is in agreement with the performed modification. The slight increase in the dispersity value from 1.2 to 1.6 could be due to side reactions during the derivatization steps.

The DSC thermogram of poly[(PDS-LA)-*co*-CL] (**e**) showed that the sample was amorphous with a $T_g = -18.4$ °C. The pyridyl disulfide groups probably allow greater mobility to the polymer chain than the bulky trityl groups.

3.2.4. Scaffold preparation and characterization

Previous results demonstrated that PCLA copolymers with a LA/CL = 75/25 molar ratio provided suitable physical properties to engineer three-dimensional porous scaffolds by the salt leaching method, and the scaffolds were able to support the proliferation and differentiation of different types of cells.³⁷

Thus, the prepared poly[(PDS-LA)-*co*-CL] (sample **e**) was blended with PCLA (LA/CL = 75/25, $M_n = 100.7$ kDa, $M_w/M_n = 1.2$) in different ratios. Porous scaffolds with different shapes and amounts of poly[(PDS-LA)-*co*-CL] were manufactured by the salt leaching method. Sodium chloride was used as the porogen agent. The particle size range was 75–500 μm , and the polymer(s)-to-salt weight ratio was 1:10.³⁷

Thick scaffolds (5 mm in thickness, 10 mm in diameter) and thin scaffolds (1 mm in thickness, 10 mm in diameter) were prepared from a blend containing poly[(PDS-LA)-*co*-CL] and PCLA (10:90 % w/w). The scaffolds completely retained their structure after salt leaching. Soft

scaffolds were obtained, and scanning electronic microscopy (SEM) was employed to analyze the structure. Representative SEM images of the fabricated porous scaffolds from the blend containing poly[(PDS-LA)-*co*-CL] and PCLA (10:90 % w/w) are shown in Figure 3.6.

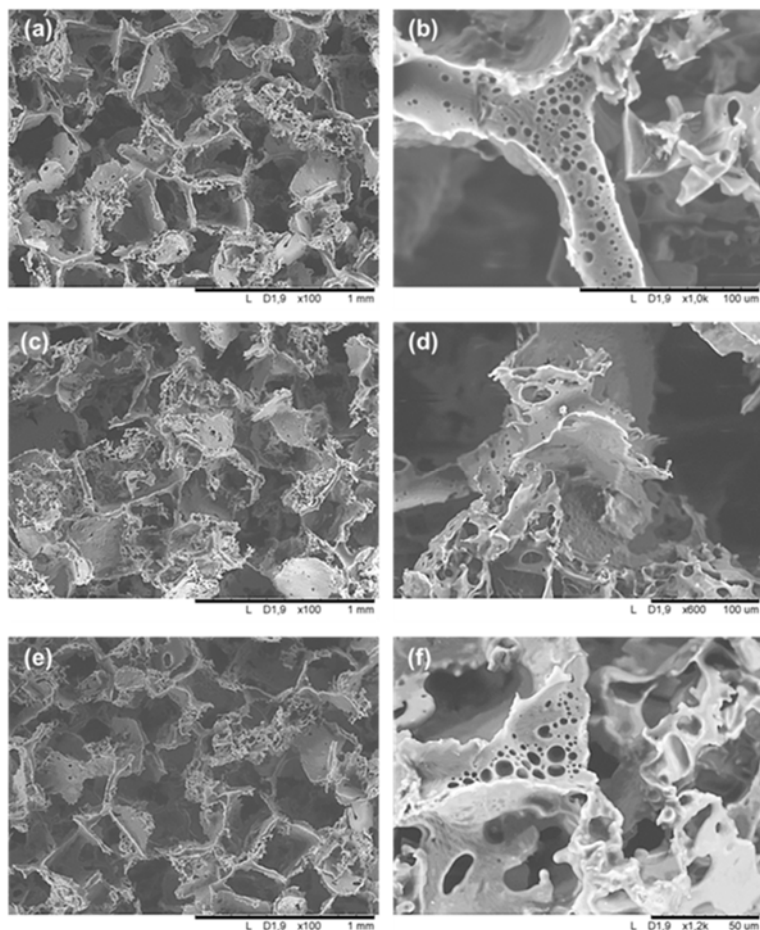


Figure 3.6. Selected SEM surface images of 3D porous scaffolds of: (a, b) copolymer PCLA; (c, d) poly[(PDS-LA)-*co*-CL]/PCLA 10:90 blend and (e, f) poly[(PDS-LA)-*co*-CL]/PCLA 10:90 blend after RGDC immobilization. Bar lengths are 1 mm (a, c and e); 100 μ m (b and d) and 50 μ m (f).

SEM images showed that the scaffolds were highly porous with pores of different sizes. The pores were also evenly distributed throughout the scaffolds, as shown in the cross-sectional SEM images. When the SEM

images of the scaffolds made from the poly[(PDS-LA)-*co*-CL]/PCLA/PCLA 10:90 blend were compared to the SEM images of the scaffolds made from PCLA, no differences were observed.

In a previous paper where only PCLA was used, a porosity higher than 83 % was determined by Micro-CT.³⁸ Those scaffolds were fabricated in the same way using the same porogen agent, and therefore a comparable porosity was assumed here.

The mechanical and thermal features were also evaluated and compared to those of PCLA-based scaffolds.

The mechanical properties were evaluated by a compression test in the *z*-direction at a rate of 10 % of the thickness/min until reaching a compressive strain of 80 %. For each sample, five parallel tests were carried out. The stress-strain compression curves and the calculated elastic modulus are reported in Figure 3.7.

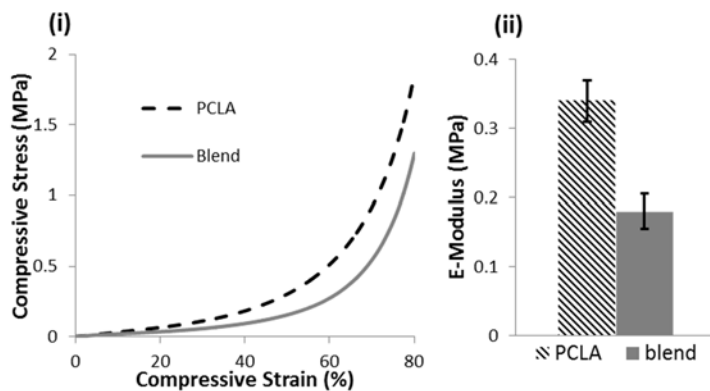


Figure 3.7. Stress-strain curves during compression tests (i) and the E-modulus (ii) of the PCLA (dashed black line) and poly[(PDS-LA)-*co*-CL]/PCLA 10:90 blend (solid grey) porous scaffolds.

The stress-strain curves obtained from the compression test showed that the mechanical behavior of the two types of scaffolds was similar. However, the poly[(PDS-LA)-*co*-CL]/PCLA 10:90 blend-based scaffold was less stiff than the PCLA-based scaffold (Figure 3.6i). More specifically, the

compressive E-modulus, calculated from the initial linear region of the stress-strain curve, decreased from 0.34 to 0.18 MPa (Figure 3.7ii).

After compression to 80 % of their thickness, the recovery of the scaffolds was measured after 1 h of relaxation. The recovery was (60 ± 4) % for the PCLA scaffolds and (55 ± 2) % for the poly[(PDS-LA)-*co*-CL]/PCLA 10:90 blend scaffolds.

Thermal analysis showed that a content of 10 % w/w of poly[(PDS-LA)-*co*-CL] in the PCLA scaffolds does not affect the thermal properties. Although the DSC thermogram of the poly[(PDS-LA)-*co*-CL] copolymer showed that the sample was amorphous with a $T_g = -18.4$ °C, the thermograms of the scaffolds made with PCLA and with the poly[(PDS-LA)-*co*-CL]/PCLA 10:90 blend were similar. In the case of the blend, a unique glass transition ($T_g = -31.8$ °C) was observed, confirming that a single phase was retained and the two copolymers were miscible. Moreover, the ^1H NMR spectra of different scaffold slices, obtained by cutting the frozen sample in liquid nitrogen, showed an equal ratio of pyridyl disulfide groups in the slides, thus indicating a homogeneous distribution of the PDS groups throughout the polymeric scaffolds.

Thus, when the content of poly[(PDS-LA)-*co*-CL] was 10 % by weight, all characterization data confirmed that it is possible to obtain an editable scaffold without significantly affecting the features of the PCLA-based scaffolds.

3.2.5. Peptide binding on 3D porous scaffolds and cytotoxicity evaluation

The side groups of functional aliphatic polyesters can be exploited to bind biologically active ligands.^{11c,39} In this case, pyridyl disulfide side groups were evenly incorporated into 3D porous scaffolds, offering the possibility to graft cell-binding motifs throughout the polymeric device. This type of

conjugate could provide a hybrid scaffold for tissue engineering with enhanced control over cell adhesion and functions.^{2,3}

As proof of concept, the simple cysteine-terminated RGD peptide (H-Arg-Gly-Asp-Cys-OH, RGDC) was chosen to investigate the ability of the pyridyl disulfide groups embedded in the polymeric scaffolds to undergo disulfide exchange with the free thiol functionality of the terminal cysteine unit (Scheme 3.5).



Scheme 3.5. RGDC peptide binding on 3D porous scaffolds by disulfide exchange.

Three different scaffolds containing different amounts of the pyridyl disulfide groups were used. In particular, blends of poly[(PSD-LA)-*co*-CL]/PCLA (10:90, 20:80 and 30:70 % w/w) were used to prepare the scaffolds by the salt leaching method, and disks, 1 mm in thickness and 10 mm in diameter, were manufactured.

The three different types of porous scaffolds, with contents of pyridyl disulfide groups of 2.9 , 4.6 and 6.6×10^{-6} mol, respectively, were allowed to react with 2.5 mL of peptide solution. The degree of immobilization was followed by UV analysis of the peptide solutions. The leaving group, 2-pyridinethiol, has a characteristic local maximum in UV absorbance at 343 nm. The concentration of the released 2-pyridinethiol was calculated according to Beer's Law with its known molar extinction coefficient.⁴⁰

The results of peptide immobilization for each type of scaffold are summarized in Figure 3.8, expressed as the mole percent of immobilized RGDC relative to the PDS groups incorporated in the scaffold.

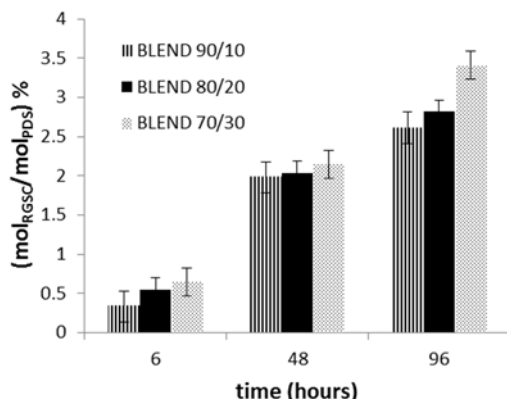


Figure 3.8. Histograms of the degree of peptide immobilization obtained for porous scaffolds made with 10:90, 20:80 and 30:70 % w/w blends of poly[(PSD–LA)-*co*-CL]/PCLA and PCLA.

The degree of immobilization increased with time, and the range of the percentage of functional groups replaced by the peptide was 2.6–3.4 % after 96 hours. However, no significant differences were observed between the different types of scaffolds. The amount of immobilized RGD peptide incorporated for each scaffold was $7.6\text{--}9.9 \times 10^{-8}$ mol.

The low percentage of functional groups replaced could be explained by the fact that the pyridyl disulfide groups are relatively hydrophobic and mainly embedded in the polymeric bulk. To estimate the amount of exposed PDS groups, one of the scaffold samples with the lowest content of functionalities (made with the poly[(PDS-LA)-*co*-CL]/PCLA 10:90 blend) was exposed to a solution of dithiothreitol (DTT; 10 equiv.) in PBS, which reacted with the disulfide bonds, releasing 2-pyridinethiol. The UV measurement of the leaving groups after 4 hours revealed that 7 % of the total PDS groups contained in the scaffold was cleaved. However, the calculated value of peptide immobilization from UV measurement of the 2-pyridinethiol concentration should be regarded with caution. This species can also be oxidized into the corresponding symmetrical disulfide, and thus

the value of immobilized RGD is probably underestimated by this method.⁴¹ Notably, Mikos *et al.* reported that an RGDS concentration of 10^{-7} mol cm⁻³, covalently linked to a poly(propylene fumarate-*co*-ethylene glycol)-based hydrogel, was sufficient to promote cell adhesion.⁴² Considering a volume of 0.08 cm³ for the entire scaffold, the calculated RGDC concentration in this case was $0.95\text{--}1.2 \times 10^{-6}$ mol cm⁻³, above the limit reported by Mikos.

SEM images were also obtained after the peptide was immobilized onto the scaffold sample and showed that the reaction did not affect the scaffold morphology and that the porous structure was completely preserved (Figure 3.7). An indirect cytotoxicity evaluation was conducted on these three different scaffolds after peptide immobilization, based on the viability of human dermal fibroblasts cultured with the extraction medium from blends of poly[(PSD-LA)-*co*-CL]/PCLA (10:90, 20:80 and 30:70 % w/w; Figure 3.9). The same evaluation was also performed with the extraction medium from a PCLA-based scaffold, used as reference.

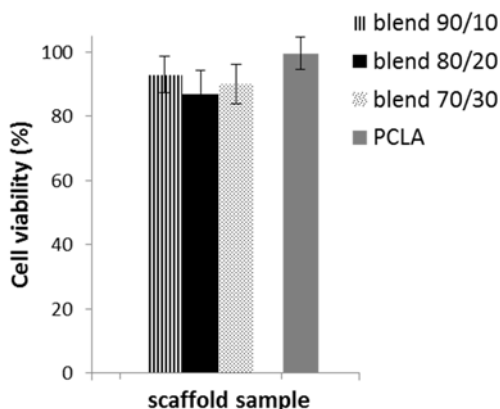


Figure 3.9. Histograms of the indirect cytotoxic evaluation based on the viability of human dermal fibroblasts obtained for porous scaffolds made with 10:90, 20:80 and 30:70 % w/w blends of poly[(PSD-LA)-*co*-CL]/PCLA and with PCLA.

A cell culture in fresh CGM served as the control. The viability of the cells, determined using an alamarBlue assay and reported as a percentage of the viability of the control, was 88–94 % for cells cultured with extraction media from scaffolds made with the different blends, whereas the viability obtained for the PCLA-based scaffold was 99 %.

CONCLUSIONS

The lack of functional groups in biodegradable aliphatic poly(ester)s is a serious drawback for the application of these materials in the biomedical field, i.e., as drug delivery systems or tissue engineering scaffolds. One of the most promising approaches towards functional polyesters is represented by the synthesis and subsequent ROP of cyclic (di)esters bearing a functional group.

The 3-methyl-6-(tritylthiomethyl)-1,4-dioxane-2,5-dione, a lactide-type monomer bearing a thiol-protected group as trityl thioether, was designed and synthesized. The co-polymerization *via* ROP of such monomer with LA and CL efficiently produced aliphatic polyesters with pendant *masked* mercapto groups. The TrtS-LA monomer was totally incorporated and the functional units were well spread along the chains.

The selected *trityl* protecting group was not only sufficiently robust to resist to the polymerization conditions but also easily removed in mild conditions. The cleavage of the protecting groups gave the “free” pendant thiols, which were subsequently converted into pyridylthiol groups, without any change in the degree of polymerizations.

Therefore, after polymerization, further modification could be carried out in specific manner without affecting the poly(ester) main chain. Notably, both functionalities, i.e. thiol and pyridylthiol, represent useful platforms for a broad range of reactions.

In this study, having in mind biomedical applications as ultimate goal, the functional *pyridyl* derivative was blended with PCLA, and editable porous scaffolds, showing a highly porous morphology, were obtained by salt leaching method.

Exploiting a disulfide exchange reaction, the binding of a peptide sequence containing a cysteine unit, RGDC, was performed to demonstrate the potential to graft any thiolated motif to the aliphatic poly(ester) main chain.

The as-prepared peptide-functionalized porous scaffolds could be promising candidates to support the proliferation and differentiation of different types of cells.

Moreover, the synthesized monomer, due to the high versatility of the thiol functionality, represents a useful *tile* for the synthesis of functional biodegradable aliphatic polyesters, opening the way to fabricate more complex polymeric architectures, stimuli responsive polymers, hybrid materials or peptide-polymer conjugates, thus, expanding and amplifying the applicability of the aliphatic polyesters materials.

The main part of this study was carried out at Department of Fibre and Polymer Technology, KTH, Royal Institute of Technology of Stockholm, where I spent a period as a visiting PhD student from February to September 2015, under the guide of Prof. Anna Finne-Wistrand.

The result presented and discussed here have been submitted for publication.⁴³

References

- ¹ (a) R. Langer, J. P. Vacanti, *Science* **1993**, *260*, 920–926. (b) P.X. Ma, *Mater. Today* **2004**, *7*, 30–40.
- ² G. Delaittre, A. M. Greiner, T. Pauloehrl, M. Bastmeyer, C. Barner-Kowollik, *Soft Matter* **2012**, *8*, 7323–7347.
- ³ (a) U. Hershel, C. Dahmen, H. Kessler, *Biomaterials* **2003**, *24*, 4385–4415. (b) L. Perlin, S. MacNeil, S. Rimmer, *Soft Matter* **2008**, *4*, 2331–2349.
- ⁴ H. Seyednejad, A. H. Ghassemi, C. F. van Nostrum, T. Vermonden, W.E. Hennink, *J. Control. Release* **2011**, *152*, 168–176.
- ⁵ (a) S. Ponsart, J. Coudane, M. Vert, *Biomacromolecules* **2000**, *1*, 275–281. (b) B. Guo, A. Finne-Wistrand, A.-C. Albertsson, *Macromolecules* **2012**, *45*, 652–659.
- ⁶ B. Saulnier, S. Ponsart, J. Coudane, H. Garreau, M. Vert, *Macromol. Biosci.* **2004**, *4*, 232–237.
- ⁷ (a) R. J. Pounder, A. P. Dove, *Polym. Chem.* **2010**, *1*, 260–271. (a) Y. Yu, J. Zou, C. Cheng, *Polym. Chem.* **2014**, *5*, 5854–5872.
- ⁸ (a) Y. Kimura, K. Shirotani, H. Yamane, T. Kitao, *Macromolecules* **1988**, *21*, 3340–3341. (b) Y. Kimura, K. Shirotani, H. Yamane, T. Kitao, *Polymer* **1993**, *34* (8), 1741–1748.
- ⁹ R. J. Pounder, A. P. Dove, *Biomacromolecules* **2010**, *11*, 1930–1939.
- ¹⁰ (a) W. W. Gerhardt, D. E. Noga, K. I. Hardcastle, A. J. García, D. M. Collard, M. Weck, *Biomacromolecules* **2006**, *7*, 1735–1742. (b) O. T. du Boullay, N. Saffon, J.-P. Diehl, B. Martin-Vaca, D. Bourissou, *Biomacromolecules* **2010**, *11*, 1921–1929.
- ¹¹ (a) M. Leemhuis, C. F. van Nostrum, J. A. W. Kruitzer, Z. Y. Zhong, ten M. R. Breteler, P. J. Dijkstra, J. Feijen, W. E. Hennink, *Macromolecules* **2006**, *39*, 3500–3508. (b) C. A. M. Loontjens, T. Vermonden, M.

Leemhuis, M. J. van Steenberg, C. F. van Nostrum, W. E. Hennink, *Macromolecules* **2007**, *40*, 7208–7216. (c) D. E. Noga, T. A. Petrie, A. Kumar, M. Weck, A. J. García, D. M. Collard, *Biomacromolecules* **2008**, *9*, 2056–2062.

¹² (a) M. Yin, G. L. Baker, *Macromolecules* **1999**, *32*, 7711–7718. (b) T. Trimaille, M. Möller, R. Gurny, *Polym. Sci., Part A: Polym. Chem.* **2004**, *42*, 4379–4391. (c) F. Jing, M. R. Smith, G. L. Baker, *Macromolecules* **2007**, *40*, 9304–9312. (d) X. Jiang, E. B. Vogel, M. R. Smith, G. L. Baker, *Macromolecules* **2008**, *41*, 1937–1944. (e) M. Leemhuis, N. Akeroyd, J. A. W. Kruijtzter, C. F. van Nostrum, W. E. Hennink, *Eur. Polym. J.* **2008**, *44*, 308–317. (f) J. Zou, C. C. Hew, E. Themistou, Y. Li, C.-K. Chen, P. Alexandridis, C. Cheng, *Adv. Mater.* **2011**, *23*, 4274–4277.

¹³ S. Deechongkit, S.-L. You, J. Kelly, *Org. Lett.* **2004**, *6*, 497–500.

¹⁴ N. Cohen-Arazi, J. Katzhendler, M. Kolitz, A. J. Domb, *Macromolecules* **2008**, *41*, 7259–7263.

¹⁵ (a) C. E. Hoyle, A. B. Lowe, C. N. Bowman, *Chem. Soc. Rev.* **2010**, *39*, 1355–1387. (b) M. Le Neindre, R. Nicolay, *Polym. Chem.* **2014**, *5*, 4601–4611.

¹⁶ M. H. Stenzel, *ACS Macro Lett.* **2013**, *2*, 14–18.

¹⁷ (a) A. Dondoni, *Angew. Chem. Int. Ed.* **2008**, *47*, 8995–8997. (b) A.B. Lowe, *Polym. Chem.* **2010**, *1*, 17–35. (c) A.B. Lowe, *Polym. Chem.* **2014**, *5*, 4820–4870.

¹⁸ (a) C. Li, J. Madsen, S. P. Armes, A. L. Lewis, *Angew. Chem. Int. Ed.* **2006**, *45*, 3510–3513. (b) D. Roy, J. N. Cambre, B. S. Sumerlin, *Prog. Polym. Sci.* **2010**, *35*, 278–301. (c) J. Zhuang, R. Chacko, D. F. Amado Torres, H. Wang, S. Thayumanavan, *ACS Macro Lett.* **2014**, *3*, 1–5.

¹⁹ (a) M. Trollsås, C. J. Hawker, J. L. Hedrick, G. Carrot, J. Hilborn, *Macromolecules* **1998**, *31*, 5960–5963. (b) G. Carrot, J. G. Hilborn, M. Trollsås, J. L. Hedrick, *Macromolecules* **1999**, *32*, 5264–5269. (c) C.

Hedfors, E. Östmark, E. Malmström, K. Hult, M. Martinelle, *Macromolecules* **2005**, *38*, 647–649. (d) M. A. Kryuchkov, Y. H. Qi, I. I. Perepichka, C. Pelletier, A. Regnaud, Z. Song, S. K. Varshney, *React. Funct. Polym.* **2015**, *90*, 1–6.

²⁰ (a) B. K. Sourkahi, A. Cunningham, Q. Zhang, J. K. Oh, *Biomacromolecules* **2011**, *12*, 3819–3825. (b) N. R. Ko, J. K. Oh, *Biomacromolecules* **2014**, *15*, 3180–3189.

²¹ (a) M. Kato, K. Toshima, S. Matsumura, *Biomacromolecules* **2009**, *10*, 366–373. (b) A. Tanaka, K. Masuri, T. Takighchi, M. Kato, S. Matsumura, *Polym. Degrad. Stabil.* **2012**, *97*, 1415–1422.

²² K. Yamamoto, A. Takasu, *Macromolecules* **2010**, *43*, 366–373.

²³ D. Pappalardo, S. Målberg, A. Finne-Wistrand, A.-C. Albertsson, *J. Polym. Sci., Part A: Polym. Chem.* **2012**, *50*, 792–800.

²⁴ (a) A.-C. Albertsson, I. K. Varma, *Biomacromolecules* **2003**, *4*, 1466–1486. (b) O. Dechy-Cabaret, B. Martin-Vaca, D. Bourissou, *Chem. Rev.* **2004**, *104*, 6147–6176. (c) R. H. Platel, L. M. Hodgson, C. K. Williams, *Polym. Rev.* **2008**, *48*, 11–63. (d) C. M. Thomas, *Chem. Soc. Rev.* **2010**, *39*, 165–173.

²⁵ T. W. Greene, P. G. M. Wuts, *Protective Groups in Organic Synthesis*, 3rd Edition, Wiley, New York, **1999**.

²⁶ K. Wisniewski, *Org. Prep. Proced. Int.* **1999**, *31*(2), 211–214.

²⁷ A. S. Scheibelhoffer, W. A. Blose, H. Harwood, *J. Polym. Prepr. (Am. Chem. Soc., Div. Polym. Chem.)* **1969**, *10*, 1375–1380.

²⁸ F. Jing, M. A. Hillmyer, *J. Am. Chem. Soc.* **2008**, *130*, 13826–13827.

²⁹ T. R. Long, A. Wongrakpanich, A.-V. Do, A. K. Salem, N. B. Bowden, *Polym. Chem.* **2015**, DOI: 10.1039/C5PY01059D.

³⁰ (a) D. Pappalardo, L. Annunziata, C. Pellicchia, *Macromolecules* **2009**, *42*, 6056–6062. (b) A. Meduri, T. Fuoco, M. Lamberti, C. Pellicchia, D. Pappalardo, *Macromolecules* **2014**, *47*, 534–543. (c) T. Fuoco, A. Meduri,

M. Lamberti, C. Pellecchia, D. Pappalardo, *J. Appl. Polym. Sci.* **2015**, *132*, 42567.

³¹ X. Lou, C. Detrembleur, R. Jerome, *Macromol. Rapid Commun.* **2003**, *24*, 161–172.

³² D. R. Grassetti, J. F., Jr. Murray, *Arch. Biochem. Biophys.* **1967**, *119*, 41–49.

³³ (a) G. T. Zugates, D. G. Anderson, S. R. Little, I. E. B. Lawhorn, R. Langer, *J. Am. Chem. Soc.* **2006**, *128*, 12726–12734. (b) J.-H. Ryu, S. Jiwanich, R. Chacko, S. Bickerton, S. Thayumanavan, *J. Am. Chem. Soc.* **2010**, *132*, 8246–8247.

³⁴ R. S. Narayan, M. S. van Nieuwenhze, *Org. Lett.* **2005**, *7* (13), 2655–2658.

³⁵ D. A. Pearson, M. Blanchette, M. L. Baker, C. A. Guindon, *Tetrahedron Lett.* **1989**, *30* (21), 2739–2742.

³⁶ W. Zhao, W. Liu, J. Ge, J. Wu, W. Zhang, X. Meng, P. Wang, *J. Mater. Chem.* **2011**, *21*, 13561–13568.

³⁷ S. Danmark, A. Finne-Wistrand, M. Wendel, K. Arvidson, A.-C. Albertsson, K. Mustafa, *J. Bioact. Compat. Polym.* **2010**, *25*, 207–223.

³⁸ S. Suliman, H. Parajuli, Y. Sun, A. C. Johannessen, A. Finne-Wistrand, E. McCormarck, K. Mustafa, D. E. Costea, *Head Neck.* **2015**, DOI: 10.1002/hed.24187.

³⁹ D. E. Borchmann, N. ten Brummelhuis, Weck, M. *Macromolecules* **2013**, *46*, 4426–4431.

⁴⁰ H. Sun, A. Wirsén, A.-C. Albertsson, *Biomacromolecules* **2004**, *5*, 2275–2280.

⁴¹ S. Stoyanov, I. Petkov, L. Antonov, T. Stoyanova, P. Karagiannidis, P. Aslandis, *Can. J. Chem.* **1990**, *68*, 1482–1489.

⁴² E. Behraves, K. Zygourakis, A. G. Mikos, *J. Biomed. Mater. Res.* **2003**, *65A* (2), 260–270.

⁴³ T. Fuoco, A. Finne-Wistrand, D. Pappalardo, *submitted*.

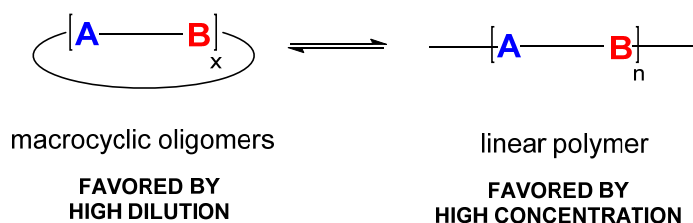
4. RING-OPENING POLYMERIZATION OF ω -6-HEXADECENYLACTONE: A ROUTE TO SEMICRYSTALLINE AND FUNCTIONAL POLY(ESTER)S

4.1. Introduction

In recent years many research studies have been devoted to the ROP of small or medium size cyclic esters: in these processes the driving force is the relief of the ring-strain, an enthalpy-driven process.¹

On the contrary, the ROP of large cyclic esters is a far less explored and now emerging field. These large lactones and macrolides were anticipated to have low polymerizability, due to the presence of an unstrained ring.² Indeed, when the ring size is large enough (usually ≥ 14 atoms), changes in enthalpy upon opening are minimal and polymerization becomes entropy-driven through an increase of conformational freedom.

The entropy-driven ROP is neither a step-growth nor a chain-growth process; however, its background lies in the step-growth polymerizations, which produce a fraction of cyclic oligomers.^{2a,3} Entropy-driven ROP exploits a ring-chain equilibrium between macrocycles and the polymer chains which leads to the most probable molecular weight distribution, i.e. $M_w/M_n \approx 2$.^{2,3} Because of the equilibrium, high dilution favors the monomers or cyclic oligomers, while high concentration favors the linear polymeric product. In other words, the absence of ring-strain results in a similar rate for polymerization and transesterification processes (Scheme 4.1).^{2c}



Scheme 4.1. Ring-chain equilibrium.

Notably, the ROP of large lactones, such as pentadecalactone (PDL), has been receiving an increasing interest because this class of monomers could be derived from bio-based feedstock and, furthermore, the related polymers are semicrystalline materials with properties comparable to polyethylene.⁴ Different approaches have been investigated for the ROP of large lactones. Anionic polymerization was explored and it produced relatively low molecular weight polymers accompanied by cyclic oligomers.⁵ Furthermore, the enzymatic method of polymerization of these large lactones proved to be successful. In particular, the lipase-catalyzed polymerization of macrolides showed higher rates affording high molecular weight products.^{4,6} However, low control on the microstructures of the polymers was achieved, due to the frequent transesterification reactions. Moreover, the production of poly(hydroxyalkanoate)s by enzymes is limited by the high cost, compared to the costs associated with the chemical route.

The polymerization of large lactones by some traditional ROP catalysts was explored, but it generally produced only low yields and low molecular weight polymers, or required long polymerization time.⁷ Organic catalysts were also used for the polymerization of pentadecalactone (PDL) and its copolymerization with ϵ -caprolactone (CL), and they also produced low molecular weight polymers.⁸

In this contest, the pioneering work of Duchateau *et al.*, with the production of high molecular weight polyesters from macrolactones by aluminum

salen complexes, emerged as a breakthrough.^{9a} This result represented a very promising route to the production of degradable “polyethylene-like” materials from renewable building block. Subsequently, few other single-site metal complexes based on aluminum, zinc and calcium were disclosed to homopolymerize the PDL to high molecular weight polymer, and, in proper conditions, to copolymerize it with smaller lactones, such as CL^{9b-d} and the branched ϵ -decalactone,^{9f} to random or block copolymers. Very recently, the “immortal” ROP of PDL by magnesium based initiator was also reported.^{9e}

It is apparent, then, that in the literature there is a paucity of catalysts capable of efficiently polymerize macrolactones. As previously reported in this thesis, dimethyl(salicylaldiminato)aluminum compounds were able to catalyze the homo- and copolymerization of LA with CL¹⁰ and with GA¹¹ to random, blocky or di-block copolymers. Such systems resulted highly efficient for the achievement of a controlled polymerization and very versatile for modulating the copolymers microstructure and the related thermal properties. Therefore, a further aim of this doctoral project was to explore the ROP of large lactones in the presence of salicylaldiminatoaluminum compounds.

The dimethyl(salicylaldiminato)aluminum compound **2** was tested as precatalyst in the ROP of the unsaturated ω -6-hexadecenlactone (6HDL). The chosen macrolactone, 6HDL, even though is commercial available and it is used in the fragrance industry with a worldwide volume of around 1.0 metric ton per year, was never described as monomer in ROP.¹² The 6HDL could represent a useful platform to design and synthesize novel polyesters aimed to be *semicrystalline* and *functional* at the same time. Indeed, the double bond does not interfere with the ring-opening polymerization and it could provide a straightforward functionality for crosslinking¹³ and/or further chemical modifications of the obtained polymeric chains. Thus, in this research project, post-polymerization modifications of the polymer

chains involving the double bonds by simple and effective reactions were performed and are described herein.

Notably, similar large unsaturated lactones, such as ambrettolide and globalide, have been previously used in enzymatic polymerization.^{6f} The globalide (11/12-pentadecen-15-olide) is a mixture of isomers with the double bond at the 11 or 12 position, whether the geometry of the double bond (*E* or *Z* isomers) is unclear.^{2c} Ambrettolide, a natural occurring unsaturated macrolactone, presents the double bond in *cis* (*Z*) configuration.^{2c} The selected macrolactone, 6HDL, instead, is commercially available as a single positional and geometric *trans* (*E*) isomer. As learned from Nature, the presence of the double bonds in “*trans*” geometry would allow a better level of order and a good packaging of the polymeric chains than that achievable when double bonds are in “*cis*” geometry.¹⁴

The polymerization of 6HDL was tested in different experimental conditions. Moreover, the feasibility of random and block copolymerization with the smaller CL and *rac*-LA was also studied. All the polymeric samples were characterized by NMR spectroscopy, GPC and DSC. In particular, the thermal and structural properties of semicrystalline poly(ω -6-hexadecenlactone) and its functional derivatives were also studied and compared.

4.2. Results and discussion

4.2.1. Ring-opening polymerization of ω -6-hexadecenlactone

The ring-opening polymerization of the 6- ω -hexadecenlactone (6HDL) was not described in the literature. The molecule was instead already described

as a starting material for the synthesis of surfactants, as a fragrance ingredient and for toner manufacturing.^{12,15}

The molecule is a large ring size unsaturated lactone. The geometry of the double bond was established by ¹³C NMR, showing a single couple of peaks (at 131.2 and 130.6 ppm) and by ¹H NMR analysis in combination with homodecoupling experiments. The calculated ³J value was 15.2 Hz, a typical value for the coupling of vicinal hydrogen atoms in *trans* (*E*) alkenes (Figure 4.1).

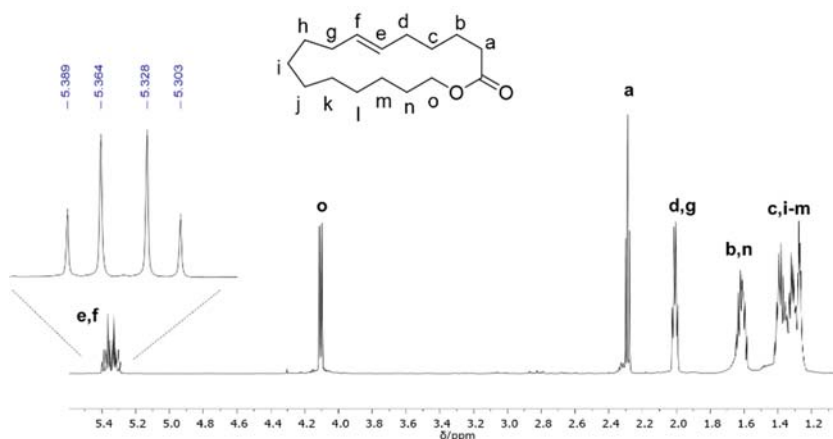
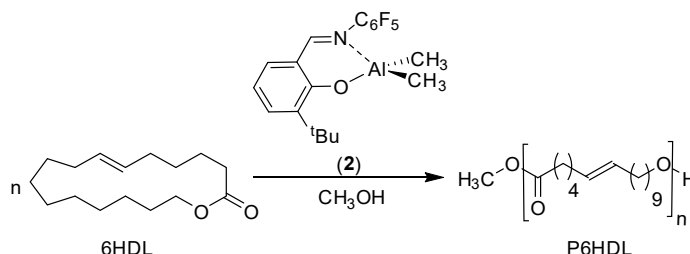


Figure 4.1. ¹H NMR (600 MHz, CDCl₃, RT) of 6HDL. In the enlargement, homonuclear-decoupled ¹H NMR of olefinic region irradiating the allylic protons ($\delta = 2.0$ ppm; **d, g**).

The polymerization of the 6HDL was performed in xylenes solution, in the presence of complex **2** and one equivalent of methanol, under different conditions (Scheme 4.2).



Scheme 4.2. ROP of ω -6-hexadecenlactone by catalyst **2**.

The obtained polymeric samples were characterized by ^1H and ^{13}C NMR spectroscopy, GPC and DSC. Illustrative results are shown in Table 4.1.

Table 4.1. Polymerization of ω -6-hexadecenlactone.

Run	[6HDL] ₀ /[2] ^c	T (°C)	t (h)	Conv (%) ^d	Yield (%)	M _{n,th} ^e (kDa)	M _{n,NMR} (kDa)	M _{n,GPC} ^f (kDa)	M _w /M _n ^f
1 ^a	100	100	4	34	28	8.6	8.9	18.3	1.6
2 ^a	100	100	8	42	34	10.5	11.4	23.1	1.6
3 ^a	100	100	16	44	40	11.1	12.0	27.2	1.6
4 ^a	100	100	24	54	47	13.6	12.7	34.9	1.6
5 ^b	100	100	27	60	60	15.1	15.4	40.0	1.6
6 ^a	10	100	18	87	n.d.	2.2	2.7	n.d.	n.d.
7 ^b	100	130	27	48	48	12.1	14.1	33.0	1.5
8 ^{b,g}	100	130	27	31	26	7.7	9.6	17.7	1.7
9 ^b	250	130	27	49	45	30.9	36.3	50.0	1.6

Polymerization conditions: ^aXylenes = 0.8 mL; precatalyst = 12 μmol ; MeOH = 12 μmol (0.12 mL of a 0.1 M toluene solution). ^bXylenes = 2.3 mL; precatalyst = 35 μmol ; MeOH = 35 μmol (0.35 mL of a 0.1 M toluene solution).

^cMol ratio of monomer to precatalyst in the feed.

^dDetermined by ^1H NMR from the ω -methylene resonances of monomer and obtained polymer.

^eCalculated from monomer conversion.

^fDetermined by GPC vs polystyrene standards.

^gReaction performed in 5 mL of xylenes.

n.d. = not determined.

A typical ^1H NMR spectrum of a poly(ω -6-hexadecenlactone) (P6HDL) is shown in Figure 4.2i. Signals due to the methylenes of the main chain and the signal due to the double bond ($\delta = 5.37$ ppm, **f**, **g**) were recognized. Conversely, inspection of the ^{13}C NMR spectrum showed a couple of peaks with the same intensity at 130.6 and 130.3 ppm, corresponding to the *trans* configuration of the double bond. Obviously, the ROP process did not affect the configuration of the double bonds.

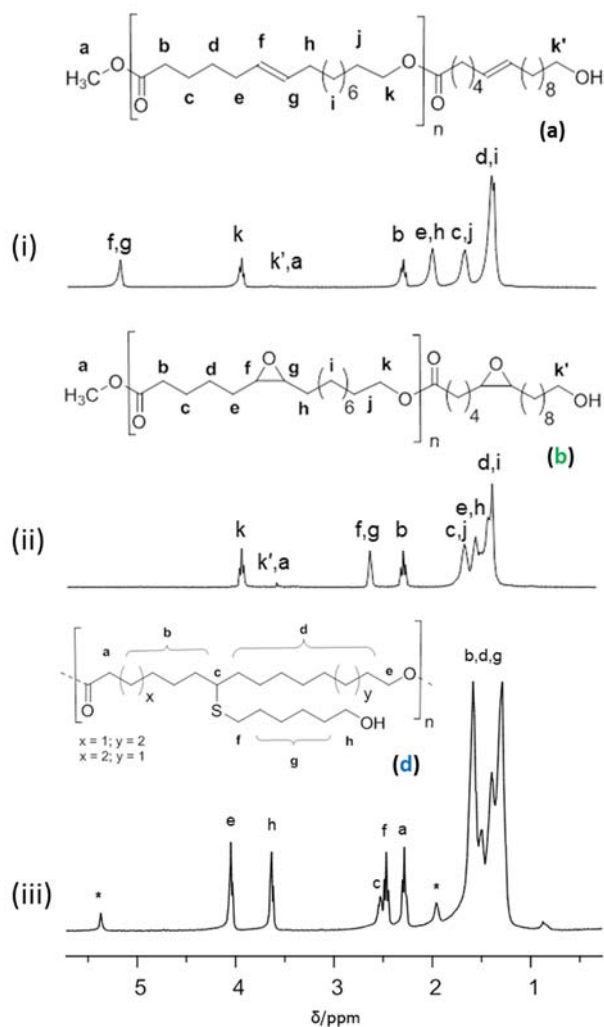


Figure 4.2. ^1H NMR (300 MHz, CDCl_3) of (i) P(6HDL); (ii) epoxidized P(6HDL); (iii) P(HDL) with pendant mercapto groups.

Significantly, in the ^1H NMR spectrum a signal attributable to the hydroxyl methylene end group ($\delta = 3.63$ ppm, $-\text{CH}_2\text{CH}_2\text{OH}$, **k'**) and a singlet relative to the methyl ester end group ($\delta = 3.66$ ppm, $-\text{COOCH}_3$, **a**) were detected. As previously observed, the methyl ester end group should be generated by insertion of the monomer unit into the Al-OCH_3 bond, formed in situ by reaction of the dimethylaluminum compound with CH_3OH ,¹⁶ while the

hydroxyl end group should be generated by hydrolysis of the growing chain. Therefore, a “coordination-insertion” mechanism proceeding through acyl-oxygen cleavage should be operative in this system also for the ROP of the macrolactone.¹⁰

The molecular weight of the samples was determined by NMR and GPC. GPC analysis showed monomodal molecular weight distribution with dispersity of 1.6. It is worth noting that since the GPC analysis was run using THF as elution solvent vs polystyrene standards, and since correction factors are not available in the literature for the studied polymers, the $M_{n,GPC}$ should be used with special care, while the $M_{n,NMR}$ values are more reliable. In detail, the $M_{n,NMR}$ were calculated from the integral ratio of the signal relative to the main chain methylene protons ($\delta = 4.04$ ppm, -CH₂-OC(O), **k**) and the singlet relative to the terminal -OCH₃ protons ($\delta = 3.66$ ppm, **a**). The $M_{n,NMR}$ values are in good agreement with the theoretical molecular weight, $M_{n,th}$ calculated on the basis of the monomer/catalyst feed ratio and the conversion (Table 4.1).

A set of polymerization runs was carried out at increasing time (Table 4.1, runs 1-5). The molecular weights of polymers linearly increased with time and conversion (Figure 4.3).

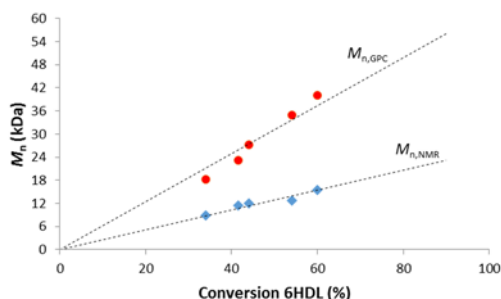


Figure 4.3. $M_{n,NMR}$ and $M_{n,GPC}$ versus conversion plot for ROP of P6HDL (Table 4.1, runs 1-5).

Notably, the dispersity values were below 2 (see Table 4.1, $M_w/M_n = 1.6$) and remained constant during the reaction time. This pseudo-*living* character of the polymerization was previously discovered for the aluminum salen based catalysts, active in the ROP of pentadecalactone (PDL). However, in the latter case, the poly(pentadecalactone) (PPDL) obtained showed higher dispersities ($M_w/M_n \geq 2$).^{9a,b,f} The values observed in the presence of compound **2**, instead, compare well with those recently reported for the best performing catalyst in the ROP of macrolactone.^{9d} The incomplete monomer conversion, leveled off around 60 %, could be due to the high viscosity of the medium, which hampered the monomer diffusion. Indeed, kinetic studies performed by ¹H NMR (Figure 4.4i) showed that full conversion was not achieved with a monomer/catalyst ratio of 100/1 and 50/1, even after prolonged reaction time (24 hours). However, when the monomer/catalyst ratio was decreased to 20/1, because of the lower molecular weight of the polymeric chains, the viscosity of the reaction medium decreased and almost full conversions were achieved with higher rates (Figure 4.4i).

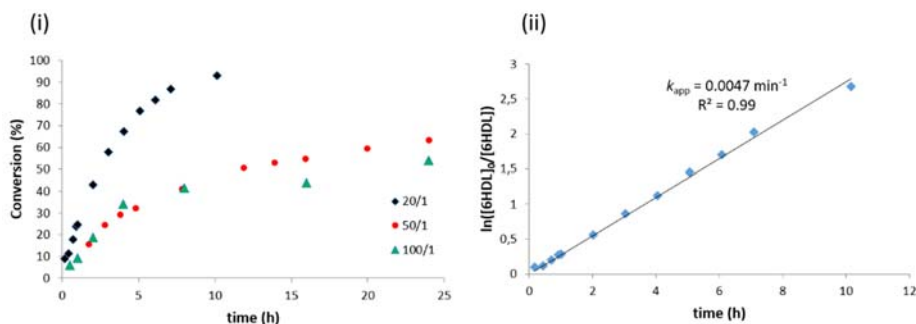


Figure 4.4. Kinetics studies for ROP of 6HDL determined by ¹H NMR spectra using toluene-*d*₈ as solvent and T = 80 °C. (i) Conversion (%) versus time (h) plots at different monomer/catalyst feed ratios: (◆) [6HDL]₀ = 1.0 M, [2] and [MeOH] = 5 × 10⁻² M; (●) [6HDL]₀ = 1.0 M; [2] and [MeOH] = 2 × 10⁻² M; (▲) [6HDL]₀ = 1.5 M, [2] and [MeOH] = 1.5 × 10⁻² M. (ii) Pseudo first-order kinetic plot; [6HDL]₀ = 1.0 M, [2] and [MeOH] = 5.0 × 10⁻² M.

More in-depth kinetics investigations were performed by ^1H NMR at $80\text{ }^\circ\text{C}$ in toluene- d_8 as solvent (Figure 4.4ii). To follow the progress of the 6HDL conversion by NMR, avoiding the viscosity problems depicted above, the initial monomer/initiator concentration ratio was fixed to 20/1. The reaction kinetics featured a pseudo-first-order dependence in the 6HDL concentration, as reported in Figure 4.4ii: the semi-logarithmic plot of $\ln([\text{6HDL}]_0/[\text{6HDL}]_t)$ versus time was linear with a slope of 0.0047 min^{-1} . This value, however, is lower than the polymerization rate of aluminum-salen based initiators.^{9a}

It is worth to note that as discussed in the Introduction, incomplete conversions may be also due to the equilibrium between monomer and polymer, which is typical feature of the “entropy-driven” polymerization of macrolactones.² This equilibrium would also affect the chain lengths and would also explain the observed dispersities.^{2a} Indeed, cyclic oligomeric species have been previously observed in the ROP of various macrolactones promoted by anionic,⁵ organic initiators,⁸ as well as by metal complexes.^{3,9a, d-f} To investigate the presence of cyclic oligomeric species also in our system, a low molecular weight P6HDL was synthesized (Table 4.1, run 6), and analyzed by MALDI-ToF-MS. The analysis showed the presence of cyclic oligomeric species, probably formed by “backbiting” side reactions, along with the major distribution of linear P6HDL chains, end-capped with methoxy groups (Figure 4.5).

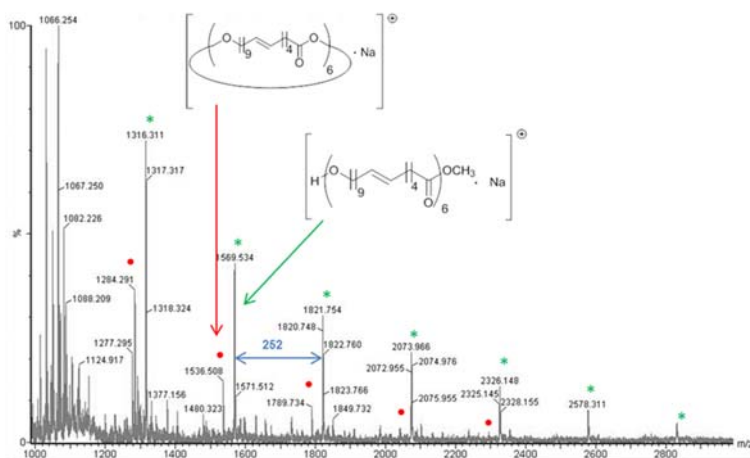


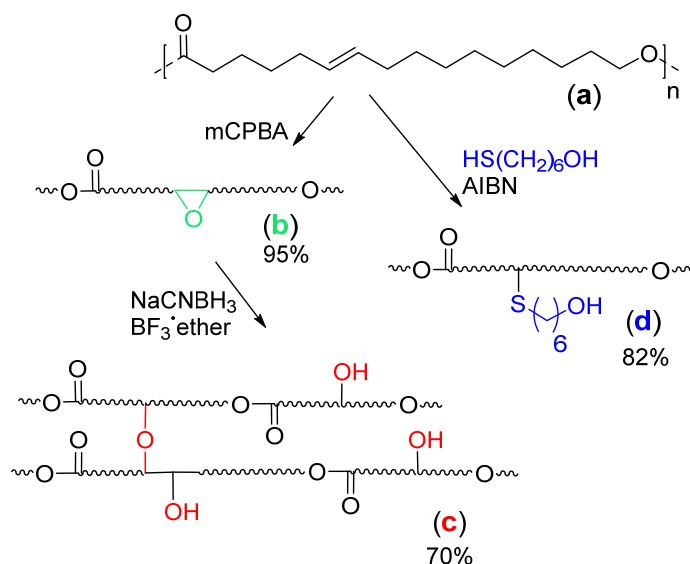
Figure 4.5. MALDI-ToF-MS of the crude P6HDL (Table 4.1, run 6). The two sets of peaks corresponding to the linear (*) and cyclic (•) polymer species (doped with Na⁺) are marked.

Further polymerization runs were performed in different conditions. Run 7 (Table 4.1) was performed at a higher temperature (130 °C), and afforded slightly lower yield and M_n , in comparison with the product obtained at 100 °C. By increasing the amount of the monomer (monomer/catalyst molar feed ratio = 250/1), a higher M_n value was obtained (Table 4.1, run 9). Therefore, the system is prone to polymerize the 6HDL to high molecular weight polymers, whose length could be modulated by the monomer/catalyst feed ratio.

The effect of dilution of the polymerization mixture was also explored (Table 4.1, run 8). Lower conversion with lower M_n were obtained, and slightly higher dispersity. As previously underlined, ROP of macrolactone is usually entropy-driven.² Thus, the dilution will favor the monomers, while high concentration favors the polymeric product. However, this effect could be also merely a consequence of the decreased monomer concentration in the case of first-order kinetics of polymerization.

4.2.2. Functionalization of poly(ω -6-hexadecenlactone)

The double bond in the poly(6- ω -hexadecenlactone) chains is a potential site for further chemical modification of the backbone, offering a wide range of possibilities to fabricate functional materials. Simple and effective reactions were selected to test the reactivity of the –ene groups embedded in the polymer (Scheme 4.3).



Scheme 4.3. Modification of poly(ω -6-hexadecenlactone).

The epoxidation of the –ene group performed on a P6HDL sample (Table 4.1, run 5) with meta-chloroperbenzoic acid (mCPBA)¹⁷ proceeded cleanly, with 95 % of yield (Scheme 4.3). In Figures 4.2i and 4.2ii the ¹H NMR spectra of the native sample **a** and of the obtained poly(6,7-epoxy- ω -hexadecalactone) (**b**) are respectively shown. The disappearance of the signal relative to the double bond protons at $\delta = 5.37$ ppm and the appearance of a new signal at $\delta = 2.65$ ppm for the protons on the epoxide ring (**f**, **g**; Figure 4.2ii) indicates that the modification was accomplished.^{17b,18} Conversely, in the ¹³C spectrum the disappearance of signals at 130.6 and 130.3 ppm and the appearance of signals at 59.0 and

58.95 ppm were observed. The number of signals in NMR spectra is compatible with the presence of a single couple of enantiomers, as expected for a non-enantioselective epoxidation mechanism proceeding with *syn* addition to the *trans* double bonds of the P6HDL.

Interestingly, the $M_{n,NMR}$ (15.6 kDa), evaluated from the integral ratio of the signal relative to the main chain methylene protons ($\delta = 4.04$ ppm; $-CH_2OC(O)-$, **k**) and the singlet relative to the terminal $-OCH_3$ protons ($\delta = 3.66$ ppm, **a**), was in good agreement with the theoretical molecular weight ($M_{n,th} = 16.1$ kDa), calculated on the basis of the $[6HDL]_0/[2]$ feed ratio and conversion, assuming that all the double bonds were epoxidized. Notably, this value was close to the $M_{n,NMR}$ (15.4 kDa) of the native polymer. The GPC analysis disclosed monomodal molecular weight distribution, with a dispersity value of 1.9. Thus, the epoxidation of the double bond could be carried out quantitatively, without side reactions. The monomodal GPC curve and the perfect accord between the numeral molecular weight before and after the epoxidation were consistent with a non-degradative derivatization reaction.^{17a}

Derivatization of the epoxide group was carried out in the presence of sodium cyanoborohydride as reducing agent and boron trifluoride (Scheme 4.3), following a literature procedure reported for the reduction of triepoxidized triglycerides to hydroxyl derivatives.¹⁹ A white solid, insoluble in most common laboratory solvents, was produced, hampering the analysis by solution NMR and GPC. The same reaction was performed on a lower molecular weight epoxidized polymer sample (Table 4.1, run 7; $M_{n,NMR} = 9.6$ kDa). The product resulted partially soluble in chloroform, thus the NMR analysis was in this case permitted. The 1H NMR spectrum of the soluble polymeric material showed the decrease of the epoxide signals of the starting material ($\delta = 2.65$ ppm), while new signals at $\delta = 3.57$ and 3.41 ppm appeared, which were respectively attributed to a methine near an

alcohol functionality $[-CHROH]$ and to vicinal ether protons $[-CHR-O-CHR-]$.²⁰ Formation of poly(hydroxy- ω -hexadecanlactone) with occasional inter and intra ether-type crosslinks was hypothesized (structure **c** of Scheme 4.3). The ether-type crosslinks would probably be generated by the following mechanism: the hydride opens an epoxide group, generating an alkoxide species which, in turn, may act as a nucleophile for a close epoxide group. Analogous polyether bridges were also obtained through the ring-opening polymerization of epoxidized methyl oleate.²¹

The FTIR characterization further supported this structure, showing broad bands for $-OH$ around 3300 cm^{-1} and ether cross-linkage bands at 1109 cm^{-1} and 1023 cm^{-1} . Conversely, the epoxide bands at 886 cm^{-1} , observed in the FTIR spectrum of the epoxidized sample corresponding to the structure **b** are lowered.²²

Among the multiple reactions that have been accepted into the click chemistry realm, the addition of thiols to $C=C$ bonds is one of the most applied, offering high yields and outstanding functional groups tolerance under simple reaction conditions.²³ The feasibility of this reaction on the double bonds embedded in the polyester chains was previously described by Heise *et al.* on poly(globalide) samples obtained by enzymatic ROP.²⁴ Following this procedure, we performed the reaction thermally, by using 2,2'-azobis(2-methylpropionitrile) (AIBN) as radical initiator in the presence of 6-mercapto-1-hexanol, which allowed the introduction of a primary alcohol terminated pendant group (Scheme 4.3, **d**).

The 1H NMR spectrum of the product (Figure 4.2iii) showed a reduction in the intensity of the peak corresponding to the double bond ($\delta = 5.37\text{ ppm}$). Conversely, a multiplet corresponding to the methine bound to the S atom ($\delta = 2.53\text{ ppm}$, **c**) belonging to polyesters main chain, and two triplets ($\delta = 3.64$ and 2.47 ppm , **h** and **f**) representative of the methylenes adjacent to

hydroxyl terminal group and thioether group respectively, belonging to the pendant chains, were observed (Figure 4.2iii).

The ^{13}C NMR spectrum confirmed this attribution: the intensity of the signals due to the carbons of the double bonds (130.3 and 130.6 ppm) was around 20 % of the initial value, while a new signal at 46.0 ppm appeared, and it was attributed, with the aid of a DEPT NMR experiment, to the methine bound to the S atom of the pendant group. GPC data analysis revealed an increase in molecular weight ($M_{n,\text{GPC}} = 36.6$ kDa) with respect to the native polymer, which is compatible with the presence of the pendant group.

4.2.2.1. Thermal and structural analysis of poly(ω -6-hexadecenlactone) and its functionalized derivatives

The obtained P6HDL and its functionalized derivatives (structures **b**, **c**, **d**, Scheme 4.3) were characterized by means of differential scanning calorimetry (DSC), in the temperature range of -80 to 150 °C, and powder X-ray diffraction analysis in the 2θ range of 3 to 40°.

In Figure 4.6 the second heating DSC runs (i) and X-ray diffraction patterns (ii) of the native poly(6- ω -hexadecenlactone) (**a**) and of its derivatives, poly(6,7-epoxy- ω -hexadecalactone) (**b**) and poly(hydroxy- ω -hexadecalactone) (**c**) samples, are reported.

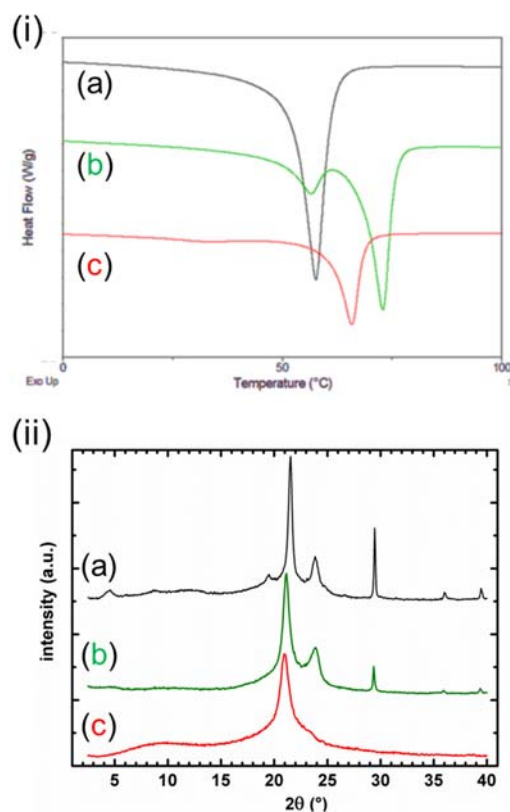


Figure 4.6. (i) DSC scans for the second heating runs and (ii) X-ray diffraction pattern of: (a) poly(6- ω -hexadecenlactone); (b) poly(6,7-epoxy- ω -hexadecalactone); (c) and poly(hydroxy- ω -hexadecalactone).

The thermogram of the P6HDL sample (Table 4.1, run 5) showed a sharp endotherm, with a melting point T_m at 57.6 °C and an enthalpy of fusion ΔH_m of 87.1 J/g, while the T_g was not detected in the scanned heating range (Figure 4.6i (a)). The T_m is slightly higher, while the ΔH_m is very similar to that observed by Heise *et al.* for the poly(ambrettolide).^{6f,14}

The X-ray diffraction pattern of P6HDL (Figure 4.6ii (a)), characterized by two strong reflections at $2\theta = 21.5$ and 23.8° , resembles that of polyethylene (PE). The similarity between the X-ray spectra of aliphatic long chain polyesters and of PE was previously reported for other polyesters obtained from saturated and unsaturated macrolactones.^{4,6d,f,25} Indeed, in the X-ray

spectrum of P6HDL (Figure 4.5ii (a)), all the reflections ($2\theta = 4.4, 19.5, 21.5, 23.8, 29.4, 36.0$ and 39.5°) are in good agreement with those calculated by Scandola *et al.* for the pseudo-orthorhombic unit cell of poly(ω -pentadecalactone) (PPDL), which is only slightly larger than those of PE. In detail, the reflection at $2\theta = 4.4^\circ$ can be attributed at the Miller index (001) of the pseudo-orthorhombic unit cell reported by these authors.^{6d} On this basis, the resulting polymer chain periodicity, $c = 20.2 \text{ \AA}$, is very similar to that observed for the PPDL ($c = 20.0 \text{ \AA}$). Such a periodicity was interpreted as the result of the inclusion of the ester groups into the polymer pseudo-orthorhombic crystal lattice, and in particular of their regular spacing along the chain axis. The close similarity observed in the polymer chain periodicity of P6HDL and PPDL suggests that, in addition to the ester groups, also the carbon-carbon double bonds are included into the polymer crystal lattice of P6HDL. Inclusion of *trans* double bonds was also observed in other “PE-like” polyesters.²⁶

The DSC thermogram of poly(6,7-epoxy- ω -hexadecalactone) (Figure 4.5i (b)) showed a large endotherm with two close melting transitions at 56.3 and 72.9°C and an enthalpy of fusion, ΔH_m of 87.9 J/g . The two very close melting peaks are probably due to a recrystallization process during which poorly-formed and small size crystals give rise to more ordered and large crystals.

The X-ray diffraction pattern of sample **b** (Figure 4.5ii) is very similar to that of P6HDL (a), except for the absence of the signals at $2\theta = 4.4$ and 19.5° . These signals were previously related to the indices 001 and 012, respectively, of the pseudo-orthorhombic unit cell of PPDL.^{6d} The absence of these two signals indicates that the polymer chain periodicity is removed, due to the presence of epoxy groups not stereoregularly arranged along the chain. In addition, the observed small differences in 2θ reflection positions indicate that the parameters a and b of the crystal lattice are slightly distorted respect to the P6HDL ones. In conclusion, the poly(6,7-epoxy- ω -

hexadecalactone) chains are presumably arranged in the crystal lattice *ab* plane, in a pseudo-orthorhombic packaging with *a* and *b* parameters similar to those of the P6HDL unit cell, while the polymer chain periodicity along the *c* axis is absent.

In spite of the absence of the polymer chain periodicity along the *c* axis, the T_m of poly(6,7-epoxy- ω -hexadecalactone) is higher than that of P6HDL. This behavior can be rationalized considering that polymer chains containing double bonds are more flexible than chains containing bulkier epoxy groups. It is well known, indeed, that flexible semicrystalline polymers have higher melting entropy and therefore lower T_m than rigid polymers, provided that they have similar enthalpy of fusion.²⁷

A DSC analysis of poly(hydroxy- ω -hexadecalactone) sample (c) (Figure 4.5i (c)) showed a melting point T_m at 65.8 °C and a ΔH_m of 61.7 J/g.

The X-ray diffraction pattern (Figure 4.5ii (c)) showed a single well defined peak at $2\theta = 20.94^\circ$. This pattern is compatible with a hexagonal crystalline structure. Therefore, the chemical modification of epoxides groups into hydroxyl groups affect the crystalline lattice: the pseudo-orthorhombic unit cell is replaced by a hexagonal structure. Indeed, hexagonal crystal structures have been proposed for ethylene/vinyl alcohol copolymers, when the ethylene molar content is in the range 14-27%.²⁸ For the poly(hydroxy- ω -hexadecalactone) a percentage of hydroxyl groups of about 15 % can be calculated on the basis of the molecular formula. Moreover, in the ethylene/vinyl alcohol copolymers described by Namakae *et al.* the strong equatorial 2θ peak around 20° corresponds to an interplanar distance $d = 4.25 \text{ \AA}$,²⁹ which is very similar to that observed for poly(hydroxy- ω -hexadecalactone) sample (c) ($d = 4.24 \text{ \AA}$).

This behavior, has been recognized also in the case of ethylene/propylene (EP) copolymers.³⁰ In detail, in the EP copolymers, with the increase of propylene molar content, the PE orthorhombic unit cell is gradually

distorted, and it is replaced by a pseudo-hexagonal structure when the propylene content is in the range 15-35 %.³⁰

The inclusion of hydroxyl units in the crystal structure of poly(hydroxy- ω -hexadecalactone) sample and the presence of strong hydrogen bonds, could also justify that the T_m is not very different from that of poly(6,7-epoxy- ω -hexadecalactone).³¹

DSC analysis of the polymer sample (**d**) bearing 6-mercapto-1-hexanol pendant groups did not show a melting transition thus indicating that the native crystalline structure is disrupted by the presence of the side moieties. An amorphous material was obtained, with a T_g of -61 °C.

4.2.3. Copolymerization of ω -6-hexadecenlactone with small and medium size lactones

The feasibility of random and block copolymerization of 6HDL with smaller CL and *rac*-LA was studied using catalyst **2** and one equivalent of MeOH in xylenes solution at 100 °C. The obtained copolymer samples were characterized by ¹H and ¹³C NMR spectroscopy, GPC and DSC. Results about composition, microstructure and molecular weight are summarized in Table 4.2. Moreover, to make comparisons, a PCL sample was also synthesized in the same condition (Table 4.2).

Table 4.2. Copolymerization of ω -6-hexadecenlactone with ϵ -caprolactone and *rac*-lactide.^a

Sample	F_{HDL}^b	F_{CL}^b	F_{LA}^b	L_{HDL}^b	L_{CL}^b	L_{LA}^b	$M_{\text{n,NMR}}^b$ (kDa) ^b	$M_{\text{n,GPC}}^c$ (kDa) ^c	$M_{\text{w}}/M_{\text{n}}^c$
PCL	-	100	-	-	-	-	8.5	23.4	1.5
P(6HDL- <i>ran</i> -CL)	50	50	-	2.2	1.9	-	15.8	36.0	1.6
PHDL- <i>block</i> -PCL	19	81	-	34	120	-	22.3	37.5	1.9
PHDL- <i>block</i> -PLA	35	-	65	66	-	125	28.4	24.3	1.5
P(HDL- <i>ran</i> -CL)- <i>block</i> -PLA	22	43	35	1.7	2.9	58	26.5	29.1	2.0

^a**Polymerization conditions:** Xylenes = 2.3 mL; precatalyst = 35 μmol ; MeOH = 35 μmol (0.35 mL of a 0.1 M toluene solution); T = 100 °C.

^bDetermined by ^1H NMR spectra.

^cDetermined by GPC in THF vs polystyrene standards.

A random copolymerization of 6HDL with CL was performed in conditions analogous to those used for the homopolymerization ($[\text{6HDL}]/[\text{CL}]/[\mathbf{2}]/[\text{MeOH}] = /5050/1/1$). ^1H NMR analysis of the obtained copolymer P(6HDL-*ran*-CL) in Table 4.2 evidenced that the composition (50/50 in the two monomers) nicely reflected the feed.

A detailed microstructure characterization of the copolymeric chains was achieved through inspection of the ^{13}C NMR spectrum. Indeed, the chemical shifts of the carbonyl, α -methylene, β -methylene and ω -methylene carbons are very sensitive to the chemical environment. By comparison with the spectra of the corresponding homopolymers, the resonance due to the hetero-sequences have been recognized and assigned. The significant ^{13}C NMR spectra regions of a P(6HDL-*ran*-CL) sample and, for comparison, of a P6HDL are shown, respectively, in Figures 4.7ii and 4.7i.

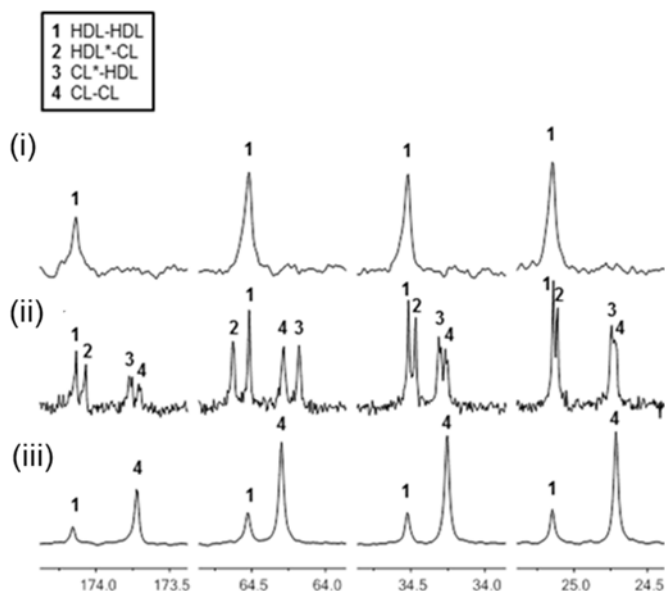


Figure 4.7. ^{13}C NMR (300 MHz, CDCl_3 , RT) spectra of: (i) P6HDL (ii) P(6HDL-*ran*-CL); (iii) P6HDL-*block*-PCL.

The average lengths of the hexadecenlactoyl (L_{HDL}) and caproyl (L_{CL}) sequences were calculated from the ^{13}C NMR data by using previously reported equations.^{9c} Interestingly, the average blocks lengths ($L_{\text{HDL}} = 2.17$; $L_{\text{CL}} = 1.85$; Table 4.2) were close to the value of 2, as expected for a random copolymer prepared with 50/50 feed. The molecular weight of the copolymer calculated from the ^1H NMR data, ($M_{\text{n,NMR}} = 15.8$ kDa) was in excellent agreement with the theoretical one ($M_{\text{n,th}} = 15.0$ kDa). The experimental GPC value ($M_{\text{n,GPC}} = 36.0$ kDa) resulted to be higher, but the above considerations hold also in this case and the GPC trace was monomodal, with dispersities $M_{\text{w}}/M_{\text{n}} = 1.6$ (Table 4.2, P(6HDL-*ran*-CL)). To further explore the ability of the catalyst in the production of copolymeric materials, the synthesis of the diblock copolymer was attempted by sequential addition of 6HDL and CL. The P6HDL-*block*-PCL copolymer (Table 4.2) was prepared in the presence of **2** by sequential addition of the two monomers in xylenes. When the 6HDL conversion

reached its maximum (60 %), a large excess of CL was added. The ^1H NMR spectrum, in addition to the resonances of the main signals due to two blocks showed peaks corresponding to the methyl ester end group at 3.66 ppm deriving from the insertion of the macrolactone monomer in the Al-OCH_3 bond, and hydroxyl methylene group at 3.63 ppm deriving from the hydrolysis of the growing chains. From these data it was possible to calculate the length of each block ($L_{\text{HDL}} = 34$; $L_{\text{CL}} = 120$) and $M_{\text{n,NMR}}$ (22.3 kDa) reported in Table 4.2. In the ^{13}C NMR spectrum (see Figure 4.7iii) the heterodiads were not observed, thus indicating that transesterification reactions were absent. Moreover, the GPC analysis disclosed unimodal chromatogram with a value $M_{\text{n,GPC}}$ of 37.5 kDa and molecular weight dispersities of 1.9 (Table 4.2).

The random and di-block copolymers obtained by copolymerizing the 6HDL with the smaller CL were also characterized by DSC and X-ray diffraction (Figure 4.8).

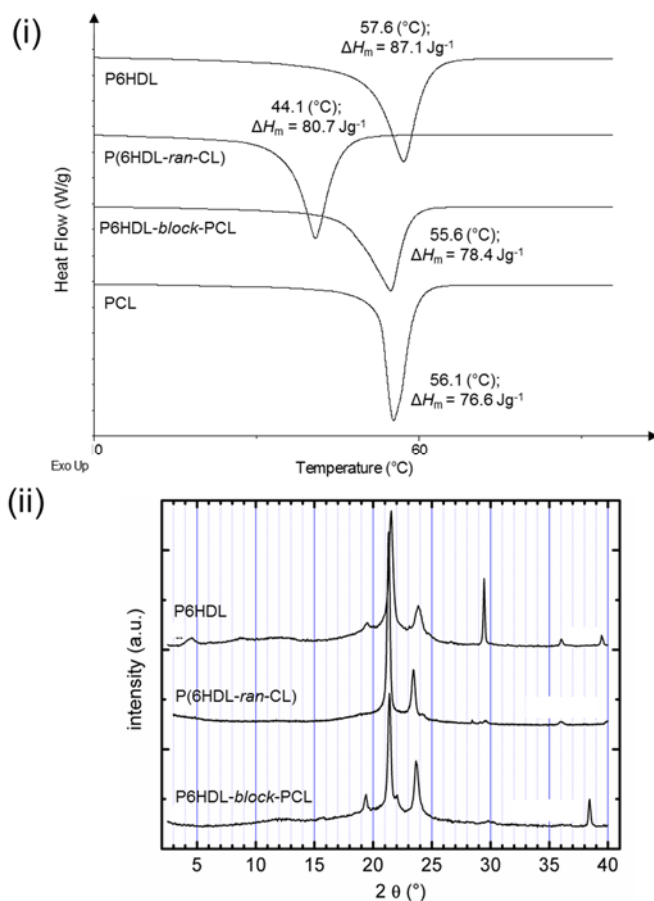


Figure 4.8. (i) DSC scans for the second heating runs of P6HDL, P(6HDL-ran-CL), P6HDL-block.PCL and PCL. (ii) X-ray diffraction pattern of P6HDL, P(6HDL-ran-CL), P6HDL-block.PCL.

DSC analysis of P(6HDL-ran-CL) evidenced a melting peak with a T_m of 44.1 °C and ΔH_m of 80.7 J/g (Figure 4.8i). The high crystallinity of this random copolymer sample is not surprising, in fact random copolymers of PDL and CL are able to cocrystallize over the whole composition range, which represent an example of macromolecular isomorphism.^{9c,32,33} The X-ray diffraction pattern (Figure 4.8ii) shows that the observed crystallinity is due to a polyethylene-like packaging, as already reported by Scandola and Gross for PDL/CL random copolymers.³² CL and 6HDL units cocrystallize

into structure whose chain packing is substantially similar to that of PE and of P6HDL, while the chain periodicity, for a composition 50/50, is lost due to random distribution of ester groups in polymer chains.

DSC analysis of P6HDL-*block*-PCL (Figure 4.8i) also showed a single melting peak T_m at 55.6 °C, with an enthalpy of fusion ΔH_m of 78.4 J/g. A similar behavior was recognized for a PCL sample (Table 4.2) obtained in the same experimental conditions ($T_m = 56.1$ °C; ΔH_m of 76.6 J/g). Indeed, the X-ray diffraction pattern of the P6HDL-*block*-PCL (Figure 4.8ii) conformed that the observed crystallinity is due to the longer caproyl blocks. These data can be rationalized by considering that the inclusion of 6HDL units in the crystalline PCL blocks probably occurs, as well as in ω -pentadecalactone/ ϵ -caprolactone copolymers the PDL units are included in the PCL crystal phase.^{8,9c,32} The absence of the crystalline phase of P6HDL blocks is not surprising, in fact it is generally accepted that the crystallization of semicrystalline block copolymers is strictly dependent on the copolymer composition³⁴ and it preferentially occurs when comparable fractions of each copolymer components are present.

Copolymerization of 6HDL with the *rac*-LA was also attempted. However, when the two monomers were mixed together in the presence of the catalyst **2** only PLA was obtained. This behaviour is probably due to the higher coordination ability of the diester lactide, in comparison to that of the macrolactone. Moreover, a computational study showed that the insertion of a macrolactone into a metal secondary alkoxy group is dramatically hampered for steric reason.^{10c} A similar effect should also be significant in our system.

However, a P6HDL-*block*-PLA copolymer was prepared in the presence of the complex **2** by sequential addition of 6HDL and *rac*-LA in xylenes (Table 4.2). As above, ¹H and ¹³C NMR analysis disclosed the presence of the two blocks, while heterosequences were not detected. Interestingly, the observed end groups were the methyl ester end group at 3.66 ppm, deriving

from the insertion of the macrolactone into the Al-OCH₃ bond, and the hydroxyl methine at 4.35 ppm due to the hydrolysis of the growing chain ending with a lactide unit.

The assignment of the end group signals allowed to determine the molecular weights copolymers, $M_{n,NMR} = 28.4$ kDa, and of the blocks lengths, $L_{6HDL} = 66$; $L_{LA} = 120$ (Table 4.2). GPC analysis disclosed unimodal chromatograms with molecular weight dispersities 1.5, in line with the presence of one kind of macromolecular chains, i.e. the expected diblock copolymers.

DSC analysis of the P6HDL-*block*-PLA sample showed a melting peak at 49.3 °C with a $\Delta H_m = 37.2$ J/g (Table 4.2). The crystallinity is due to the crystallizable P6HDL block, while, of course, the stereoirregular LA sequences do not crystallize. The observed decrease of T_m and ΔH_m with respect to the P6HDL homopolymer could be due to the greater difficulty of 6HDL units to crystallize in the presence of long LA blocks.

The achievement of the described diblock copolymers is a further indication of the *pseudo-living* nature of ROP catalyzed by this system. Taking advantage of this feature, we attempted to synthesize a diblock copolymer of the type P(6HDL-*ran*-CL)-*block*-PLA by first copolymerizing 6HDL and CL, and subsequently adding *rac*-LA (see Table 4.2). The first random block was obtained by polymerization of the 6HDL and CL (50/ 50) in xylenes at 100 °C for one day. Subsequently, 50 equivalents of *rac*-LA were added, and after 3 days a conversion of 93% of *rac*-LA was observed. Also in this case, GPC analysis confirmed the di-block nature of this copolymer, showing a monomodal trace and a value of 2.0 for the molecular weight dispersity.

DSC analysis of this sample showed a single melting peak, with a T_m of 38.8 °C and a ΔH_m of 46.9 J/g. Also in this case the stereoirregular LA sequences do not crystallize, therefore the crystallinity is due to cocrystallization of random sequences of 6HDL and CL units. The observed decrease of T_m with respect to the P(6HDL-*ran*-CL) ($T_m = 44.1$ °C), could

be due to the greater difficulty of random 6HDL/CL block to crystallize in the presence of the LA block.

GPC showed monomodal distribution for all the copolymers, which is a clear indication that the samples were block copolymers, and not mechanical mixtures of homopolymers. Moreover, the same conclusion can be derived from the 2D DOSY NMR carried out on all the copolymers. Representative DOSY NMR experiments of P(6HDL-*ran*-CL)-*block*-PLA is reported in Figure 4.9.

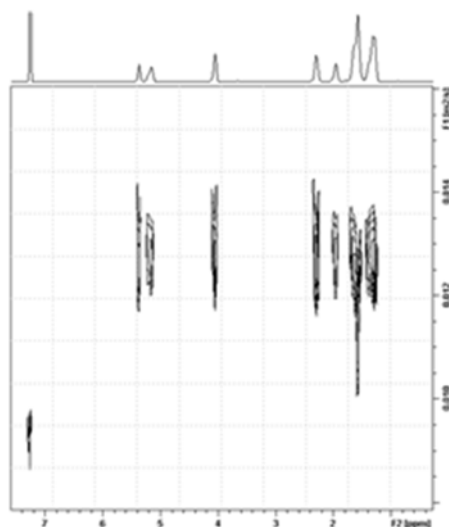


Figure 4.9. 2D DOSY NMR (400 MHz, CDCl₃, RT) of P(6HDL-*ran*-CL)-*block*-PLA, recorded employing $\delta = 1000 \mu\text{s}$ and $\Delta = 0.8 \text{ s}$. Signals at 7.26 and 1.56 ppm are relative to deuterated solvent residual protic signal (CHCl₃) and to adventitious water, respectively.

DOSY NMR experiments of all the described copolymers showed that the signals of the first block and those of the second block lied at the same diffusion coefficient, and therefore belonged to the same polymeric chains, thus confirming the di-block nature.

Notably, most of the reported catalytic systems (enzymatic, organic and metal-based) active in the polymerization of macrolactones, undergo intra- and inter-molecular transesterification reactions preventing the formation

of diblock copolymers. In particular, several aluminum based complexes have been explored in the sequential polymerization of macrolide and small lactones.^{9c,d} Actually, when the copolymers were allowed to react for longer time, they showed an increased randomness with increasing reaction time. Beside the dimethyl(salicylaldiminato) aluminum complex **2**, only two catalysts, based on calcium and zinc, able to produce poly(PHDL)-block-poly(CL) copolymers have been reported in the literature.^{9d} The salicylaldiminato aluminium compound represents the first example of aluminum based catalyst able to produce perfect block copolymers with the desired composition even if the reaction is carried out for prolonged reaction times.

CONCLUSIONS

In recent years, great research interest has been devoted to the ROP of small or medium size cyclic esters for the production of aliphatic polyesters. On the contrary, the ROP of strainless large cyclic esters by a non-enzymatic route is a far less explored field. To the best of current knowledge, the synthesis and characterization of poly(ω -6-hexadecenlactone) has been investigated in this thesis for the first time. The dimethyl(salicylaldiminato) aluminum compound **2** resulted active catalysts for the ROP of ω -6-hexadecenlactone to high molecular weight polymer, in a controlled fashion. The used catalyst offered better control in comparison to the enzymatic and/or metal based traditional macrolactone catalysts furnishing polymers with narrower dispersities and higher molecular weights. Since the ROP process does not affect the unsaturation of the main chain, this functionality was used for further chemical modifications. Thiol-ene coupling of the 6-mercapto-1-hexanol to the polymeric chains was carried out by radical approach affording polyesters bearing pendant alcohol functionalized groups. Epoxidation of the double bond occurred quantitatively, without any change in the degree of polymerization. The epoxide opening by hydrides was performed, as a result alcohol-substituted polyester chains with occasional inter and intra ether-type crosslinks were formed. The epoxide function could be a further useful platform for the introduction of other usable groups or the attachment of bioactive substances, thus opening the way to fabricate functional materials.

Thermal and structural characterization showed that not only the poly(ω -6-hexadecenlactone) itself, but also the epoxy-functionalized and the hydroxylated derivative are semicrystalline. While the poly(ω -6-hexadecenlactone), containing unsaturated groups, has a crystal structure very similar to that of orthorhombic PE, in the presence of bulkier and more stereoirregularly arranged epoxy groups the structure is deformed and the

periodicity along the chain axis is lost. Conversely, the polymer chains containing the randomly arranged hydroxyl groups are packaged into a hexagonal crystal lattice. Therefore, the chemical modifications, which occurred without any change in the degree of polymerization, modified thermal and structural polymer features.

Copolymerization of the macrolactone with the smaller ring size CL produced a random semicrystalline copolymer, with average sequence blocks lengths around 2, having both the monomers included in the crystal lattice. The *pseudo-living* behaviour of the catalytic system and the absence of transesterification reactions allowed the preparation of linear block copolymers of 6HDL with CL and/or *rac*-LA by sequential addition of the monomers. These block copolymers were also semicrystalline. Due to their *poly(ethylene) like* behaviour, 6HDL/*rac*-LA based di-block copolymers may be of interest as compatibilizers for poly(ethylene)/poly(esters) mixtures. Recently PPDL/PLLA block copolymers have been indeed investigated as compatibilizers for blends of high density polyethylene and PLLA.³⁵

The ROP of macrolactones is a vivid research area as showed by the recent literature.^{35,36} The results reported and discussed here have been published in *Polymer Chemistry*.³⁷

References

- ¹ (a) A. Duda, A. Kowalski, J. Libiszowski, S. Penczek, *Macromol. Symp.* **2005**, *224*, 71-83. (b) A. Duda in *Polymer Science: A Comprehensive Reference*. Amsterdam, Elsevier, **2012**, *4*, 213-245.
- ² (a) P. Hodge, H.M. Colquhoun, *Polym. Adv. Technol.* **2005**, *16*, 84-94 (b) S. Strandman, J. E. Gautrot, X. X. Zhu, *Polym. Chem.* **2011**, *2*, 791-799. (c) P. Hodge, *Chem. Rev.* **2014**, *114*, 2278-2312.
- ³ M. P. F. Pepels, P. Souljé, R. Peters, R. Duchateau, *Macromolecules* **2014**, *47*, 5542-5550.
- ⁴ M. L. Focarete, M. Scandola, A. Kumar, R. A. Gross, *J. Polym. Sci., Part B: Polym. Phys.* **2001**, *39*, 1721-1729.
- ⁵ (a) R. Nomura, A. Ueno, T. Endo, *Macromolecules* **1994**, *27*, 620-621. (b) Z. Jedlinski, M. Juswa, G. Adamus, M. Kowalczyk, *Macromol. Chem. Phys.* **1996**, *197*, 2923-2929.
- ⁶ (a) K. S. Bisht, L. A. Henderson, R. A. Gross, D. L. Kaplan, G. Swift, *Macromolecules* **1997**, *30*, 2705-2711. (b) P. Skoglund, Å. Fransson, *Polymer* **1998**, *39*, 1899-1906. (c) S. Namekawa, S. Suda, H. Uyama, S. Kobayashi, *Int. J. Biol. Macromol.* **1999**, *25*, 145-151. (d) M. Gazzano, V. Malta, M. L. Focarete, M. Scandola, R. A. Gross, *J. Polym. Sci., Part B: Polym. Phys.* **2003**, *41*, 1009-1013. (e) L. van der Mee, F. Helmich, R. de Bruijn, J. A. J. M. Vekemans, A. R. A. Palmans, E. W. Meijer, *Macromolecules* **2006**, *39*, 5021-5027. (f) I. van der Meulen, M. de Geus, H. Antheunis, R. Deumens, E. A. J. Joosten, C. E. Koning, A. Heise, *Biomacromolecules* **2008**, *9*, 3404-3410.
- ⁷ (a) Y. Hori, H. Hongo, T. Hagiwara, *Macromolecules* **1999**, *32*, 3537-3539. (b) Z. Zhong, P. J. Dijkstra, J. Feijen, *Macromol. Chem. Phys.* **2000**, *201*, 1329-1333. (c) A. Duda, A. Kowalski, S. Penczek, H. Uyama, S.

Kobayashi, *Macromolecules* **2002**, *35*, 4266–4270. (d) R. Slivniak, J. A. Domb, *Biomacromolecules* **2005**, *6*, 1679–1688. (e) Y. Nakayama, N. Watanabe, K. Kusaba, K. Sasaki, Z. Cai, T. Shiono, C. Tsutsumi, *J. Appl. Polym. Sci.* **2011**, *121*, 2098–2103.

⁸ M. Bouyahyi, M. P. F. Pepels, A. Heise, R. Duchateau, *Macromolecules* **2012**, *45*, 3356–3366.

⁹ (a) I. Van der Meulen, E. Gubbels, S. Huijser, R. Sablong, C. E. Koning, A. Heise, R. Duchateau, *Macromolecules* **2011**, *44*, 4301–4305. (b) B. A. J. Noordover, L. Jasinska-Walc, I. van der Meulen, R. Duchateau, C. E. Koning, in *Biobased Monomers, Polymers, and Materials*, ed. P. B. Smith and A. R. Gross., American Chemical Society, Washington, DC, **2012**, ACS Symposium Series vol. 1105, ch. 9, pp 281–322. (c) M. P. F. Pepels, M. Bouyahyi, A. Heise, R. Duchateau, *Macromolecules* **2013**, *46*, 4324–4334. (d) M. Bouyahyi, R. Duchateau, *Macromolecules* **2014**, *47*, 517–524. (e) J. A. Wilson, S. A.; Hopkins, P. M. M. Wright, A. P. Dove, *Polym. Chem.*, 2014, *5*, 2691–2694. (f) L. Jasinska-Walk, M. R. Hansen, D. Dudenko, A. Rozanski, M. Bouyahyi, M. Wagner, R. Graft, R. Duchateau, *Polym. Chem.* **2014**, *5*, 3306–3310.

¹⁰ D. Pappalardo, L. Annunziata, C. Pellecchia, *Macromolecules* **2009**, *42*, 6056–6062.

¹¹ (a) A. Meduri, T. Fuoco, M. Lamberti, C. Pellecchia, D. Pappalardo, *Macromolecules* **2014**, *47*, 534–543. (b) T. Fuoco, A. Meduri, M. Lamberti, C. Pellecchia, D. Pappalardo, *J. Appl. Polym. Sci.* **2015**, *132*, 42567 (1–11).

¹² D. McGinty, C. S. Letizia, A. M. Api, *Food Chem. Toxicol.* **2011**, *49*(Suppl. 2), S207–S211.

¹³ I. van der Meulen, Y. Li, R. Deumens, E. A. Joosten, C. E. Koning, A. Heise, *Biomacromolecules* **2011**, *12*, 837–843.

¹⁴ S. P. Soni, J. A. Ward, S. E. Sen, S. E. Feller, S. R. Wassall, *Biochemistry* **2009**, *48*, 11097–11107.

- ¹⁵ (a) J. Wosnick, Eur. Pat.t Appl. EP2 63950A1, **2010**. (b) A. K. L. Yuen, F. Heinroth, A. J. Ward, A. F. Masters, T. Maschmeyer, *Phys. Chem. Phys.* **2013**, *15*(32), 13343-13353.
- ¹⁶ V. C. Gibson, E. L. Marshall, in *Comprehensive Coordination Chemistry II*, ed. J. A. McCleverty and T. J. Meyer, Elsevier, Amsterdam, **2003**, vol. 9, ch. 1, pp 1–74.
- ¹⁷ (a) A. Finne, A.-C. Albertsson, *J. Polym. Sci., Part A: Polym. Chem.* **2004**, *42*, 444–452. (b) P. -J. Roumanet, F. Laflèche, N. Jarroux, Y. Raoul, S. Claude, P. Guégan, *Eur. Polym. J.* **2013**, *49*, 813–822.
- ¹⁸ Y. Yang, W. Lu, X. Zhang, W. Xie, M. Cai, R. Gross, *Biomacromolecules* **2010**, *11*, 259–268.
- ¹⁹ H. -P. Zhao, J. -F. Zhang, X. S. Sun, D. H. Hua, *J. Appl. Polym. Sci.* **2008**, *110*, 647–656.
- ²⁰ B. J. K. Ahn, S. Kraft, X. S. Sun, *J. Agric. Food Chem.* **2012**, *60*, 2179–2189.
- ²¹ G. Lligadas, J. C. Ronda, M. Galià, U. Biermann, J. O. Metzger, *J. Polym. Sci., Part A: Polym. Chem.* **2006**, *44*, 634–645.
- ²² R. M. Silverstein, G. C. Bassler, T. C. Morrill, in *Spectroscopic Identification of Organic Compounds*, John Wiley & Sons, New York, 4th Edn., **1981**, pp. 115–116.
- ²³ A. Dondoni, *Angew. Chem., Int. Ed.* **2008**, *47*, 8995–8997.
- ²⁴ Z. Ates, P. D. Thornton, A. Heise, *Polym. Chem.*, **2011** *2*, 309–312.
- ²⁵ M. P. F. Pepels, M. Bouyahyi, A. Heise, R. Duchateaus, *Macromolecules* **2013**, *46*, 7668-7677.
- ²⁶ G. Maglio, C. Marchetta, A. Botta, R. Palumbo, M. Pracella, *Eur. Polym. J.* **1979**, *15*, 695-699.
- ²⁷ 28 F. W. Billmeyer, in *Textbook of Polymer Science*, Wiley & Sons, 3rd edn., **1984**.
- ²⁸ M. Takahashi, K. Tashiro, A. Shigetoshi, *Macromolecules* **1999**, *32*, 5860-5871.

- ²⁹ K. Namakae, M. Kameyama, T. Matsumoto, *Polymer Eng. Sci.* **1979**, *19*, 572-578.
- ³⁰ (a) G. Guerra, O. R. De Ballesteros, V. Venditto, M. Galimberti, F. Sartori, R. Pucciariello, *J. Polym. Sci., Part B: Polym. Phys.* **1999**, *37*, 1095-1103. (b) S. Antinucci, G. Guerra, L. Oliva, O. R. De Ballesteros, V. Venditto, *Macromol. Chem. Phys.* **2001**, *202*, 382-387.
- ³¹ Y. Mori, H. Sumi, T. Hirabayashi, Y. Ynai, K. Yokota, *Macromolecules* **1994**, *27*, 1051-1056.
- ³² G. Ceccorulli, M. Scandola, A. Kumar, B. Kalra, R. A. Gross, *Biomacromolecules* **2005**, *6*, 902-907.
- ³³ P. Pan, Y. Inoue, *Prog. Polym. Sci.* **2009**, *34*, 605-640.
- ³⁴ (a) I. W. Hamley, *Adv. Polym. Sci.* **1999**, *148*, 113-137. (b) W. N. He, J. T. Xu, *Prog. Polym. Sci.* **2012**, *37*, 1350-1400. (c) S. Nojima, M. Ono, T. Ashida, *Polymer* **1991**, *24*, 1271-1280.
- ³⁵ (b) M. P. F. Pepels, W. P. Hofman, R. Kleijnen, A. B. Spoelstra, C. E. Koning, H. Goossens, R. Duchateau, *Macromolecules* **2015**, *48*, 6909-6921.
- ³⁶ (a) R. Todd, S. Tempelaar, G. Lo Re, S. Spinella, S. A. McCallum, R. A. Gross, J.-M. Raquez, P. Dubois, *ACS Macro Lett.* **2015**, *4*, 408-410. (b) L. Jasinska-Walc, M. Bouyahyi, A. Rozanski, R. Graf, M. R. Hansen, R. Duchateau, *Macromolecules* **2015**, *48*, 502-510. (c) J. A. Wilson, S. A. Hopkins, P. M. Wright, A. P. Dove, *Macromolecules* **2015**, *48*, 950-958. (d) M. P. F. Pepels, R. A. C. Koeken, S. J. J. van der Linden, A. Heise, R. Duchateau, *Macromolecules* **2015**, *48*, 4779-4792. (e) M. P. F. Pepels, L. E. Govaert, R. Duchateau, *Macromolecules* **2015**, *48*, 5845-5854. (f) C. Qing, L. Li, Y. Dalei, Z. Mingyao, T.-T. Minh-Tan, H. Wei, L. Shuai, *Chem. Res. Chin. Univ.* **2015**, *31*, 640-644. (g) S. Naumann, P. B. V. Scholten, J. A. Wilson, A. P. Dove, *J. Am. Chem. Soc.* **2015**, *137*, 14439-

14445. (h) J. A. Wilson, S. A. Hopkins, P. M. Wright, A. P. Dove, *Biomacromolecules* **2015**, *16*, 3191-3200.

³⁷ T. Fuoco, A. Meduri, M. Lamberti, V. Venditto, C. Pellicchia, D. Pappalardo, *Polym. Chem.* **2015**, *6*, 1727-1740.

CONCLUDING REMARKS

Aliphatic polyesters, by far the most interesting biodegradable polymers, suffer from several drawbacks. For example, the brittleness of PLA, the poor solubility of PGA in most organic solvent, the quite long degradation time of PCL and the lack of functional groups strongly limit their applications, especially in biomedical field.

The copolymerization of different monomers represents the most efficient strategy to overcome these disadvantages and to modulate the properties of polymers by properly matching the homopolymers features. A controlled design of the macromolecular structure opens the way to tune the mechanical, thermal and chemical properties of the obtained copolymers.

The ring-opening polymerization industrial catalysts, such as tin (II) octanoate, do not allow a precise control over the chain growth, which is a very disadvantage especially for copolymers production. On the contrary, recently developed *single-site* catalysts are very promising systems for the synthesis of copolymers with the desired microstructure.

In this PhD project the development of synthetic approaches for the preparation of linear aliphatic copolyesters with controlled microstructures and functional groups by ring-opening polymerization of suitable monomers was pursued. Extending previous expertise in the copolymerization of lactides and ϵ -caprolactone by dimethyl(salicylaldiminato)aluminum compounds, the homo- and copolymerization of glycolide and *rac*-lactide were carried out in the presence of this class of catalysts. PLGA copolymers, by far the most used biodegradable polymers for biomedical applications, were prepared. A good control on the microstructure (from random to block to microblocks) was achieved, depending on the experimental conditions. The same catalytic approach was subsequently exploited in copolymerizations of

glycolide with ϵ -caprolactone and in terpolymerizations of glycolide, ϵ -caprolactone and *rac*-lactide, producing random copolyesters. The effect of the microstructure on thermal properties was demonstrated. Interestingly, all terpolymer samples were amorphous with T_g below the body temperature. These copolymeric materials may have applications in the biomedical fields.

The lack of functional groups in aliphatic polyesters limits their use especially in application where the binding of biological motifs could enable interactions with cells. With this purpose in mind, a new functional monomer, bearing a thiol protected group and able to polymerize by ring-opening, was designed and synthesized. The 3-methyl-6-(tritylthiomethyl)-1,4-dioxane-2,5-dione appeared a versatile “building block” for the preparation of functionalized aliphatic polyesters by copolymerization with other cyclic esters. After polymerization, modifications of the side groups were carried out without any change in the degree of polymerization. The functional copolymer was used to fabricate 3D porous scaffolds. The usability of the functional groups embedded in the 3D structure was demonstrated by grafting, as proof of concept, a cysteine terminated RGD peptide. Given the large pliability of the thiol functionality, this molecule could be used to manufacture a plethora of advanced materials. For example, the preparation of PEG-PLA based micelles with –S–S– crosslinks, useful for stimuli responsive drug-delivery applications, could be pursued in future studies. Another possible use of the molecule would be the functionalization of gold nanoparticles with biodegradable polymers, exploiting the sulfur-gold affinity.

The last aim of this thesis was the synthesis of functional and semicrystalline “polyethylene-like” polyesters. This purpose was achieved by the ring-opening polymerization of an unsaturated large lactone, the ω -6-hexadecenlactone. The polymerization reactions catalyzed by one of

the dimethyl(salicylaldiminato)aluminum compounds gave unsaturated polyesters with a good control over the chain growth following a *pseudo*-first order kinetic. The high versatility of this class of catalysts was further demonstrated by copolymerization of the ω -6-hexadecenlactone with the smaller ring size ϵ -caprolactone and *rac*-lactide. Random and block copolymer were obtained. The possibility to further modify the polyesters chains was demonstrated by simple and effective reactions on the double bond, which occurred without any change in the degree of polymerization. All the polymeric materials resulted semicrystalline. It was demonstrated that the crystalline structure, as well as thermal properties, could be changed by chemical modifications. The main limit of the poly(ω -6-hexadecenlactone) and related copolymers is the low melting point, however, these materials could be tested as compatibilizers for polyolefin/polyester mixtures and, of course, further modifications of the double bond might be carry out to enhance the properties of such materials.

5. EXPERIMENTAL SECTION

5.1. General experimental methods

5.1.1. Materials and methods

Moisture and air-sensitive materials were manipulated under nitrogen using Schlenk techniques or in an MBraun Labmaster glove box. Before use, glassware was dried overnight in an oven at 120 °C. Solvents were refluxed over a drying agent (indicated below) and distilled under nitrogen: toluene and methanol (MeOH) over Na; xylenes, benzene and tetrahydrofuran (THF) over Na/benzophenone; and dichloromethane (CH₂Cl₂) over LiAlH₄. Acetonitrile (CH₃CN) was dried over Na₂SO₄ and stored over molecular sieves.

Monomers (Sigma-Aldrich) were purified prior to use. L-Lactide (LA) was purified by recrystallization from dry toluene and then dried *in vacuo* with phosphorous pentoxide (P₂O₅) for 96 hours and stored in drybox. *Rac*-lactide was dried *in vacuo* with P₂O₅ for 96 hours and stored in drybox. Glycolide was recrystallized from THF, dried *in vacuo* with P₂O₅ for 48 hours and stored in drybox. ε-Caprolactone (CL) and ω-6-hexadecenlactone were distilled *in vacuo* over CaH₂ and stored over molecular sieves in a drybox.

Benzoyl peroxide was purified by recrystallization from CH₂Cl₂ and MeOH and dried in a desiccator for two days. Trimethylamine (NEt₃) was dried over molecular sieves for two days. meta-Chloroperoxybenzoic acid (mCPBA) was dissolved in CH₂Cl₂ and dried over Na₂SO₄. The solution was filtered, the solvent evaporated *in vacuo* and then the mCPBA was crystallized from n-hexane/Et₂O 10/1 at -20 °C.

All other reagents and solvents were purchased from Sigma-Aldrich. Solvent and chemicals were used as received unless stated otherwise.

The H-Arg-Gly-Asp-Cys-OH peptide (RGDC) was purchased from Bachem and used as received. Dulbecco's modified Eagle's medium, phosphate-buffered saline (10x) and trypsin-EDTA solution were purchased from Sigma-Aldrich. Fetal bovine serum, penicillin-streptomycin and alamarBlue cell viability reagent were purchased from Fisher and used as received.

Human dermal fibroblasts were purchased from ATCC and cultured according to standard protocols.

5.1.2. Instruments and measurements

NMR spectra of polymers were performed on Bruker Avance 300, 400 or 600 spectrometers (^1H : 300.13, 400.13, 600.13 MHz; ^{13}C : 75.47, 100.62, 150.92 MHz; respectively). The resonances are reported in ppm (δ) and coupling constants in Hz (J), and they are referenced to the residual solvent peak versus $\text{Si}(\text{CH}_3)_4$. Spectra recording was performed on Bruker TopSpin v2.1 software. Data processing was performed on TopSpin v2.1 or MestReNova v6.0.2 software.

Molecular weights (M_n and M_w) and molecular weight dispersities (M_w/M_n) were measured by gel permeation chromatography (GPC). The measurements were performed at 30 °C on a Waters 1525 binary system equipped with a Waters 2414 Refractive Index (RI) detector and a Waters 2487 Dual λ Absorbtion (UV, $\lambda_{\text{abs}} = 220$ nm) detector, using tetrahydrofuran as eluent (1.0 mL min^{-1}) and employing a system of four Styragel HR columns (7.8×300 mm; range $10^3 - 10^6$ Å). Narrow polystyrene standards were used as reference and Waters Breeze v3.30 software for data processing.

Molecular weights (M_n and M_w) and molecular weight dispersities (M_w/M_n) were also performed at 30 °C on a Verotech PL-GPC 50 Plus system equipped with two PLgel 5 μm MIXED-D (300×7.5 mm) columns, a PL-

RI detector (Varian, Germany) and a PL-GPC 50 Plus autosampler using CHCl_3 as the eluent (1.0 mL min^{-1}). Narrow polystyrene standards were used as reference, and the flow rate fluctuations were corrected using toluene as an internal standard.

A MALDI-ToF-MS analysis was performed on a Waters Maldi Micro MX equipped with a 337 nm nitrogen laser. An acceleration voltage of 25 kV was applied. The polymer sample was dissolved in THF with Milli-Q water containing 0.1% formic acid at a concentration of 0.8 mg mL^{-1} . The matrix used was 2,5-dihydroxybenzoic acid (DHBA) (Pierce) and was dissolved in THF at a concentration of 30 mg mL^{-1} . Solutions of the matrix and the polymer were mixed in a volume ratio of 1:1. The mixed solution was hand-spotted on a stainless steel MALDI target and left to dry. The spectra were recorded in reflection mode.

Glass transition temperatures (T_g), melting points (T_m) and enthalpy of fusion (ΔH_m) of the polymer samples were measured by differential scanning calorimetry (DSC) using aluminum pans and a DSC 2920 TA Instruments apparatus, calibrated with indium. Measurements were performed in nitrogen flow with a heating rate of $10 \text{ }^\circ\text{C min}^{-1}$ in the range of -80 to $+220 \text{ }^\circ\text{C}$. DSC data were processed with TA Universal Analysis v2.3 software and are reported for the second heating cycle.

Infrared spectra of polymers were recorded on KBr disk samples by using a Bruker - Vertex 70 FT-IR spectrometer with a Globar (silicon carbide) light source.

X-ray diffraction measurements were performed on a Philips PW1710 powder diffractometer using a Ni-filtered $\text{CuK}\alpha$ radiation ($\lambda = 1.5418 \text{ \AA}$) at 40 kV and 20 mA. The scans were carried out, on as polymerized samples, in the 2θ range of 3 to 40° with a 0.05° step in 2θ and an acquisition time of 3 s. Data were processed with Origin 7.0 software.

Mechanical properties were measured by a compression test using an Instron 5566 universal tester (Instron Corp., High Wycombe, UK) with a

500 N load cell. All samples were cylinders approximately 5.0 mm in thickness and 10 mm in diameter. The cylinders were vertically compressed of a rate of 10 % of the thickness/min until the scaffolds achieved 80 % deformation. For each sample, five parallel tests were carried out after conditioning at 23 °C and 50 % humidity for 24 hours. The compressive modulus was then determined from the slope of the initial linear portion of the stress-strain curve.

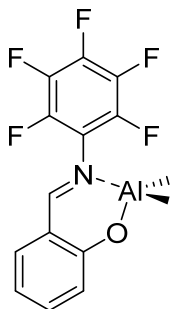
UV spectra were recorded on UV-vis spectrophotometer 2550 over a range of 200-900 nm, and UV data were processed with UV Probe software.

Cell viability was evaluated by fluorescence measurements performed on a Tecan Infinite 200 PRO multifunctional microplate reader with an excitation wavelength = 560 nm and an emission wavelength = 590 nm.

Scanning electron microscopy (SEM) was performed on a Table-Top SEM Hitachi TM-1000 using an acceleration voltage of 15 kV. Samples were sputter-coated with a layer of gold-platinum.

5.2. Catalysts synthesis and characterization

5.2.1. Synthesis of $\{[2\text{-O-C}_6\text{H}_4]\text{CH=NC}_6\text{F}_5\}\text{Al}(\text{CH}_3)_2$ (1)



To a toluene solution (15 mL) of **Lig1**, synthesized according to literature,¹ (1.5 g, 5.1 mmol), 10 mL of a *n*-hexane solution 0.56 M of $\text{Al}(\text{CH}_3)_3$ (5.5 mmol) was added dropwise via cannula at 0 °C. The reaction mixture was magnetically stirred for 1 h at 0 °C, then for 1.5 h at room temperature.

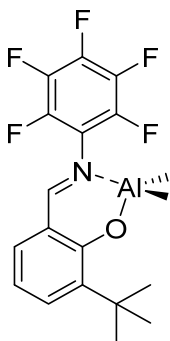
After this time, the solvent was removed, the solid was washed with *n*-pentane and dried in vacuo. Yield: 1.417 g (81 %).

^1H NMR (400 MHz, C_6D_6 , 25 °C) δ 7.18 (s, 1H; N=CH), 7.04 (td, $J = 8.6$, 1.4 Hz, 1H; ArH), 6.89 (d, $J = 8.6$ Hz, 1H; ArH), 6.63 (d, $J = 7.8$ Hz, 1H; ArH), 6.40 (t, $J = 7.8$ Hz, 1H; ArH), -0.28 (bs, 6H; Al-CH₃).

^{13}C NMR (101 MHz, C_6D_6 , 25 °C) δ 176.5 (ArC=N), 174.4 (ArC-O), 167.3, 137.9 (ArC-F), 140.3, 135.2 (ArC-F), 136.2, 123.1, 118.1 (ArC-H), 122.0 (ArC-C=N), 118.0 (ArC-N), -9.9 (Al-CH₃).

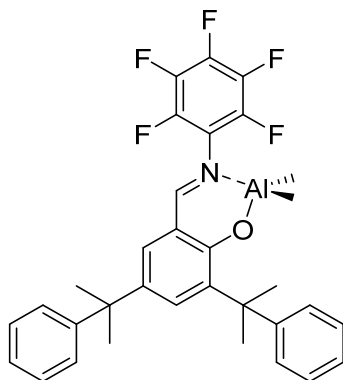
^{19}F NMR (376 MHz, C_6D_6 , 25 °C) δ -148.44 (d, $J = 18.8$ Hz, 2F; *o*-F), -154.07 (t, $J = 22.5$ Hz, 1F; *p*-F), -160.50 (td, $J = 22.5$, 5.4 Hz, 2F; *m*-F).

5.2.2. Synthesis of $\{[3\text{-}^i\text{Bu-2-O-C}_6\text{H}_3]\text{CH=NC}_6\text{F}_5\}\text{Al}(\text{CH}_3)_2$ (2).



Catalyst **2** was prepared as previous reported.²

5.2.3. Synthesis of $\{[3,5\text{-C}(\text{CH}_3)_2\text{C}_6\text{H}_3\text{-2-O-C}_6\text{H}_2]\text{CH=NC}_6\text{F}_5\}\text{Al}(\text{CH}_3)_2$ (3).



To a toluene (25 mL) solution of **Lig3**, synthesized according to literature,³ (0.97 g, 1.86 mmol), 3 mL of a toluene solution 0.68 M of $\text{Al}(\text{CH}_3)_3$ (2.05 M) was added dropwise via cannula at 0 °C. The reaction mixture was magnetically stirred for 1 h at 0 °C, then for 2 h at room temperature. After this time, the solvent was removed and the solid dried in vacuo. Yield: 0.918 g (83 %).

^1H NMR (400 MHz, C_6D_6 , 25 °C) δ 7.73 (d, $J = 2.5$ Hz, 1H; ArH), 7.29 – 7.13 (m, 8H; ArH cumyl), 7.12 – 7.06 (m, 2H; *p*-ArH cumyl), 7.03 (s, 1H; N=CH), 6.77 (d, $J = 2.5$ Hz, 1H; ArH), 1.63 (s, 6H; CH_3), 1.62 (s, 6H; CH_3), -0.57 (s, 6H; Al- CH_3).

^{13}C NMR (101 MHz, C_6D_6 , 25 °C) δ 176.7 (ArC=N), 164.2 (C-O), 150.3, 150.0 (ArC cumyl), 142.5, 139.9 136.7 (ArC-F), 131.5, 128.7, 127.1, 126.5, 125.8, 125.6 (ArC cumyl), 118.5 (ArC-C=N), 42.7, 42.4 ($\text{C}(\text{CH}_3)_2$), 30.9, 29.0 ($\text{C}(\text{CH}_3)_2$), -10.3 (Al- CH_3).

^{19}F NMR (376 MHz, C_6D_6 , 25 °C) δ -148.28 (dd, $J = 18.2, 5.6$ Hz, 2F; *o*-F), -154.76 (t, $J = 22.3$ Hz, 1F; *p*-F), -160.87 (td, $J = 22.3, 5.6$ Hz, 2F; *m*-F).

5.3. Copolymerization of *rac*-lactide and glycolide

5.3.1. Hopolymerization in bulk

In a typical homopolymerization run, a vial (20 mL) was charged sequentially with monomer (2.50 mmol), precatalyst (25 μmol) and MeOH (25 μmol ; 0.25 mL of a 0.1 M toluene solution). The vial was put into an oil bath, preheated and thermostated at 140 $^{\circ}\text{C}$, and was magnetically stirred. After 75 min, the vial was allowed to cool at room temperature. Product purification was obtained by dissolving the reaction mixture in CH_2Cl_2 , followed by a dropwise addition of this solution to rapidly stirring methanol. The precipitated polymer was recovered by filtration, washed with methanol and dried at 60 $^{\circ}\text{C}$ in a vacuum oven overnight.

Poly(glycolide) = ^1H NMR (300 MHz, DMSO-d_6 , 100 $^{\circ}\text{C}$) 4.87 (s, 2H; $\text{CH}_2\text{C}(\text{O})\text{O}$), 4.13 (s, 2H; CH_2OH), 3.72 (s, 3H; OCH_3).

Poly(*rac*-lactide) = ^1H NMR (300 MHz, DMSO-d_6 , 100 $^{\circ}\text{C}$) δ 5.25 – 5.16 (m, 1H; $\text{CH}(\text{CH}_3)\text{C}(\text{O})\text{O}$), 4.23 (m, 1H; $\text{CH}(\text{CH}_3)\text{OH}$), 3.70 (s, 3H; CH_3O), 1.53 – 1.45 (m, 3H; $\text{CH}(\text{CH}_3)\text{C}(\text{O})\text{O}$), 1.32 (d, $J = 7.0$ Hz, 3H; $\text{CH}(\text{CH}_3)\text{OH}$).

^{13}C NMR (75 MHz, DMSO-d_6) δ 168.3, 168.15, 168.1 ($\text{CH}(\text{CH}_3)\text{C}(\text{O})\text{O}$), 68.5, 68.3 ($\text{CH}(\text{CH}_3)\text{C}(\text{O})\text{O}$), 15.8, 15.7 ($\text{CH}(\text{CH}_3)\text{C}(\text{O})\text{O}$).

5.3.2. Copolymerization in bulk

In a typical copolymerization run, a vial (20 mL) was charged sequentially with monomers (total amount = 2.50 mmol, if not stated otherwise), precatalyst (25 μmol) and MeOH (25 μmol ; 0.25 mL of a 0.1 M toluene solution). The vial was put into an oil bath, preheated and thermostated at 140 $^{\circ}\text{C}$, and was magnetically stirred. The polymerization workup was performed as above.

Poly(glycolide-*co-rac*-lactide) = ^1H NMR (300 MHz, DMSO-d_6 , 100 $^{\circ}\text{C}$) δ 5.34 – 5.14 (m, 1H; $\text{CH}(\text{CH}_3)\text{C}(\text{O})\text{O}$), 4.98 – 4.71 (m, 2H; $\text{CH}_2\text{C}(\text{O})\text{O}$), 1.57 – 1.44 (m, 3H; $\text{CH}(\text{CH}_3)\text{C}(\text{O})\text{O}$). ^{13}C NMR (75 MHz, DMSO) δ 168.4, 168.3, 168.2, 168.15, 168.1 ($\text{CH}(\text{CH}_3)\text{C}(\text{O})\text{O}$), 165.8, 165.7 ($\text{CH}_2\text{C}(\text{O})\text{O}$),

68.5, 68.3 ($\text{CH}(\text{CH}_3)\text{C}(\text{O})\text{O}$), 60.3, 60.2 ($\text{CH}_2\text{C}(\text{O})\text{O}$), 15.8, 15.7 ($\text{CH}(\text{CH}_3)\text{C}(\text{O})\text{O}$).

^1H NMR (300 MHz, CDCl_3 , 25 °C) δ 5.31 – 5.11 (m, 1H; $\text{CH}(\text{CH}_3)\text{C}(\text{O})\text{O}$), 4.92 – 4.57 (m, 2H; $\text{CH}_2\text{C}(\text{O})\text{O}$), 1.65 – 1.52 (m, 3H; $\text{CH}(\text{CH}_3)\text{C}(\text{O})\text{O}$). ^{13}C NMR (75 MHz, DMSO) δ 169.6, 169.4, 169.3, 169.2 ($\text{CH}(\text{CH}_3)\text{C}(\text{O})\text{O}$), 166.4, 166.74 ($\text{CH}_2\text{C}(\text{O})\text{O}$), 69.3, 69.2, 69.0 ($\text{CH}(\text{CH}_3)\text{C}(\text{O})\text{O}$), 60.9, 60.8, 60.7 ($\text{CH}_2\text{C}(\text{O})\text{O}$), 16.7, 16.6 ($\text{CH}(\text{CH}_3)\text{C}(\text{O})\text{O}$).

Low molecular weight poly(glycolide-*co-rac*-lactide) copolymers were prepared as above, but 0.50 mmol of glycolide and 0.50 mmol of *rac*-lactide were used.

^1H NMR (300 MHz, DMSO- d_6 , 100 °C) δ 5.34 – 5.14 (m, 1H; $\text{CH}(\text{CH}_3)\text{C}(\text{O})\text{O}$), 4.98 – 4.71 (m, 2H; $\text{CH}_2\text{C}(\text{O})\text{O}$), 4.23 (m, 1H; $\text{CH}(\text{CH}_3)\text{OH}$), 4.29 – 4.18 (m, 1H; $\text{CH}(\text{CH}_3)\text{OH}$), 4.13 (s, 2H; CH_2OH), 4.09 (m, 2H; CH_2OH), 3.72 (s, 3H; OCH_3), 3.70 (s, 3H; CH_3O), 1.57 – 1.44 (m, 3H; $\text{CH}(\text{CH}_3)\text{C}(\text{O})\text{O}$), 1.32 (d, $J = 7.0$ Hz, 3H; $\text{CH}(\text{CH}_3)\text{OH}$). ^{13}C NMR (75 MHz, DMSO- d_6) δ 168.4, 168.3, 168.2, 168.15, 168.1 ($\text{CH}(\text{CH}_3)\text{C}(\text{O})\text{O}$), 165.8, 165.7 ($\text{CH}_2\text{C}(\text{O})\text{O}$), 68.5, 68.3 ($\text{CH}(\text{CH}_3)\text{C}(\text{O})\text{O}$), 60.3, 60.2 ($\text{CH}_2\text{C}(\text{O})\text{O}$), 59.1 (CH_2OH), 15.8, 15.7 ($\text{CH}(\text{CH}_3)\text{C}(\text{O})\text{O}$).

^1H NMR (300 MHz, CDCl_3 , 25 °C) δ 5.34 – 5.10 (m, 1H; $\text{CH}(\text{CH}_3)\text{C}(\text{O})\text{O}$), 4.95 – 4.55 (m, 2H; $\text{CH}_2\text{C}(\text{O})\text{O}$), 4.46 – 4.34 (m, 1H; $\text{CH}(\text{CH}_3)\text{OH}$), 4.30 (s, 2H; CH_2OH), 4.28 – 4.23 (m, 2H; CH_2OH), 3.72 (s, 3H; OCH_3), 3.70 (s, 3H; OCH_3), 1.65 – 1.48 (m, 3H; $\text{CH}(\text{CH}_3)\text{C}(\text{O})\text{O}$), 1.32 (d, $J = 7.0$ Hz, 3H; $\text{CH}(\text{CH}_3)\text{OH}$).

5.3.3. Copolymerization in solution

In a typical polymerization run, a Schlenk tube (10 mL) was charged sequentially with monomer(s) (total = 5.00 mmol), precatalyst (25 μmol ; 5 mM in each solvent), the solvent and MeOH (25 μmol ; 0.25 mL of a 0.1 M

toluene solution). The Schlenk tube was put into an oil bath, preheated and thermostated at the desired temperature, and was magnetically stirred. After the established time, the mixture was cooled to room temperature. Product purification was attained by dropwise addition of the reaction mixture, dissolved in CH_2Cl_2 , to rapidly stirring methanol. The precipitated polymers were recovered by filtration, washed with methanol and dried at $60\text{ }^\circ\text{C}$ overnight in a vacuum oven.

Poly(glycolide-*co-rac*-lactide) = ^1H NMR (300 MHz, DMSO-d_6 , $100\text{ }^\circ\text{C}$) δ 5.34 – 5.14 (m, 1H; $\text{CH}(\text{CH}_3)\text{C}(\text{O})\text{O}$), 4.98 – 4.71 (m, 2H; $\text{CH}_2\text{C}(\text{O})\text{O}$), 1.57 – 1.44 (m, 3H; $\text{CH}(\text{CH}_3)\text{C}(\text{O})\text{O}$). ^{13}C NMR (75 MHz, DMSO-d_6) δ 168.4, 168.3, 168.2, 168.15, 168.1 ($\text{CH}(\text{CH}_3)\text{C}(\text{O})\text{O}$), 165.8, 165.7 ($\text{CH}_2\text{C}(\text{O})\text{O}$), 68.5, 68.3 ($\text{CH}(\text{CH}_3)\text{C}(\text{O})\text{O}$), 60.3, 60.2 ($\text{CH}_2\text{C}(\text{O})\text{O}$), 15.8, 15.7 ($\text{CH}(\text{CH}_3)\text{C}(\text{O})\text{O}$).

5.3.4. Synthesis of poly(glycolide)-*block*-poly(*rac*-lactide)]

A Schlenk tube (10 mL) was charged sequentially with *rac*-lactide (1.25 mmol), precatalyst (25 μmol ; 5 mM in xylenes), xylenes and MeOH (25 μmol ; 0.25 mL of a 0.1 M toluene solution). The Schlenk tube was put into an oil bath, thermostated at $130\text{ }^\circ\text{C}$. After 4.5 h, glycolide (0.39 mmol) was added as a solid to the reaction mixture. The reaction was quenched after 10' by addition of 2 mL of wet CH_2Cl_2 . The mixture was then added to methanol (20 mL). The precipitated polymer was recovered by filtration, washed with methanol and dried at $60\text{ }^\circ\text{C}$ overnight in a vacuum oven. The $M_{n,\text{NMR}}$ evaluated by ^1H NMR was 3.7 kDa.

^1H NMR (300 MHz, DMSO-d_6 , $100\text{ }^\circ\text{C}$) δ 5.27 – 5.14 (m, 1H; $\text{CH}(\text{CH}_3)\text{C}(\text{O})\text{O}$), 4.87 (s, 2H; $\text{CH}_2\text{C}(\text{O})\text{O}$), 1.54 – 1.44 (m, 3H; $\text{CH}(\text{CH}_3)\text{C}(\text{O})\text{O}$). ^{13}C NMR (75 MHz, DMSO-d_6) δ 168.3, 168.15, 168.1 ($\text{CH}(\text{CH}_3)\text{C}(\text{O})\text{O}$), 165.8 ($\text{CH}_2\text{C}(\text{O})\text{O}$), 68.5, 68.3 ($\text{CH}(\text{CH}_3)\text{C}(\text{O})\text{O}$), 60.3 ($\text{CH}_2\text{C}(\text{O})\text{O}$), 15.8, 15.7 ($\text{CH}(\text{CH}_3)\text{C}(\text{O})\text{O}$).

5.4. Copolymerization of glycolide and ϵ -caprolactone.

In a typical copolymerization run, a screw vial (20 mL) was charged sequentially with monomers (total amount = 2.50 mmol), precatalyst (12 μ mol) and MeOH (0.12 mL of a 0.1 M toluene solution; 12 μ mol). The vial was put into an oil bath, preheated and thermostated at 140 °C and was magnetically stirred. After 75 min, product isolation was attained by dissolving the reaction mixture in CH_2Cl_2 and by dropwise pouring this solution into rapidly stirring methanol. Precipitated polymer was recovered by filtration, washed with methanol and dried at 60 °C in vacuum oven overnight.

Poly[(glycolide)-*co*-(ϵ -caprolactone)] = ^1H NMR (300 MHz, DMSO-d_6 , 100 °C) δ 4.87 (s, 2H; $-\text{C}(\text{O})\text{OCH}_2-$; GGGG), 4.85 (s, 2H; $-\text{C}(\text{O})\text{OCH}_2-$; CapGGGG and GGGGCap), 4.83 (s, 2H; $-\text{C}(\text{O})\text{OCH}_2-$; CapGGGCap), 4.75 (s, 2H; $-\text{C}(\text{O})\text{OCH}_2-$; GGGGCap), 4.73 (s, 2H; $-\text{C}(\text{O})\text{OCH}_2-$; CapGGGG and CapGGGCap), 4.71 (s, 2H; $-\text{C}(\text{O})\text{OCH}_2-$; CapGGCap), 4.61 (s, 2H; $-\text{C}(\text{O})\text{OCH}_2$; CapGCap), 4.13 (m, 2H; $-\text{C}(\text{O})\text{OCH}_2-$; CapG), 4.02 (t, $J = 6.6$ Hz, 2H; $-\text{C}(\text{O})\text{OCH}_2-$; CapCap), 3.71 (s, 3H; $\text{CH}_3\text{O-GG}$), 3.70 (s, 3H; $\text{CH}_3\text{O-GGCap}$), 3.605 (s, 3H; $\text{CH}_3\text{O-Cap}$), 3.42 (t, $J = 6.4$ Hz, 3H; Cap-OH), 2.39 (m, 2H; $-\text{CH}_2\text{CO}-$; CapG), 2.28 (m, 2H; $-\text{CH}_2\text{CO}-$; CapCap), 1.60 (m, 4H; $-\text{CH}_2\text{CH}_2\text{CO}-$ and $-\text{C}(\text{O})\text{OCH}_2\text{CH}_2-$), 1.37 (m, 2H; $-\text{C}(\text{O})\text{O}(\text{CH}_2)_2\text{CH}_2(\text{CH}_2)_2\text{CO}-$).

^{13}C NMR (75 MHz, DMSO-d_6 , 100 °C) δ 172.0 ($-\text{C}(\text{O})\text{O}-$; CapCap), 171.6 ($-\text{C}(\text{O})\text{O}-$; CapGCap), 171.4 ($-\text{C}(\text{O})\text{O}-$; CapGG), 167.0 ($-\text{C}(\text{O})\text{O}-$; CapGCap), 166.7 ($-\text{C}(\text{O})\text{O}-$; CapGGCap), 166.6 ($-\text{C}(\text{O})\text{O}-$; CapGGGG), 166.4 ($-\text{C}(\text{O})\text{O}-$; CapGGGCap), 166.3 ($-\text{C}(\text{O})\text{O}-$; GGGGCap), 166.05 ($-\text{C}(\text{O})\text{O}-$; CapGGGCap), 166.0 ($-\text{C}(\text{O})\text{O}-$; CapGGGG), 165.95 ($-\text{C}(\text{O})\text{O}-$; GGGGCap), 165.9 ($-\text{C}(\text{O})\text{O}-$; GGGG), 64.2 ($-\text{C}(\text{O})\text{OCH}_2-$; GGCap), 64.15 ($-\text{C}(\text{O})\text{OCH}_2-$; GGCap), 64.0 ($-\text{C}(\text{O})\text{OCH}_2-$; CapGCap), 62.9 ($-\text{C}(\text{O})\text{OCH}_2-$; CapCap), 60.7 ($-\text{C}(\text{O})\text{OCH}_2-$; CapGGGCap), 60.6 ($-\text{C}(\text{O})\text{OCH}_2-$; CapGGGCap).

C(O)OCH_2^- ; CapGGG), 60.3 ($-\text{C(O)OCH}_2^-$; GGGG), 60.1 ($-\text{C(O)OCH}_2^-$; GGGGCap), 60.0 ($-\text{C(O)OCH}_2^-$; CapGCap), 59.55 ($-\text{C(O)OCH}_2^-$; GGCap); 33.0 ($-\text{CH}_2\text{CO}-$; CapCap), 32.95 ($-\text{CH}_2\text{CO}-$; CapGG), 32.5 ($-\text{CH}_2\text{CO}-$; CapGCap), 32.5 ($-\text{CH}_2\text{CO}-$; CapGG), 32.45 ($-\text{CH}_2\text{CO}-$; CapGG); 27.3 ($-\text{C(O)OCH}_2\text{CH}_2^-$; CapCap), 27.3 ($-\text{C(O)OCH}_2\text{CH}_2^-$; CapGG), 27.15 ($-\text{C(O)OCH}_2\text{CH}_2^-$; CapGCap), 27.1 ($-\text{C(O)OCH}_2\text{CH}_2^-$; CapGG), 27.05 ($-\text{C(O)OCH}_2\text{CH}_2^-$; CapGG); 24.4 ($-\text{CH}_2\text{CH}_2\text{CO}-$; CapCap), 24.3 ($-\text{CH}_2\text{CH}_2\text{CO}-$; CapGCap), 24.25 ($-\text{CH}_2\text{CH}_2\text{CO}-$; CapGG), 24.1 ($-\text{CH}_2\text{CH}_2\text{CO}-$; CapGG); 23.5 ($-\text{C(O)O}(\text{CH}_2)_2\text{CH}_2(\text{CH}_2)_2\text{CO}-$; CapCap), 23.45 ($-\text{C(O)O}(\text{CH}_2)_2\text{CH}_2(\text{CH}_2)_2\text{CO}-$; CapGCap), 23.4 ($-\text{C(O)O}(\text{CH}_2)_2\text{CH}_2(\text{CH}_2)_2\text{CO}-$; CapGCap), 23.35 ($-\text{C(O)O}(\text{CH}_2)_2\text{CH}_2(\text{CH}_2)_2\text{CO}-$; CapGCap), 23.3 ($-\text{C(O)O}(\text{CH}_2)_2\text{CH}_2(\text{CH}_2)_2\text{CO}-$; CapGG), 23.3 ($-\text{C(O)O}(\text{CH}_2)_2\text{CH}_2(\text{CH}_2)_2\text{CO}-$; CapGG).

5.5. Terpolymerization of glycolide, ϵ -caprolactone and *rac*-lactide.

In a typical terpolymerization run, a screw vial (20 mL) was charged sequentially with monomers (total amount = 2.50 mmol), precatalyst (25 μmol) and MeOH (0.25 mL of a 0.1 M toluene solution; 25 μmol). The vial was put into an oil bath, preheated and thermostated at 140 $^\circ\text{C}$, and was magnetically stirred. After 75 min, workup was performed as described above.

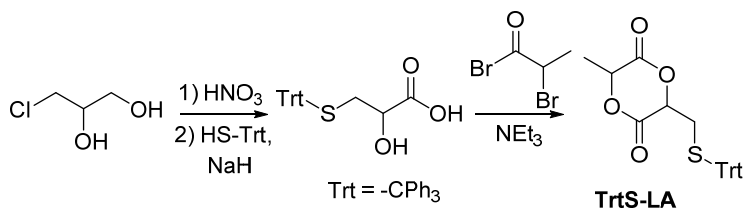
Poly[(glycolide)-*co*-(*rac*-lactide)-*co*-(ϵ -caprolactone)] = ^1H NMR (300 MHz, DMSO- d_6 , 100 $^\circ\text{C}$) δ 5.32 – 5.17 (m, 1H; $-\text{C(O)OCH}(\text{CH}_3)-$; LLLL) 5.17 – 5.05 (m, 1H; $-\text{C(O)OCH}(\text{CH}_3)-$; LLGG+LLCap+CapLL+GGLL); 4.88 (s, 2H; $-\text{C(O)OCH}_2-$; GGGG), 4.86 (s, 2H; $-\text{C(O)OCH}_2-$; CapGGGG and GG $\underline{\underline{G}}$ Cap), 4.85 (s, 2H; $-\text{C(O)OCH}_2-$; GGL and LGG); 4.84 (s, 2H; $-\text{C(O)OCH}_2-$; CapGG $\underline{\underline{G}}$ Cap), 4.83 (s, 2H; $-\text{C(O)OCH}_2-$; LGL); 4.75 (s,

2H; $-\text{C}(\text{O})\text{OCH}_2-$; GGGGCap), 4.73 (s, 2H; $-\text{C}(\text{O})\text{OCH}_2-$; CapGGG and CapGGGCap), 4.71 (s, 2H; $-\text{C}(\text{O})\text{OCH}_2-$; CapGGCap), 4.61 (s, 2H; $-\text{C}(\text{O})\text{OCH}_2$; CapGCap), 4.20–4.07 (m, 2H; $-\text{C}(\text{O})\text{OCH}_2-$; CapG and CapL), 4.03 (t, $J = 6.6$ Hz, 2H; $-\text{C}(\text{O})\text{OCH}_2-$; CapCap), 3.71 (s, 3H; $\text{CH}_3\text{O}-\text{GG}$), 3.69 (s, 3H; $\text{CH}_3\text{O}-\text{LL}$), 3.61 (s, 3H; $\text{CH}_3\text{O}-\text{Cap}$), 3.42 (t, $J = 6.4$ Hz, 3H; Cap-OH), 2.43 – 2.32 (m, 2H; $-\text{CH}_2\text{CO}-$; CapG), 2.28 (t, $J = 7.3$ Hz; 2H; $-\text{CH}_2\text{CO}-$; CapCap), 1.75 – 1.55 (m, 4H; $-\text{CH}_2\text{CH}_2\text{CO}-$, $-\text{C}(\text{O})\text{OCH}_2\text{CH}_2-$ and $-\text{CH}(\text{CH}_3)-$), 1.45 – 1.20 (m, 2H; $-\text{C}(\text{O})\text{O}(\text{CH}_2)_2\text{CH}_2(\text{CH}_2)_2\text{CO}-$).

^{13}C NMR (75 MHz, DMSO- d_6 , 100 °C) δ 172.0 ($-\text{C}(\text{O})\text{O}-$; CapCap), 171.6 ($-\text{C}(\text{O})\text{O}-$; CapGCap), 171.4 ($-\text{C}(\text{O})\text{O}-$; CapGG+CapLL), 169.0 and 168.95 ($-\text{C}(\text{O})\text{O}-$; CapLL+LLCap), 168.4 ($-\text{C}(\text{O})\text{O}-$; LLGG), 168.3 ($-\text{C}(\text{O})\text{O}-$; LLLL), 168.25 ($-\text{C}(\text{O})\text{O}-$; GLG), 168.20 and 168.1 ($-\text{C}(\text{O})\text{O}-$; LLLL), 167.0 ($-\text{C}(\text{O})\text{O}-$; CapGCap), 166.6 ($-\text{C}(\text{O})\text{O}-$; CapGGGG), 166.5 ($-\text{C}(\text{O})\text{O}-$; CapGGGCap), 166.4, 166.3 and 166.0 ($-\text{C}(\text{O})\text{O}-$; GGGGCap), 165.85 ($-\text{C}(\text{O})\text{O}-$; GGGG), 165.8 and 165.7 ($-\text{C}(\text{O})\text{O}-$; GGLL), 68.7, 68.5, 68.45, 68.4, 68.35, 68.3, 68.2, 68.0, 67.4, 67.3 and 67.25 ($-\text{CH}(\text{CH}_3)-$), 64.7, 64.3, 64.2, 63.95, 63.9 and 62.9 ($-\text{CH}_2\text{OC}(\text{O})-$; Cap), 60.7, 60.6, 60.55, 60.3, 60.25, 60.2, 60.1, 60.0, 59.6, 59.5, 59.4, 59.2, 59.15, 59.1 ($-\text{CH}_2\text{OC}(\text{O})-$; G), 32.95, 32.6, 32.5, 32.4, 27.3, 27.25, 27.2, 27.1, 27.05, 24.4, 24.3, 24.25, 24.2, 24.1, 23.5, 23.45, 23.4, 23.35 and 23.3 ($-\text{CH}_2-$; Cap), 15.85, 15.8, 15.7 ($-\text{CH}_3$).

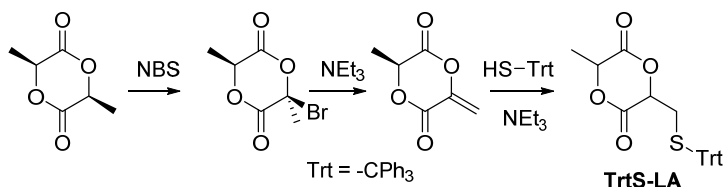
5.6. Synthesis and ROP of TrtS-LA, post-polymerization modification and scaffolding

5.6.1. Synthesis of 3-methyl-6-(tritylthiomethyl)-1,4-dioxane-2,5-dione (TrtS-LA)



Route a. The synthesis of 2-hydroxy-3-triphenylmethylthiopropanoic acid was performed according to a reported literature procedure by oxidizing 3-chloro-1,2-propanediol with HNO₃, followed by reaction with triphenylmethanethiol.⁴

Then, to a solution of 2-hydroxy-3-triphenylmethylthiopropanoic acid (2.15 g; 5.9 mmol) and NEt₃ (0.82 mL; 5.9 mmol) in dry CH₃CN (150 mL), 2-bromopropanoyl bromide (0.62 mL; 5.9 mmol) was added at 0 °C under nitrogen. The reaction was allowed to stir for 1 hour at 0 °C. Then, NEt₃ (0.82 mL; 5.9 mmol) was added at 0 °C. The temperature was slowly increased to 70 °C over 1 hour, and the reaction mixture was stirred for an additional 3 hours at 70 °C. The mixture was cooled to room temperature, concentrated to ~100 mL, dissolved in ethyl acetate (250 mL) and washed with HCl (200 mL x 3; 1 M). The organic layer was dried over Na₂SO₄, and the solvent was evaporated to dryness. The obtained brown oil was purified by column chromatography (silica gel; eluent, n-hexane/ethyl acetate gradient) to give the target compound in 30 % yield as a diastereomeric mixture ((3*S*,6*R*)/(3*S*,6*S*) 90:10).



Route b. The synthesis of (6*S*)-3-methylene-6-methyl-1,4-dioxane-2,5-dione was performed in two steps. L-Lactide was converted into (3*S*,6*S*)-3-bromo-3,6-dimethyl-1,4-dioxane-2,5-dione by radical bromination with *N*-bromosuccinimide (NBS). Then, dehydrobromination of the latter with

trimethylamine (NEt_3) gave (6*S*)-3-methylene-6-methyl-1,4-dioxane-2,5-dione.⁵

To a solution of triphenylmethanethiol (8.20 g; 29.6 mmol) and triethylamine (800 μL ; 5.6 mmol) in dry CH_3CN (200 mL) was added dropwise a solution of (6*S*)-3-methylene-6-methyl-1,4-dioxane-2,5-dione (4.00 g; 28.2 mmol), dissolved in dry CH_3CN (80 mL), over 40 min at 0 °C under nitrogen. The reaction mixture was stirred for 1.5 hours at 0 °C. The mixture was concentrated *in vacuo* to ~100 mL, dissolved in ethyl acetate (400 mL) and washed with HCl (200 mL x 3; 0.1 M). The organic layer was dried over Na_2SO_4 . Then, the solvent was evaporated to dryness. The resulting solid was purified by column chromatography (silica gel; eluent, n-hexane/ethyl acetate gradient) to give the target compound in 68 % yield as a diastereomeric mixture ((3*S*,6*R*)/(3*S*,6*S*) 83:17).

(3*S*,6*R*) diastereomer = ^1H NMR (600 MHz; CDCl_3) δ 7.48 (6H, d, $^3J = 7.6$ Hz, *o*-ArH), 7.31 (6, t, $^3J = 7.8$ Hz, *m*-ArH), 7.25–7.22 (3H, m, *p*-ArH), 4.58 (1H, q, $^3J = 6.6$ Hz, $-\text{CHCH}_3-$), 3.54 (1H, dd, $^3J = 7.8$ Hz, $^3J = 5.4$ Hz, $-\text{CHCH}_2\text{S}-$), 3.01 (1H, dd, $^2J = 15.0$ Hz, $^3J = 5.4$ Hz, $-\text{CHCH}_2\text{S}-$), 2.85 (1H, dd, $^2J = 15.0$ Hz, $^3J = 7.8$ Hz, $-\text{CHCH}_2\text{S}-$), 1.57 (3H, d, $^3J = 6.6$ Hz, $-\text{CHCH}_3-$).

^{13}C NMR (100 MHz; CDCl_3) δ 166.5 ($-\text{C}(\text{O})\text{CHCH}_3-$); 165.8 ($-\text{C}(\text{O})\text{CHCH}_2\text{S}-$); 144.1 ($^{\text{Ar}}\text{C}$); 129.5, 128.2 and 127.0 ($^{\text{Ar}}\text{CH}$); 74.4 ($-\text{CHCH}_2\text{S}-$); 72.2 ($-\text{CHCH}_3-$); 67.7 ($-\text{SC}(\text{Ph})_3$); 31.5 ($-\text{CHCH}_2\text{S}-$); 15.6 ($-\text{CH}_3$).

(3*S*,6*S*) diastereomer = selected ^1H NMR resonances (600 MHz; CDCl_3) δ 7.44 (6H, d, $^3J = 7.8$ Hz), 4.92 (1H, q, $^3J = 7.2$ Hz), 4.22 (1H, dd, $^3J = 7.2$ Hz, $^3J = 4.8$ Hz), 2.92 (1H, dd, $^2J = 13.8$ Hz, $^3J = 4.8$ Hz), 2.86 (1H, dd, $^2J = 13.8$ Hz, $^3J = 7.2$ Hz), 1.54 (3H, d, $^3J = 7.2$ Hz). Selected ^{13}C NMR resonances (100 MHz; CDCl_3) δ 165.6, 144.0, 129.9, 128.0, 127.3, 75.0, 73.1, 33.6 and 17.7.

5.6.2. Copolymerization of 3-methyl-6-(tritylthiomethyl)-1,4-dioxane-2,5-dione (TrtS-LA) with L-lactide (LA).

Prior to polymerization, TrtS-LA was dried as follows: the solid was dissolved in 100 mL of toluene and the solution was dried over Na₂SO₄. After filtration, the solvent was evaporated and the monomer was dissolved in dry toluene. The toluene was removed *in vacuo* trap by trap, and the monomer was further dried with P₂O₅ for 96 hours and stored in a glove box at -30 °C.

A 25 mL Schlenk Flask was sequentially charged with the salicylaldiminato aluminum complex **2** (10.0 mg; 25 μmol), LA (306 mg; 2.12 mmol) and Trt-LA (156 mg; 0.38 mmol) as monomers; toluene (2.0 mL); and MeOH (0.25 mL of a 0.1 M toluene solution; 25 μmol). The polymerization mixture was thermostated at 70 °C and magnetically stirred for 96 hours. Then, the mixture was cooled to room temperature and poured into n-hexane. The precipitate was filtered, washed sequentially with n-hexane and MeOH and dried *in vacuo* at 30 °C overnight. Yield = 90 %.

Poly[(TrtS-LA)-*co*-LA] (**a**) = ¹H NMR (400 MHz; CDCl₃) δ 7.42–7.37 (6H, m, ArH), 7.33–7.18 (9H, m, ArH), 5.16 (2H, q, ³J = 7.2 Hz, -CHCH₃-), 5.01 (1H, q, ³J = 6.0 Hz, -CHCH₃O-C(O)CHCH₂S-), 4.53 (1H, dd, ³J = 8.7 Hz, ³J = 3.3 Hz, -CHCH₂S-), 3.74 (3H, s, CH₃OC(O)-), 2.87–2.78 (1H, m, -CHCH₂S-), 2.70–2.64 (1H, m, -CHCH₂S-), 1.58 (3H, d, ³J = 7.2 Hz, -CHCH₃), 1.50–1.45 (3H, m, -CHCH₃).

¹³C NMR (75 MHz; CDCl₃) δ 169.8, 169.4 and 169.3 (-OC(O)CHCH₃-); 167.5 (-OC(O)CHCH₂S-); 144.3, 129.7, 128.2 and 127.0 (-C^{Ar}); 72.0 (-CHCH₂S-); 69.2 (-CHCH₃-); 67.6 (-SC(Ph)₃); 32.7 (-CHCH₂S-); 16.8 (-CHCH₃).

5.6.3. Copolymerization of 3-methyl-6-(tritylthiomethyl)-1,4-dioxane-2,5-dione (TrtS-LA) with ε-caprolactone (CL)

The polymerization was performed as above, but for TrtS-LA (314 mg; 0.75 mmol) and CL (200 mg; 1.75 mmol) were used as monomers. Yield = 92 %. Poly[(TrtS-LA)-*co*-CL] (**b**) = ^1H NMR (400 MHz; CDCl_3) δ 7.45–7.35 (6H, m, ArH), 7.30–7.20 (9H, m, ArH), 5.20–5.12 (1H, m, $-\text{CHCH}_3\text{O}-$), 5.00–4.93 (1H, m, $-\text{CHCH}_3\text{O}-$), 4.72–4.65 (1H, m, $-\text{CHCH}_2\text{S}(\text{CPh}_3)-$), 4.56–4.45 (1H, m, $-\text{CHCH}_2\text{S}(\text{CPh}_3)-$), 4.05 (2H, t, $^3J = 6.3$ Hz, $-\text{CH}_2\text{OC}(\text{O})-$), 3.66 (3H, s, $\text{CH}_3\text{OC}(\text{O})-$), 2.88–2.53 (2H, m, $-\text{CHCH}_2\text{S}(\text{CPh}_3)-$), 2.40–2.25 (2H, m, $-\text{OC}(\text{O})\text{CH}_2-$), 1.70–1.55 (overlapped signals: 4H, m, $-\text{CH}_2-$; 3H, m, $-\text{CHCH}_3$), 1.44–1.30 (2H, m, $-\text{CH}_2-$).

^{13}C NMR (75 MHz; CDCl_3) δ 173.6, 173.55, 172.7 and 172.6 ($-\text{OC}(\text{O})\text{CH}_2-$); 170.0 and 169.9 ($-\text{OC}(\text{O})\text{CHCH}_3-$); 168.1 and 168.0 ($-\text{OC}(\text{O})\text{CHCH}_2\text{S}-$); 144.4, 144.3, 129.7, 129.65, 128.2 and 127.0 ($-\text{C}^{\text{Ar}}$); 71.8 and 71.4 ($-\text{CHCH}_2\text{S}-$); 69.4 and 68.1 ($-\text{CHCH}_3-$); 67.5 and 67.2 ($-\text{SC}(\text{Ph})_3$); 65.6, 65.3 and 64.3 ($-\text{CH}_2\text{OC}(\text{O})-$); 34.2, 34.15, 33.8 and 33.7 ($-\text{C}(\text{O})\text{CH}_2-$); 32.9 ($-\text{CHCH}_2\text{S}-$); 28.5, 28.2, 25.6, 25.5, 25.4, 24.7 and 24.6 ($-\text{CH}_2-$); 17.0 and 16.9 ($-\text{CHCH}_3$).

5.6.4. Copolymerization of 3-methyl-6-(tritylthiomethyl)-1,4-dioxane-2,5-dione (TrtS-LA) with ϵ -caprolactone (CL) and L-lactide (LA)

The polymerization was performed as above, but TrtS-LA (105 mg; 0.25 mmol), CL (57.0 mg; 0.50 mmol) and LA (252 mg; 1.75 mmol) were used as monomers. Yield = 84 %.

Poly[(TrtS-LA)-*co*-CL-*co*-LA] (**c**) = ^1H NMR (400 MHz; CDCl_3) δ 7.46–7.37 (6H, m, ArH); 7.30–7.19 (9H, m, ArH), 5.19–5.07 (1H, m, $-\text{CHCH}_3\text{OC}(\text{O})-$), 5.03–4.97 (1H, m, $-\text{CHCH}_3\text{O}-\text{C}(\text{O})\text{CHCH}_2\text{S}-$), 4.74–4.68 (1H, m, $-\text{CHCH}_2(\text{SCPh}_3)-\text{C}(\text{O})-$), 4.53–4.47 (1H, m,

–CHCH₂S(CPh₃)–C(O)–), 4.16–4.09 (2H, m, –CH₂OC(O)CH–), 4.06 (2H, t, ³J = 6.8 Hz, –CH₂OC(O)CH–), 3.74 (3H, s, CH₃OC(O)–), 2.88–2.78 (2H, m, –CHCH₂S(CPh₃)–), 2.69–2.74 (2H, m, –CHCH₂S(CPh₃)–), 2.45–2.34 (2H, m, –CHOC(O)CH₂–), 2.32–2.28 (2H, m, –OC(O)CH₂–), 1.75–1.45 (overlapped signals: 4H, m, –CH₂–; 3H, m, –CHCH₃), 1.45–1.30 (2H, m, –CH₂–).

¹³C NMR (75 MHz; CDCl₃) δ 173.7, 173.6, 173.05 and 173.0 (–OC(O)CH₂–); 170.5, 170.2, 169.9, 169.75 and 169.70 (–OC(O)CH–); 144.3, 129.7, 128.2 and 127.0 (–C^{Ar}); 69.4, 69.1, 69.0, and 68.3 (–CH–); 67.6 (–SC(Ph)₃); 65.4 and 64.3 (–CH₂OC(O)–); 34.2, 34.15, 33.8 and 33.7 (–C(O)CH₂–); 32.0 (–CHCH₂S–); 28.5, 28.4, 28.35, 28.3, 25.6, 25.5, 25.4, 25.3, 24.7, 24.6, 24.5 and 24.4 (–CH₂–); 16.95, 16.9 and 16.8 (–CHCH₃).

5.6.5. Cleavage of trityl groups of poly[(TrtS–LA)-*co*-CL]

To a solution of poly[(TrtS–LA)-*co*-CL] (835 mg; 1.15 mmol of TrtS–groups) and Et₃SiH (220 μL; 1.38 mmol) in CH₂Cl₂ (10 mL) TFA was added (600 μL; 8.0 mmol) dropwise over 10 min under nitrogen. The solution was stirred for 1 hour. Then, the volatiles were evaporated *in vacuo*. The crude product was washed with n-hexane and used in the next step without further purification.

Poly[(HS–LA)-*co*-CL] (**d**) = ¹H NMR (400 MHz; CDCl₃) δ 5.39–5.23 (1H, m, –CHCH₂S–), 5.22–5.12 (1H, m, –CHCH₃–), 4.21–4.13 (2H, m, –CH₂OC(O)CH–), 4.06 (2H, t, ³J = 6.8 Hz, –CH₂OC(O)–), 3.11–2.95 (2H, m, –CHCH₂S–), 2.48–2.38 (2H, m, –CH₂C(O)OCH–), 2.31 (2H, t, ³J = 7.6 Hz, –CH₂C(O)O–), 1.67–1.57 (4H, m, –CH₂–), 1.53 (3H, d, ³J = 7.2 Hz, –CHCH₃–), 1.43–1.38 (2H, m, –CH₂–).

¹³C NMR (75 MHz; CDCl₃) δ 174.6, 173.4, 173.1 (–OC(O)CH₂–); 170.5 and 170.3 (–OC(O)CHCH₃–); 167.9 and 167.8 (–OC(O)CHCH₂S–); 73.4

and 73.0 (–CHCH₂S–); 69.7 and 68.5(–CHCH₃–); 65.9, 65.6 and 64.7 (–CH₂OC(O)–); 34.3, 34.2, 33.8 and 33.7 (–C(O)CH₂–); 31.7 (–CHCH₂S–); 28.4, 28.2, 25.8, 25.6, 25.4, 24.7 and 24.6 (–CH₂–); 17.0 and 16.9 (–CHCH₃).

5.6.6. Reaction of poly[(HS–LA)-*co*-CL] with 2,2'-dipyridyl disulfide

The poly[(HS–LA)-*co*-CL] obtained in the above step was dissolved in CH₂Cl₂ (45 mL). The solution was added dropwise over 1 hour to a solution of 2,2'-dipyridyl disulfide (1.00 g; 4.6 mmol) in CH₂Cl₂ (5 mL) under nitrogen. The mixture turned yellow and was stirred for three hours. Then, it was concentrated to ~10 mL and poured into 200 mL of hexane. The precipitated polymer was washed three times with MeOH, then dried under nitrogen flow and later *in vacuo* until constant weight. The obtained poly[(PDS–LA)-*co*-CL] (**e**) was collected as a clear waxy solid (535 mg; 90 % overall yield of the two steps). $M_n = 18.2$ kDa; $M_w/M_n = 1.6$.

Poly[(PDS–LA)-*co*-CL] (**e**) = ¹H NMR (400 MHz; CDCl₃) δ 8.46 (1H, s, pyridyl–H), 7.64 (2H, s, pyridyl–H), 7.10 (1H, s, pyridyl–H), 5.44–5.33 (1H, m, –CHCH₂S–), 5.25–5.08 (1H, m, –CHCH₃–), 4.18–4.00 (2H, m, –CH₂OC(O)–), 3.47–3.19 (2H, m, –CHCH₂S–), 2.44–2.26 (2H, m, –CH₂C(O)O–), 1.71–1.61 (4H, m, –CH₂–), 1.56 (3H, d, ³J = 6.3 Hz, –CHCH₃–), 1.48 (3H, d, ³J = 7.0 Hz, –CHCH₃–), 1.42–1.34 (2H, m, –CH₂–).

¹³C NMR (100 MHz; CDCl₃) δ 173.7, 173.6, 172.8 and 172.7 (–OC(O)CH₂–); 170.1 (–OC(O)CHCH₃–); 168.1 and 168.0 (–OC(O)CHCH₂S–); 159.2, 149.7, 137.4, 121.2 and 120.2 (–C^{Ar}); 71.4 and 70.8 (–CHCH₂S–); 69.7 and 68.2 (–CHCH₃–); 65.9, 65.6 and 64.3 (–CH₂OC(O)–); 34.3, 34.2, 33.8 and 33.7 (–C(O)CH₂–); 31.8

($-\text{CHCH}_2\text{S}-$); 28.5, 28.3, 28.25, 25.7, 25.6, 25.4, 24.7, 24.6, and 24.5 ($-\text{CH}_2-$); 17.0 and 16.9 ($-\text{CHCH}_3$).

5.6.7. Synthesis of poly(L-lactide-co- ϵ -caprolactone) (PCLA)

The copolymer was prepared according to a literature procedure.⁶ A previously silanized 25 mL round-bottom flask was charged with stannous octoate SnOct_2 (9.0 mg; 22.0 μmol), ethylene glycol (23.0 mg; 0.37 mmol), LA (18.2 g; 0.126 mol) and CL (11.8; 0.103 mol) under nitrogen. The polymerization mixture was thermostated at 110 °C and magnetically stirred for 24 hours. Then, the mixture was cooled to room temperature, and the crude copolymer was dissolved in CHCl_3 and precipitated three times in a cold n-hexane/MeOH 95:5 solution. The precipitate was dried *in vacuo* at 60 °C overnight and collected as a white solid (21.7 g; 72 % yield). $M_n = 100.7$ kDa; $M_w/M_n = 1.2$. Composition: LA/CL 75:25.

PCLA = ^1H NMR (400 MHz; CDCl_3) δ 5.19–5.09 (m, 2H), 4.15–4.04 (m, 2H), 2.40–2.29 (m, 2H), 1.63–1.62 (m, 4H), 1.57–1.49 (m, 6H), 1.40–1.36 (m, 2H).

^{13}C NMR (100 MHz; CDCl_3) δ 173.7, 173.6, 173.55, 173.0, 172.95, 170.5, 170.45, 170.4, 170.2, 169.9, 169.75, 169.7, 69.4, 69.1, 68.9, 68.4, 65.45, 65.4, 64.3, 34.3, 34.2, 33.8, 33.75, 28.5, 28.45, 28.35, 28.3, 25.7, 25.55, 25.5, 25.3, 24.7, 24.6, 24.5, 24.4, 17.0, 16.9, 16.8.

5.6.8. Scaffold preparation

Porous scaffolds were prepared by a salt leaching method⁶ using blends of poly[(PDS–LA)-co-CL] and PCLA.

Scaffolds containing different amounts of poly[(PDS–LA)-co-CL] (0, 10, 20 and 30 % by weight) were prepared by dissolving poly[(PDS–LA)-co-

CL] and PCLA in CHCl_3 to form a 10 % w/w homogeneous solution. The obtained solution was poured over the porogen agent (NaCl; particle size in the range of 75–500 μm) in a mold. The polymer-to-salt weight ratio was 1:10. The mixture was slowly air-dried under a lid for 1 week. The scaffold was removed from the mold and subsequently cut into the desired shape. The salt particles were leached out with deionized water. Salt-leached samples were dried in a vacuum desiccator for 3 days before use.

5.6.9. Binding of the H-Arg-Gly-Asp-Cys-OH (RGDC) peptide to the scaffolds

The binding of the RGDC (H-Arg-Gly-Asp-Cys-OH) to the scaffolds was performed according to a slightly modified literature procedure.⁷ Porous scaffolds (1 mm in thickness and 10 mm in diameter; weight in the range of 15.1–11.4 mg; content of pyridyl disulfide groups in the range of 2.9–6.6 $\times 10^{-6}$ mol) were presoaked in ethanol and then in phosphate-buffered saline (PBS). Afterwards, the scaffolds were transferred to 2.5 mL of peptide solution ($C = 5.00 \times 10^{-3}$ M) in PBS ($C = 0.01$ M; $\text{pH} = 7.4$) and shaken in the dark at room temperature. UV spectroscopy of the peptide solution was used to follow the reaction; the absorbance of the released 2-pyridinethiol at 343 nm was detected to calculate the degree of immobilization according to Beer's law with a known the molar extinction coefficient, $\epsilon = 8.06 \times 10^3 \text{ M}^{-1} \text{ cm}^{-1}$, at 343 nm. A UV spectrum of the peptide solution before reaction was recorded and used as a blank.

5.6.10. Cytotoxicity of the scaffolds' extracted liquid

The cytotoxicity of the RGDC-modified scaffolds described in the above paragraph was assessed using human dermal fibroblasts (hDFs) stained by the alamarBlue assay. For each sample, three parallel tests were carried out.

Porous scaffold disks (1 mm in thickness and 10 mm in diameter, weight in the range of 15.1–11.4 mg) were sterilized with 70 % ethanol, washed three times with phosphate-buffered saline (PBS) buffer and placed into the wells of a 48-well tissue-culture polystyrene plate. Each sample was immersed in 250 μL of complete growth medium (CGM; Dulbecco's modified Eagle's medium supplemented with 10 % fetal bovine serum and 1 % antibiotics, penicillin/streptomycin).

After 24 hours of incubation at 37 °C under an atmosphere of 5 % CO_2 , 140 μL of extraction medium from each sample were added into each well of a 96-well plate, and 8×10^3 cells were seeded in each well (10 μL of the hDF cell suspension; density = 8×10^5 cells/mL; passage 10). A cell culture in fresh CGM was used as a control. The plate was incubated for 24 hours at 37 °C under an atmosphere of 5 % CO_2 .

Then, the extraction media were removed, and 100 μL of resazurin (Invitrogen alamarBlue cell viability reagent) solution in PBS were added to each well. The plate was incubated for approximately 1 hour. The fluorescence of each well was measured by a Tecan Infinite 200 PRO multifunctional microplate reader (excitation wavelength = 560 nm; emission wavelength = 590). The viability of the cells in each well was determined according to a titration curve and compared to the cell viability obtained for PCLA-based scaffolds evaluated by the same method.

5.7. Ring-opening of 6HDL and post-polymerization modifications.

5.7.1. Synthesis of poly(6- ω -hexadecenlactone)

A typical polymerization is described herein for the sample of run 5 in Table 4.1. A Schlenk tube was charged sequentially with the precatalyst (14.0 mg, 35 μmol), the monomer (883 mg, 3.5 mmol), xylenes (2.3 mL) and

methanol (0.35 mL of a 0.1 M toluene solution, 35 μmol). The mixture was thermostated at 100 °C and magnetically stirred for 27 h, then cooled to room temperature. Volatiles were removed *in vacuo*, the product was dissolved in a minimal amount of CH_2Cl_2 , then added dropwise to rapidly stirring methanol. The precipitated polymer was recovered by filtration, washed with methanol and dried at 30 °C overnight in a vacuum oven. Yield = 60 %.

^1H NMR (300 MHz, CDCl_3 , RT) δ 5.37 (bs, 2H; $-\text{C}(\text{H})=$), 4.04 (t, $J = 6.6$ Hz, 2H; $-\text{CH}_2\text{O}-$), 3.66 (s, $-\text{OCH}_3$), 3.63 (t, $-\text{CH}_2\text{OH}$), 2.28 (t, $J = 7.4$ Hz, 2H; $-\text{C}(\text{O})\text{CH}_2-$), 1.96 (bs, 4H; $-\text{CH}_2\text{C}(\text{H})=$), 1.75–1.55 (m, 4H; $-\text{C}(\text{O})\text{CH}_2\text{CH}_2-$ and $-\text{CH}_2\text{CH}_2\text{O}-$), 1.45–1.25 (m, 14H; CH_2). ^{13}C NMR (75 MHz, CDCl_3 , RT) δ 174.15 ($-\text{C}(\text{O})\text{O}-$), 130.6 ($-\text{CH}=\text{}$), 130.3 ($-\text{CH}=\text{}$), 64.5 ($-\text{C}(\text{O})\text{OCH}_2-$), 34.5 ($-\text{CH}_2\text{C}(\text{O})\text{O}-$), 32.7, 32.6, 29.7 and 29.6 (CH_2), 29.3 (2 C; CH_2), 29.15 ($-\text{CH}_2\text{CH}=\text{}$), 28.9 ($-\text{CH}_2\text{CH}=\text{}$), 28.8, 25.95 and 25.15 (CH_2).

5.7.2. Kinetic experiments

In a Braun Labmaster glovebox, a Teflon-valved J. Young NMR tube was charged with a solution of the initiator, the monomer and dry methanol in toluene- d_8 (0.5 mL). The sample was thermostated at 80 °C. The polymerization reaction was monitored *via* ^1H NMR analysis.

5.7.3. Epoxidation of poly(6,7-epoxy- ω -hexadecenlactone)

The epoxidation procedure is based on a modification of previously reported literature methodologies.⁸ In a screw vial, poly(6- ω -hexadecenlactone) (obtained in run 5 in Table 4.1, 252 mg, 1.0 mmol alkene function) was dissolved in dry CHCl_3 (5.0 mL) at room temperature. Then, mCPBA was added (260 mg, 1.5 mmol) at 0 °C. The mixture was stirred for 3 days at 20 °C. The epoxidized polymer was precipitated in methanol,

recovered by filtration, washed with methanol and dried *in vacuo* at 20 °C. Yield = 95 %. $M_{n,th}$ = 16.4 kDa. $M_{n,NMR}$ = 15.6 kDa. $M_{n,GPC}$ = 37.2 kDa. M_n/M_w = 1.9.

^1H NMR (300 MHz, CDCl_3 , RT) δ 4.04 (t, J = 6.6 Hz, 2H; $-\text{CH}_2\text{O}-$), 3.66 (s, $-\text{OCH}_3$), 3.63 (t, $-\text{CH}_2\text{OH}$), 2.65 (bs, 2H; $-\text{CHO}-$), 2.28 (t, J = 7.4 Hz, 2H; $-\text{C}(\text{O})\text{CH}_2-$), 1.75–1.55 (m, 4H; $-\text{C}(\text{O})\text{CH}_2\text{CH}_2-$ and $-\text{CH}_2\text{CH}_2\text{O}-$), 1.55–1.45 (m, 2H; $\text{CH}_2\text{CHO}-$) 1.45–1.15 (m, 14H; CH_2). ^{13}C NMR (75 MHz, CDCl_3 , RT) δ 174.15 ($-\text{C}(\text{O})\text{O}-$), 64.5 ($-\text{C}(\text{O})\text{OCH}_2-$), 59.0 ($-\text{CHO}-$), 58.95 ($-\text{CHO}-$), 34.45 ($-\text{CH}_2\text{C}(\text{O})\text{O}-$), 32.2, 32.15, 29.4 and 29.3 (CH_2), 29.2 (2C; CH_2), 28.65 (CH_2), 26.15 and 26.1 ($-\text{CH}_2\text{CHO}-$), 25.95 and 25.05 (CH_2).

5.7.4. Reaction of poly(6,7-epoxy- ω -hexadecenlactone) with NaCNBH_3

The reaction procedure is based on a modification of a literature methodology.⁹ In a Schlenk flask, the poly(6,7-epoxy- ω -hexadecenlactone) described above (88 mg, 0.33 mmol epoxy function) was dissolved in dry THF (33.0 mL) at room temperature. Then, NaCNBH_3 (82.5 mg, 1.3 mmol) and $\text{BF}_3 \cdot \text{ether}$ (82.0 μL , 0.66 mmol) were added at 0 °C. The mixture was stirred for 8 h at 20 °C. The polymer was recovered by filtration, washed with methanol five times and dried in vacuum at 20 °C. Yield = 69 %. The same procedure was performed on a lower molecular weight epoxidized sample (Table 1, Run 3).

^1H NMR (300 MHz, CDCl_3 , RT) δ 4.04 (t, J = 6.6 Hz, 2H; $-\text{CH}_2\text{O}-$), 3.57 (bs, 1H; CHOH), 3.41 (bs, 2H; $-\text{CH}-\text{O}-\text{CH}-$), 2.28 (t, J = 7.4 Hz, 2H; $-\text{C}(\text{O})\text{CH}_2-$), 1.75–1.50 (m, 8H; $-\text{CH}_2-$), 1.50–1.15 (m, 16H; CH_2).

5.7.5. Reaction of poly(6- ω -hexadecenlactone) with 6-mercapto-1-hexanol

In a screw vial, 6-mercapto-1-hexanol (250 mg, 2.1 mmol) and 2,2'-azobis(2-methylproprionitrile) (5 mg) were added under N₂ atmosphere to poly(6- ω -hexadecenlactone) (104 mg of the sample of run 7 in Table 4.1, $M_{n,NMR} = 14.1$ kDa), dissolved in dry THF (1.0 mL). The mixture was stirred for 24 h at 80 °C. The product was precipitated in methanol, recovered by filtration, washed with methanol and dried in vacuum at 20 °C. Yield = 62 %. $M_{n,NMR} = 21.5$ kDa. $M_{n,GPC} = 36.6$ kDa. $M_n/M_w = 1.8$.

¹H NMR (400 MHz, CDCl₃, RT) δ 4.05 (t, $J = 6.4$ Hz, 2H; -CH₂O-), 3.64 (t, $J = 6.8$ Hz, 2H; -CH₂OH), 2.54-2.51 (m, 1H; -CHS-), 2.47 (t, $J = 7.2$ Hz, 2H; -CH₂S-), 2.29 (t, $J = 7.2$ Hz, 2H; -C(O)CH₂-), 1.68-1.46 (m, 14H; -CH₂-), 1.46-1.20 (m, 18H; -CH₂-). ¹³C NMR (100 MHz, CDCl₃, RT) δ 174.2 (-C(O)O-), 64.5 (-C(O)OCH₂-) 63.0 (-CH₂OH), 46.0 (-CS-), 35.0 (-CS-), 34.5 (-CH₂C(O)O-), 32.8, 30.4, 30.0, 29.7, 29.6 and 29.5 (CH₂), 29.4 (2C; CH₂), 29.3, 28.9, 28.8, 26.9, 26.85, 26.0, 25.6 and 25.1 (CH₂).

5.7.6. Synthesis of poly[(6- ω -hexadecenlactone)-*ran*-(ϵ -caprolactone)]

A Schlenk tube was charged with precatalyst (14.0 mg, 35 μ mol), 6HDL (442 mg, 1.75 mmol), ϵ -CL (200 mg, 1.75 mmol), xylenes (2.3 mL) and methanol (0.35 mL of a 0.1 M toluene solution, 35 μ mol). The mixture was thermostated at 100 °C and magnetically stirred for 29 h, then cooled to room temperature. Product purification was attained by removal of xylenes under vacuum, followed by dropwise addition of the crude reaction mixture, dissolved in a minimal amount of CH₂Cl₂, to rapidly stirring methanol. The precipitated polymer was recovered by filtration, washed with methanol and dried at 30 °C overnight in a vacuum oven. Yield = 75 %. Composition ϵ -CL = 50 %; 6HDL = 50 %. $M_{n,th} = 15.0$ kDa. $M_{n,NMR} = 15.8$ kDa. $M_{n,GPC} = 36.0$ kDa. $M_n/M_w = 1.6$.

^1H NMR (300 MHz, CDCl_3 , RT) δ 5.37 (bs, 2H; $-\text{C}(\text{H})=$), 4.05 (t, $J = 6.3$ Hz, 4H; $-\text{CH}_2\text{O}-$), 3.66 (s, 3H; $-\text{OCH}_3$), 3.63 (t, 2H; $-\text{CH}_2\text{OH}$), 2.35–2.25 (m, 4H; $-\text{C}(\text{O})\text{CH}_2-$), 1.96 (bs, 4H; $-\text{CH}_2\text{CH}=\text{}$), 1.75 – 1.55 (m, 8H; $-\text{C}(\text{O})\text{CH}_2\text{CH}_2-$ and $-\text{CH}_2\text{CH}_2\text{O}-$), 1.45 – 1.25 (m, 16 H; CH_2). ^{13}C NMR (75 MHz, CDCl_3 , RT) δ 174.15 ($-\text{C}(\text{O})\text{O}-$; HDL-HDL), 174.1 ($-\text{C}(\text{O})\text{O}-$; HDL*-CL), 173.8 ($-\text{C}(\text{O})\text{O}-$; CL*-HDL), 173.7 ($-\text{C}(\text{O})\text{O}-$; CL-CL), 130.6 ($-\text{CH}=\text{}$), 130.3 ($-\text{CH}=\text{}$), 64.6 ($-\text{C}(\text{O})\text{OCH}_2-$; HDL*-CL), 64.5 ($-\text{C}(\text{O})\text{OCH}_2-$; HDL-HDL), 64.3 ($-\text{C}(\text{O})\text{OCH}_2-$; CL-CL), 64.2 (CL*-HDL), 34.5 ($-\text{CH}_2\text{C}(\text{O})\text{O}-$; HDL-HDL), 34.45 ($-\text{CH}_2\text{C}(\text{O})\text{O}-$; HDL*-CL), 34.3 ($-\text{CH}_2\text{C}(\text{O})\text{O}-$; CL*-HDL), 34.25 ($-\text{CH}_2\text{C}(\text{O})\text{O}-$; CL-CL), 32.7, 32.6, 29.7 and 29.6 (CH_2 , HDL), 29.3 (2C; CH_2 , HDL), 29.15 ($-\text{CH}_2\text{CH}=\text{}$), 28.9 ($-\text{CH}_2\text{CH}=\text{}$), 28.8 (CH_2 , HDL), 28.5 ($-\text{C}(\text{O})\text{OCH}_2\text{CH}_2-$), 25.95 (CH_2 , HDL), 25.7 ($-\text{CH}_2\text{CH}_2\text{CH}_2\text{C}(\text{O})\text{O}-$, CL), 25.15 ($\text{CH}_2\text{CH}_2\text{C}(\text{O})\text{O}-$; HDL-HDL), 25.1 ($\text{CH}_2\text{CH}_2\text{C}(\text{O})\text{O}-$; HDL*-CL), 24.75 ($\text{CH}_2\text{CH}_2\text{C}(\text{O})\text{O}-$; CL*-HDL), 24.7 ($\text{CH}_2\text{CH}_2\text{C}(\text{O})\text{O}-$; CL-CL).

5.7. 7. Synthesis of poly(6- ω -hexadecenlactone)-*block*-poly(ϵ -caprolactone)

A Schlenk tube was charged with precatalyst (14.0 mg, 35 μmol), 6HDL (442 mg, 1.75 mmol), xylenes (0.7 mL) and methanol (0.35 mL of a 0.1 M toluene solution, 35 μmol). The mixture was thermostated at 100 $^\circ\text{C}$ and magnetically stirred. After 21 h, an aliquot was withdrawn from the reaction mixture, dissolved in CDCl_3 and analyzed by ^1H NMR, the macrolactone conversion was 60 %. Afterwards, ϵ -CL (515 mg, 4.50 mmol) was added and the reaction mixture was stirred for 20 h. Finally, the mixture was cooled to room temperature. Product purification was attained by removal of xylenes under vacuum, followed by dropwise addition of the residue, dissolved in a minimal amount of CH_2Cl_2 , to rapidly stirring methanol. The precipitated polymer was recovered by filtration, washed with methanol

and dried at 30 °C overnight in a vacuum oven. Yield = 84 %. $M_{n,th} = 22.4$ kDa. $M_{n,NMR} = 22.3$ kDa. $M_{n,GPC} = 37.5$ kDa. $M_n/M_w = 1.9$.

^1H NMR (300 MHz, CDCl_3 , RT) δ 5.37 (bs, 2H; $-\text{C}(\text{H})=$), 4.15 – 3.95 (m, 4H), 3.66 (s, 3H; $-\text{OCH}_3$), 3.63 (t, 2H; $-\text{CH}_2\text{OH}$), 2.35 – 2.20 (m, 4H; $-\text{C}(\text{O})\text{CH}_2-$), 1.96 (bs, 4H; $-\text{CH}_2\text{C}(\text{H})=$), 1.75–1.55 (m, 8H; $-\text{C}(\text{O})\text{CH}_2\text{CH}_2-$ and $-\text{CH}_2\text{CH}_2\text{O}-$), 1.45–1.25 (m, 16H; CH_2). ^{13}C NMR (75 MHz, CDCl_3 , RT) δ 174.15 ($-\text{C}(\text{O})\text{O}-$, HDL), 173.7 ($-\text{C}(\text{O})\text{O}-$, CL), 130.6 ($-\text{C}(\text{H})=$), 130.3 ($-\text{C}(\text{H})=$), 64.5 ($-\text{C}(\text{O})\text{OCH}_2-$, HDL), 64.3 ($-\text{C}(\text{O})\text{OCH}_2-$, CL), 34.5 ($-\text{CH}_2\text{C}(\text{O})\text{O}-$, HDL), 34.25 ($-\text{CH}_2\text{C}(\text{O})\text{O}-$, CL), 32.7 (CH_2 , HDL), 32.6 (CH_2 , HDL), 29.7 (CH_2 , HDL), 29.6 (CH_2 , HDL), 29.3 (2C; CH_2 , HDL), 29.15 ($-\text{CH}_2\text{CH}=\text{}$), 28.9 ($-\text{CH}_2\text{CH}=\text{}$), 28.8 (CH_2 , HDL), 28.5 (CH_2 , CL), 25.95 (CH_2 , HDL), 25.7 (CH_2 , CL), 25.15 (CH_2 , HDL), 24.75 (CH_2 , CL).

5.7.8. Synthesis of poly(6- ω -hexadecenlactone)-*block*-poly(*rac*-lactide)

A Schlenk tube was charged with precatalyst (14.0 mg, 35 μmol), 6HDL (442 mg, 1.75 mmol), xylenes (2.3 mL) and methanol (0.35 mL of a 0.1 M toluene solution, 35 μmol). The mixture was thermostated at 100 °C and magnetically stirred for 24 h. Then, an aliquot was withdrawn, dissolved in CDCl_3 and analyzed by ^1H NMR, resulting in a macrolactone conversion of 50 %. Afterwards, *rac*-LA (252.2 mg, 1.75 mmol) was added and the reaction mixture was stirred for other 17 h (*rac*-LA conversion = 95 %). Finally, the mixture was cooled to room temperature. Product purification was attained by dropwise addition of the reaction mixture, dissolved in CH_2Cl_2 , to rapidly stirring *n*-hexane. The precipitated polymer was recovered by filtration, washed with *n*-hexane and dried at 60 °C overnight in a vacuum oven. Yield = 51 %. $M_{n,th} = 16.9$ kDa. $M_{n,NMR} = 28.4$ kDa. $M_{n,GPC} = 24.3$ kDa. $M_n/M_w = 1.5$.

^1H NMR (300 MHz, CDCl_3 , RT) δ 5.37 (bs, 2H; $-\text{CH}=\text{}$), 5.30 – 5.05 (m, 1H; $-\text{CHCH}_3-$), 4.04 (t, $J = 6.6$ Hz, 2H; $-\text{CH}_2\text{O}-$), 3.66 (s, 3H; $-\text{OCH}_3$), 3.63 (t, 2H; $-\text{CH}_2\text{OH}$), 2.28 (t, $J = 7.4$ Hz, 2H; $-\text{C}(\text{O})\text{CH}_2-$), 1.96 (bs, 4H; $-\text{CH}_2\text{CH}=\text{}$), 1.75 – 1.55 (m, 7H; $-\text{C}(\text{O})\text{CH}_2\text{CH}_2-$, $-\text{CH}_2\text{CH}_2\text{O}-$ and $-\text{CH}_3$), 1.45 – 1.20 (m, 14 H; CH_2). ^{13}C NMR (75 MHz, CDCl_3 , RT) δ 174.15 ($-\text{C}(\text{O})\text{O}-$, HDL-HDL), 169.8, 169.6, 169.55, 169.5 and 169.3 ($-\text{C}(\text{O})\text{O}-$, LA-LA), 130.6 ($-\text{C}(\text{H})=\text{}$), 130.3 ($-\text{CH}=\text{}$), 69.3 and 69.15 ($-\text{C}(\text{O})\text{OCH}-$), 64.5 ($-\text{C}(\text{O})\text{OCH}_2-$), 34.5 ($-\text{CH}_2\text{C}(\text{O})\text{O}-$), 32.7, 32.6, 29.7 and 29.6 (CH_2), 29.3 (2C; CH_2), 29.15 ($-\text{CH}_2\text{CH}=\text{}$), 28.9 ($-\text{CH}_2\text{CH}=\text{}$), 28.8, 25.95 and 25.15 (CH_2), 16.9 and 16.8 ($\text{C}(\text{O})\text{OCHCH}_3-$).

5.7.9. Synthesis of poly[(6- ω -hexadecenlactone)-*ran*-(ϵ -caprolactone)]-*block*-poly(*rac*-lactide)

A Schlenk tube was charged sequentially with precatalyst (14.0 mg, 35 μmol), HDL (442 mg, 1.75 mmol), ϵ -CL (200 mg, 1.75 mmol), xylenes (2.3 mL) and methanol (0.35 mL of a 0.1 M toluene solution, 35 μmol). The Schlenk tube was thermostated at 100 $^\circ\text{C}$ and magnetically stirred for 24 h then *rac*-LA (252.2 mg, 1.75 mmol) was added and the reaction mixture was stirred for 23 h. Finally, the mixture was cooled to room temperature. Product purification was attained by dropwise addition of the reaction mixture, dissolved in CH_2Cl_2 , to rapidly stirring *n*-hexane. The precipitated polymer was recovered by filtration, washed with *n*-hexane (x 3) and dried at 60 $^\circ\text{C}$ overnight in a vacuum oven. Yield = 48 %. $M_{n,\text{th}} = 15.2$ kDa. $M_{n,\text{GPC}} = 29.1$ kDa. $M_{n,\text{NMR}} = 26.5$ kDa. $M_n/M_w = 2.0$. Sequences block lengths, as evaluated by ^1H NMR: $L_{(\text{HDL-}i\text{ran-CL})} = 110$; $L_{\text{LL}} = 58$. Average sequence block lengths of the random HDL/CL block: $L_{\text{HDL}} = 1.73$; $L_{\text{CL}} = 2.93$.

^1H NMR (300 MHz, CDCl_3 , RT) δ 5.37 (bs, 2H; $-\text{CH}=\text{}$), 5.30 – 5.05 (m, 1H; $-\text{CHCH}_3-$), 4.04 (t, $J = 5.7$ Hz, 2H; $-\text{CH}_2\text{O}-$), 3.66 (s, 3H; $-\text{OCH}_3$), 3.63 (t, 2H; $-\text{CH}_2\text{OH}$), 2.28 (q, $J = 7.4$ Hz, 4H; $-\text{C}(\text{O})\text{CH}_2-$), 1.96 (bs, 4H;

$-CH_2CH=$), 1.75 – 1.45 (m, 11H, $-C(O)CH_2CH_2-$, $-CH_2CH_2O-$ and $-CHCH_3-$), 1.45 – 1.15 (m, 16H, CH_2). ^{13}C NMR (75 MHz, $CDCl_3$, RT) δ 174.15 ($-C(O)O-$; HDL-HDL), 174.1 ($-C(O)O-$; HDL*-CL), 173.8 ($-C(O)O-$; CL*-HDL), 173.7 ($-C(O)O-$; CL-CL), 169.8, 169.6, 169.55, 169.5 and 169.3 ($-C(O)O-$, LA-LA), 130.6 ($-CH=$), 130.3 ($-CH=$), 69.3 and 69.15 ($-C(O)OCH-$, LA), 64.6 ($-C(O)OCH_2-$; HDL*-CL), 64.5 ($-C(O)OCH_2-$; HDL-HDL), 64.3 ($-C(O)OCH_2-$; CL-CL), 64.2 (CL*-HDL), 34.5 ($-CH_2C(O)O-$; HDL-HDL), 34.45 ($-CH_2C(O)O-$; HDL*-CL), 34.3 ($-CH_2C(O)O-$; CL*-HDL), 34.25 ($-CH_2C(O)O-$; CL-CL), 32.7, 32.6, 29.7 and 29.6 (CH_2 , HDL), 29.3 (2C; CH_2 , HDL), 29.15 ($-CH_2CH=$), 28.9 ($-CH_2CH=$), 28.8 (CH_2 , HDL), 28.5 ($-C(O)OCH_2CH_2-$), 25.95 (CH_2 , HDL), 25.7 ($-CH_2CH_2CH_2C(O)O-$, CL), 25.15 ($CH_2CH_2C(O)O-$; HDL-HDL), 25.1 ($CH_2CH_2C(O)O-$; HDL*-CL), 24.75 ($CH_2CH_2C(O)O-$; CL-CL), 24.7 ($CH_2CH_2C(O)O-$; CL*-HDL), 16.9 and 16.8 ($C(O)OCH(CH_3)-$).

References

- ¹ D.-P. Song, Y.-G. Li, R. Lu, N.-H. Hu, Y.-S. Li, *Appl. Organomet. Chem.* **2008**, *22*, 333-340.
- ² D. Pappalardo, C. Tedesco, C. Pellicchia, *Eur. J. Inorg. Chem.* **2002**, 621-628.
- ³ K. V. Axenov, M. Klinga, O. Lehtonen, H. T. Laskela, T. Repo, *Organometallics* **2007**, *26*, 1444-1460.
- ⁴ K. Wisniewski, *Org. Prep. Proced. Int.* **1999**, *31(2)*, 211–214.
- ⁵ (a) A. S. Scheibelhoffer, W. A. Blose, H. Harwood, *J. Polym. Prepr. (Am. Chem. Soc., Di V. Polym. Chem.)* **1969**, *10*, 1375–1380. (b) F. Jing, M. A. Hillmyer, *J. Am. Chem. Soc.* **2008**, *130*, 13826–13827.
- ⁶ S. Dånmark, A. Finne-Wistrand, M. Wendel, K. Arvidson, A.-C. Albertsson, K. Mustafa, *J. Bioact. Compat. Polym.* **2010**, *25*, 207–223.
- ⁷ H. Sun, A. Wirsén, A.-C. Albertsson, *Biomacromolecules* **2004**, *5*, 2275–2280.
- ⁸ (a) A. Finne, A.-C. Albertsson, *J. Polym. Sci., Part A: Polym. Chem.* **2004**, *42*, 444–452. (b) P. -J. Roumanet, F. Laflèche, N. Jarroux, Y. Raoul, S. Claude, P. Guégan, *Eur. Polym. J.* **2013**, *49*, 813–822.
- ⁹ H. -P. Zhao, J. -F. Zhang, X. S. Sun, D. H. Hua, *J. Appl. Polym. Sci.* **2008**, *110*, 647–656.

ACKNOWLEDGEMENTS

During my PhD I had the great pleasure to work with wonderful and professional people and I would like to express my gratitude to each of them, for the fundamental research experience they have granted me.

First and foremost, I would like to thank Prof. Daniela Pappalardo, my tutor, for her help, her many precious suggestions and her constant encouragement during my PhD. She has been a true mentor for me, an essential and constant point of reference. It was always a pleasure to work with Daniela throughout the ups and downs of the last three years.

I would like also to express my gratitude to my co-tutor, Prof. Marina Lamberti for her collaboration, her patience and her constructive and critical opinions.

I wish also to express my sincere gratitude to my external co-tutor, Prof. Anna Finne-Wistrand, for the great experience I had at KTH Royal Institute of Technology in Stockholm. Furthermore, I would like to thank the "VINNOVA, Mobility for Growth; the Marie Curie Actions FP7-PEOPLE-2011-COFUND (GROWTH 291,795)" for the financial support during my period of research at KTH.

Thanks to Prof. Claudio Pellecchia, the head of my research group, for his valuable advices and essential scientific support. I was privileged to carry out my PhD project in his group, whose atmosphere contributed significantly to the success of my studies. My time in this group has been the most enjoyable, and I believe that it is necessary condition for successful research.

I am also grateful to all the friends and people with whom I shared part of my research. In particular, the friends of the Lab. 3, and my colleagues of the Department of Chemistry and Biology.

Finally, I would like to thank my family for supporting me.